



THE UNIVERSITY *of* EDINBURGH

Edinburgh Research Explorer

Measurement of inclusive jet charged-particle fragmentation functions in Pb+Pb collisions at $\sqrt{s_{NN}}=2.76$ TeV with the ATLAS detector

Citation for published version:

Clark, PJ, Leonidopoulos, C, Martin, VJ, Mills, C & Collaboration, A 2014, 'Measurement of inclusive jet charged-particle fragmentation functions in Pb+Pb collisions at $\sqrt{s_{NN}}=2.76$ TeV with the ATLAS detector', *Physics Letters B*, vol. B739, Aad:2014wha, pp. 320-342.
<https://doi.org/10.1016/j.physletb.2014.10.065>

Digital Object Identifier (DOI):

[10.1016/j.physletb.2014.10.065](https://doi.org/10.1016/j.physletb.2014.10.065)

Link:

[Link to publication record in Edinburgh Research Explorer](#)

Document Version:

Publisher's PDF, also known as Version of record

Published In:

Physics Letters B

General rights

Copyright for the publications made accessible via the Edinburgh Research Explorer is retained by the author(s) and / or other copyright owners and it is a condition of accessing these publications that users recognise and abide by the legal requirements associated with these rights.

Take down policy

The University of Edinburgh has made every reasonable effort to ensure that Edinburgh Research Explorer content complies with UK legislation. If you believe that the public display of this file breaches copyright please contact openaccess@ed.ac.uk providing details, and we will remove access to the work immediately and investigate your claim.





Measurement of inclusive jet charged-particle fragmentation functions in Pb+Pb collisions at $\sqrt{s_{NN}} = 2.76$ TeV with the ATLAS detector

ATLAS Collaboration ^{*}

ARTICLE INFO

Article history:

Received 11 June 2014

Received in revised form 27 October 2014

Accepted 30 October 2014

Available online 4 November 2014

Editor: D.F. Geesaman

ABSTRACT

Measurements of charged-particle fragmentation functions of jets produced in ultra-relativistic nuclear collisions can provide insight into the modification of parton showers in the hot, dense medium created in the collisions. ATLAS has measured jets in $\sqrt{s_{NN}} = 2.76$ TeV Pb+Pb collisions at the LHC using a data set recorded in 2011 with an integrated luminosity of 0.14 nb^{-1} . Jets were reconstructed using the anti- k_t algorithm with distance parameter values $R = 0.2, 0.3$, and 0.4 . Distributions of charged-particle transverse momentum and longitudinal momentum fraction are reported for seven bins in collision centrality for $R = 0.4$ jets with $p_T^{\text{jet}} > 100$ GeV. Commensurate minimum p_T values are used for the other radii. Ratios of fragment distributions in each centrality bin to those measured in the most peripheral bin are presented. These ratios show a reduction of fragment yield in central collisions relative to peripheral collisions at intermediate z values, $0.04 \lesssim z \lesssim 0.2$, and an enhancement in fragment yield for $z \lesssim 0.04$. A smaller, less significant enhancement is observed at large z and large p_T in central collisions.

© 2014 The Authors. Published by Elsevier B.V. This is an open access article under the CC BY license (<http://creativecommons.org/licenses/by/3.0/>). Funded by SCOAP³.

1. Introduction

Collisions between lead nuclei at the LHC are thought to produce a quark–gluon plasma (QGP), a form of strongly interacting matter in which quarks and gluons become locally deconfined. One predicted consequence of QGP formation is the “quenching” of jets generated in hard-scattering processes during the initial stages of the nuclear collisions [1]. Jet quenching refers, collectively, to a set of possible modifications of parton showers by the QGP through interactions of the constituents of the shower with the colour charges in the plasma [2,3]. In particular, quarks and gluons in the shower may be elastically or inelastically scattered resulting in both deflection and energy loss of the constituents of the shower. The deflection and the extra radiation associated with inelastic processes may broaden the parton shower and eject partons out of an experimental jet cone [4–9]. As a result, jet quenching can potentially both soften the spectrum of the momentum of hadrons inside the jet and reduce the total energy of the reconstructed jet. A complete characterization of the effects of jet quenching therefore requires measurements of both the single-jet suppression and the jet fragment distributions.

Observations of modified dijet asymmetry distributions [10–12], modified balance-jet transverse momentum (p_T) distributions in $\gamma + \text{jet}$ events [13], and suppressed inclusive jet yield in Pb+Pb collisions at the LHC [14,15] are consistent with theoretical calcu-

lations of jet quenching. However, it has been argued that those measurements do not sufficiently discriminate between calculations that make different assumptions regarding the relative importance of the contributions described above [16]. Based on the above arguments, theoretical analyses are incomplete without experimental constraints on the theoretical description of jet fragmentation distributions.

This Letter presents measurements of charged-particle jet fragmentation functions in $\sqrt{s_{NN}} = 2.76$ TeV Pb+Pb collisions using 0.14 nb^{-1} of data recorded in 2011. The jets used in the measurements were reconstructed with the anti- k_t [17] algorithm using distance parameter values $R = 0.2, 0.3$, and 0.4 . Results are presented for the charged-particle transverse momentum (\vec{p}_T^{ch}) and longitudinal momentum fraction ($z \equiv \vec{p}_T^{\text{ch}} \cdot \vec{p}_T^{\text{jet}} / |\vec{p}_T^{\text{jet}}|^2$) distributions,

$$D(p_T) \equiv \frac{1}{N_{\text{jet}}} \frac{dN_{\text{ch}}}{dp_T^{\text{ch}}}, \quad (1)$$

$$D(z) \equiv \frac{1}{N_{\text{jet}}} \frac{dN_{\text{ch}}}{dz}, \quad (2)$$

of charged particles with $p_T^{\text{ch}} > 2$ GeV produced within an angular range $\Delta R = 0.4$ of the reconstructed jet directions for jets with $p_T^{\text{jet}} > 85, 92$, and 100 GeV for $R = 0.2, 0.3$, and 0.4 , respectively. Here, $\Delta R = \sqrt{(\Delta\phi)^2 + (\Delta\eta)^2}$ where $\Delta\phi$ ($\Delta\eta$) is the difference in azimuthal angles (pseudorapidities) between the charged

^{*} E-mail address: atlas.publications@cern.ch.

particle and jet directions.¹ The p_T^{jet} thresholds for the three R values were chosen to match the R -dependence of the measured transverse momentum of a typical jet. For simplicity, the terms “fragmentation functions” are used to describe the distributions defined in Eq. (2) with the understanding that $D(z)$ is different from a theoretical fragmentation function, $D(z, Q^2)$, calculated using unquenched jet energies and with no restriction on the angles of particles with respect to the jet axis. Earlier measurements by CMS of jet fragmentation functions [18] in Pb+Pb collisions at the LHC show no significant modification, but the uncertainties on that measurement were not sufficient to exclude modifications at the level of $\sim 10\%$. CMS recently released a new result [19] using higher statistics data from 2011 that show fragmentation function modifications which are consistent with the results presented in this Letter.

2. Experimental setup

The measurements presented in this Letter were performed using the ATLAS calorimeter, inner detector, muon spectrometer, trigger, and data acquisition systems [20]. The ATLAS calorimeter system consists of a liquid argon (LAr) electromagnetic (EM) calorimeter covering $|\eta| < 3.2$, a steel-scintillator sampling hadronic calorimeter covering $|\eta| < 1.7$, a LAr hadronic calorimeter covering $1.5 < |\eta| < 3.2$, and two LAr forward calorimeters (FCal) covering $3.2 < |\eta| < 4.9$. The hadronic calorimeter has three sampling layers longitudinal in shower depth and has a $\Delta\eta \times \Delta\phi$ granularity of 0.1×0.1 for $|\eta| < 2.5$ and 0.2×0.2 for $2.5 < |\eta| < 4.9$.² The EM calorimeters are segmented longitudinally in shower depth into three compartments with an additional pre-sampler layer. The EM calorimeter has a granularity that varies with layer and pseudorapidity, but which is generally much finer than that of the hadronic calorimeter. The middle sampling layer, which typically has the largest energy deposit in EM showers, has a granularity of 0.025×0.025 over $|\eta| < 2.5$.

The inner detector [21] measures charged particles within the pseudorapidity interval $|\eta| < 2.5$ using a combination of silicon pixel detectors, silicon microstrip detectors (SCT), and a straw-tube transition radiation tracker (TRT), all immersed in a 2 T axial magnetic field. All three detectors are composed of a barrel and two symmetrically placed end-cap sections. The pixel detector is composed of 3 layers of sensors with nominal feature size $50 \mu\text{m} \times 400 \mu\text{m}$. The SCT barrel section contains 4 layers of modules with $80 \mu\text{m}$ pitch sensors on both sides, while each end-cap consists of nine layers of double-sided modules with radial strips having a mean pitch of $80 \mu\text{m}$. The two sides of each SCT layer in both the barrel and the end-caps have a relative stereo angle of 40 mrad. The TRT contains up to 73 (160) layers of staggered straws interleaved with fibres in the barrel (end-cap). Charged particles with $p_T^{\text{ch}} \gtrsim 0.5$ GeV typically traverse three layers of pixel sensors, four layers of double-sided SCT sensors, and, in the case of $|\eta| < 2.0$, 36 TRT straws.

Minimum bias Pb+Pb collisions were identified using measurements from the zero degree calorimeters (ZDCs) and the minimum-bias trigger scintillator (MBTS) counters [20]. The ZDCs are located symmetrically at $z = \pm 140$ m and cover $|\eta| > 8.3$.

In Pb+Pb collisions the ZDCs measure primarily “spectator” neutrons, which originate from the incident nuclei and do not interact hadronically. The MBTS detects charged particles over $2.1 < |\eta| < 3.9$ using two counters placed at $z = \pm 3.6$ m. MBTS counters are divided into 16 modules with 8 different positions in azimuth and covering 2 different $|\eta|$ intervals. Each counter provides measurement of both the pulse heights and arrival times of ionization energy deposits.

Events used in this analysis were selected for recording by a combination of Level-1 minimum-bias and High Level Trigger (HLT) jet triggers. The Level-1 trigger required a total transverse energy measured in the calorimeter of greater than 10 GeV. The HLT jet trigger ran the offline Pb+Pb jet reconstruction algorithm, described below, for $R = 0.2$ jets except for the application of the final hadronic energy scale correction. The HLT trigger selected events containing an $R = 0.2$ jet with transverse energy $E_T > 20$ GeV.

3. Event selection and data sets

This analysis uses a total integrated luminosity of 0.14 nb^{-1} of Pb+Pb collisions recorded by ATLAS in 2011. Events selected by the HLT jet trigger were required to have a reconstructed primary vertex and a time difference between hits in the two sides of the MBTS detector of less than 3 ns. The primary vertices were reconstructed from charged-particle tracks with $p_T^{\text{ch}} > 0.5$ GeV. The tracks were reconstructed from hits in the inner detector using the ATLAS track reconstruction algorithm described in Ref. [22] with settings optimized for the high hit density in heavy-ion collisions [23]. A total of 14.2 million events passed the described selections.

The centrality of Pb+Pb collisions was characterized by $\sum E_T^{\text{FCal}}$, the total transverse energy measured in the forward calorimeters [23]. Jet fragmentation functions were measured in seven centrality bins defined according to successive percentiles of the $\sum E_T^{\text{FCal}}$ distribution ordered from the most central to the most peripheral collisions: 0–10%, 10–20%, 20–30%, 30–40%, 40–50%, 50–60%, and 60–80%. The percentiles were defined after correcting the $\sum E_T^{\text{FCal}}$ distribution for a 2% minimum-bias trigger inefficiency that affects the most peripheral events which are not included in this analysis.

The performance of the ATLAS detector and offline analysis in measuring jets and charged particles in the environment of Pb+Pb collisions was evaluated using a large Monte Carlo (MC) event sample obtained by overlaying simulated [24] PYTHIA [25] pp hard-scattering events at $\sqrt{s} = 2.76$ TeV onto 1.2 million minimum-bias Pb+Pb events recorded in 2011. The same number of PYTHIA events was produced for each of five intervals of \hat{p}_T , the transverse momentum of outgoing partons in the $2 \rightarrow 2$ hard-scattering, with boundaries 17, 35, 70, 140, 280, and 560 GeV. The detector response to the PYTHIA events was simulated using Geant4 [26], and the simulated hits were combined with the data from the minimum-bias Pb+Pb events to produce 1.2 million overlaid events for each \hat{p}_T interval.

4. Jet and charged-particle analysis

Charged particles included in the fragmentation measurements were required to have at least two hits in the pixel detector, including a hit in the first pixel layer if the track trajectory makes such a hit expected, and seven hits in the silicon microstrip detector. In addition, the transverse (d_0) and longitudinal ($z_0 \sin \theta$) impact parameters of the tracks measured with respect to the primary vertex were required to satisfy $|d_0/\sigma_{d_0}| < 3$ and $|z_0 \sin \theta/\sigma_z| < 3$, where σ_{d_0} and σ_z are uncertainties on d_0 and $z_0 \sin \theta$, respectively, obtained from the track-fit covariance matrix.

¹ ATLAS uses a right-handed coordinate system with its origin at the nominal interaction point (IP) in the centre of the detector and the z -axis along the beam pipe. The x -axis points from the IP to the centre of the LHC ring, and the y axis points upward. Cylindrical coordinates (r, ϕ) are used in the transverse plane, ϕ being the azimuthal angle around the beam pipe. The pseudorapidity is defined in terms of the polar angle θ as $\eta = -\text{Intan}(\theta/2)$.

² An exception is the third sampling layer that has a segmentation of 0.2×0.1 up to $|\eta| = 1.4$.

Table 1

Number of jets for two centrality bins in data as a function of the selection criteria applied. Each line specifies the number of jets passing all cuts for the given line and above.

Cut description	N_{jet}	
	0–10%	60–80%
All jets	41 191	2579
UE jet rejection	41 116	2570
Isolation	40 986	2554
Muon rejection	40 525	2523
Inactive area exclusion	39 548	2458
Trigger jet match	39 548	2458

Jets were reconstructed using the techniques described in Ref. [14], which are briefly summarized here.

The anti- k_t algorithm was first run in four-momentum recombination mode, on $\Delta\eta \times \Delta\phi = 0.1 \times 0.1$ logical towers and for three values of the anti- k_t distance parameter, $R = 0.2, 0.3$, and 0.4 . The tower kinematics were obtained by summing electromagnetic-scale energies of calorimeter cells within the tower boundaries. Then, an iterative procedure was used to estimate a layer- and η -dependent underlying event (UE) energy density while excluding actual jets from that estimate. The UE energy was subtracted from each calorimeter cell within the towers included in the reconstructed jet. The correction takes into account a $\cos 2\phi$ modulation of the calorimeter response due to elliptic flow of the medium [23] which is estimated by measurement of the amplitude of that modulation in the calorimeter. The final jet kinematics were calculated via a four-momentum sum of all (assumed massless) cells contained within the jets using subtracted E_T values. A correction was applied to the reconstructed jet to account for jets not excluded or only partially excluded from the UE estimate. Then, a final jet η - and E_T -dependent hadronic energy scale calibration factor was applied.

After the reconstruction, additional selections were applied for the purposes of this analysis. “UE jets” generated by fluctuations in the underlying event, were removed using techniques described in Ref. [14].

To prevent neighbouring jets from distorting the measurement of the fragmentation functions, jets were required to be isolated. The isolation cut required that there be no other jet within $\Delta R = 1$ having $p_T > p_T^{\text{iso}}$ where p_T^{iso} , the isolation threshold, is set to half of the analysis threshold for each R value, $p_T^{\text{iso}} = 42.5, 46$, and 50 GeV for $R = 0.2, 0.3$, and 0.4 , respectively. To prevent muons from semileptonic heavy-flavour decays from influencing the measured fragmentation functions, all jets with reconstructed muons having $p_T > 4$ GeV within a cone of size $\Delta R = 0.4$ were excluded from the analysis. To prevent inactive regions in the calorimeters from producing artificial high z fragments, jets were required to have more than 90% of their energy contained within fully functional regions of the calorimeter. Finally, all jets included in the analysis were required to match HLT jets reconstructed with transverse momenta greater than the trigger threshold of 20 GeV. The HLT jets were found to be fully efficient for the jet kinematic selection used in this analysis. Table 1 shows the impact of the cuts on the number of measured jets in central (0–10%) and peripheral (60–80%) collisions. All these cuts together retain more than 96% of all jets.

5. Jet and track reconstruction performance

The performance of the ATLAS detector and analysis procedures in measuring jets was evaluated from the MC sample using the procedures described in Ref. [14]. Reconstructed MC jets were matched to “truth” jets obtained by separately running the anti- k_t

Table 2

The relationship between the mean truth-jet transverse momenta, $\langle p_{T\text{true}}^{\text{jet}} \rangle$, and corresponding reconstructed jet transverse momenta, $p_{T\text{rec}}^{\text{jet}}$. Sample values of α and β obtained from linear fits to $\langle p_{T\text{true}}^{\text{jet}} \rangle (p_{T\text{rec}}^{\text{jet}})$ (see text) according to Eq. (3) and the resulting $\langle p_{T\text{true}}^{\text{jet}} \rangle$ for $p_{T\text{rec}}^{\text{jet}} = 100$ GeV.

Centrality	Jet R	α	β (GeV)	$\langle p_{T\text{true}}^{\text{jet}} \rangle$ (100 GeV)
0–10%	0.2	0.995 ± 0.003	-7.6 ± 0.5	91.9 GeV
60–80%	0.2	0.989 ± 0.002	-6.0 ± 0.3	92.9 GeV
0–10%	0.4	1.027 ± 0.004	-17.7 ± 0.5	85.0 GeV
60–80%	0.4	0.964 ± 0.002	-2.3 ± 0.2	94.1 GeV

algorithm on the final-state PYTHIA particles³ for the three jet R values used in this analysis. For the jet fragmentation measurements, the most important aspect of the jet performance is the jet energy resolution (JER). For jet energies $\gtrsim 100$ GeV, the JER in central (0–10%) collisions for $R = 0.4$ jets has comparable contributions from UE fluctuations and “intrinsic” resolution of the calorimetric jet measurement. For peripheral collisions and $R = 0.2$ jets, the intrinsic calorimeter resolution dominates the JER. The value of JER evaluated for jets with $p_T = 100$ GeV in 0–10% collisions is 0.18, 0.15, and 0.13 for $R = 0.4$, $R = 0.3$, and $R = 0.2$ jets, respectively.

The combination of the finite JER and the steeply falling jet p_T spectrum produces a net migration of jets from lower p_T to higher p_T values (hereafter referred to as “upfeeding”) such that a jet reconstructed with a given $p_{T\text{rec}}^{\text{jet}}$ corresponds, on average, to a lower truth-jet p_T , $\langle p_{T\text{true}}^{\text{jet}} \rangle$. The relationship between $\langle p_{T\text{true}}^{\text{jet}} \rangle$ and $p_{T\text{rec}}^{\text{jet}}$ was evaluated from the MC data set for the different centrality bins and three R values used in this analysis. For the jet $p_{T\text{rec}}^{\text{jet}}$ values used in this analysis, that relationship is well described by a linear dependence,

$$\langle p_{T\text{true}}^{\text{jet}} \rangle = \alpha p_{T\text{rec}}^{\text{jet}} + \beta. \quad (3)$$

Sample values for α and β and the resulting $\langle p_{T\text{true}}^{\text{jet}} \rangle$ values for $R = 0.2$ and $R = 0.4$ jets in peripheral and central collisions are listed in Table 2. The extracted relationships between $p_{T\text{rec}}^{\text{jet}}$ and $\langle p_{T\text{true}}^{\text{jet}} \rangle$ will be used in the fragmentation analysis to correct for the average shift in the measured jet energy.

MC studies indicate that the efficiency for PYTHIA jets to be reconstructed and to pass UE jet rejection exceeds 98% for $p_T^{\text{jet}} > 60$ GeV in the 0–10% centrality bin. For kinematic selection of jets used in this study, the jet reconstruction was fully efficient.

The efficiency for reconstructing charged particles within jets in Pb+Pb collisions was evaluated using the MC sample. Fig. 1 shows comparisons of distributions of four important track-quality variables between data and MC simulation for reconstructed tracks over a narrow p_T^{ch} interval, $5 < p_T^{\text{ch}} < 7$ GeV, to minimize the impact of differences in MC and data charged-particle p_T^{ch} distributions. The ratios of the data to MC distributions also shown in the figure indicate better than 1% agreement in the η dependence of the average number of pixel and SCT hits associated with the tracks. The distributions of d_0 and $z_0 \sin \theta$ agree to $\lesssim 10\%$ except in the tails of the distributions, which contribute a negligible fraction of the distribution. For the purpose of evaluating the track reconstruction performance and for the evaluation of response matrices that are used in the unfolding (described below), the reference “truth” particles were taken from the set of final-state PYTHIA charged particles. These were matched to re-

³ Final-state PYTHIA particles are defined as all generated particles with lifetimes longer than $0.3 \cdot 10^{-10}$ s originating from the primary interaction or from subsequent decay of particles with shorter lifetimes.

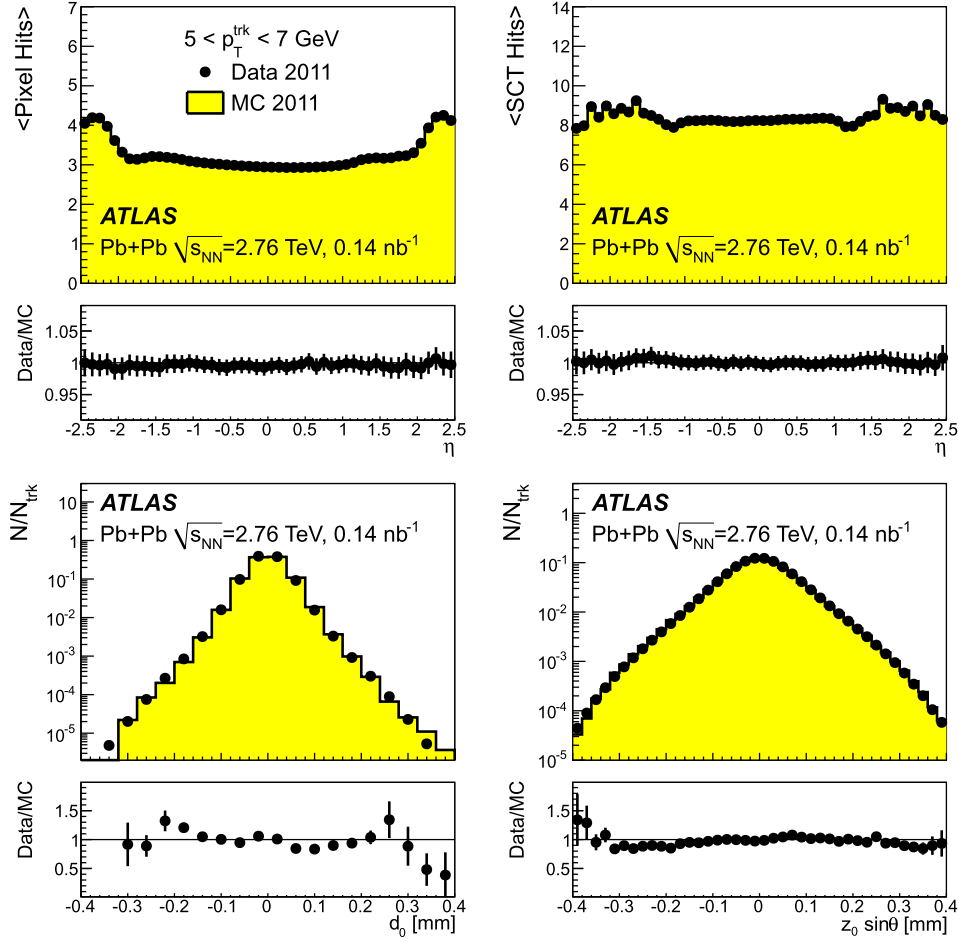


Fig. 1. Comparison between data and MC distributions for four different charged-particle reconstruction selection parameters. The distributions are shown for the 0–10% centrality bin and for charged-particle transverse momenta in the range $5 < p_T^{\text{ch}} < 7$ GeV. Top: average number of pixel (left) and SCT (right) hits per track. Bottom: distribution of track impact parameters with respect to the reconstructed primary vertex; both transverse, d_0 (left), and longitudinal, $z_0 \sin \theta$ (right), impact parameters are shown. Ratios of distributions in data to those in MC simulation are shown for each quantity.

constructed charged particles using associations between detector hits and truth tracks recorded by the ATLAS Geant4 simulations. Truth particles for which no matching reconstructed particle was found were considered lost due to inefficiency.

The charged-particle reconstruction efficiency, $\varepsilon(p_T, \eta)$, was evaluated separately in each of the seven centrality bins used in this analysis for truth particles within $\Delta R = 0.4$ of $R = 0.4$ truth jets having $p_{T, \text{jet}}^{\text{jet}} > 100$ GeV. Fig. 2 shows the efficiency as a function of truth-particle p_T averaged over $|\eta| < 1$ (top) and $1 < |\eta| < 2.5$ (bottom) for the 0–10% and 60–80% centrality bins. For $p_T < 8$ GeV, $\varepsilon(p_T, \eta)$ was directly evaluated using fine bins in p_T and η . For $p_T > 8$ GeV the p_T dependence of the efficiencies were parameterized separately in the two pseudorapidity intervals shown in Fig. 2 using a functional form that describes trends at low p_T as well as at high p_T . An example of the resulting parameterizations is shown by the solid curves in Fig. 2. A centrality-dependent systematic uncertainty in the parameterized efficiencies, shown by the shaded bands in Fig. 2, was evaluated based on both the uncertainties in the parameterization and on observed variations of the efficiency with p_T , which largely result from loss of hits in the SCT at higher detector occupancy. Thus, the systematic uncertainty in the 60–80% centrality bin is small because no significant variation of the efficiency is observed at low detector occupancy, while the uncertainties are largest for the 0–10% centrality bin with the largest detector occupancies.

The efficiencies shown in Fig. 2 decrease by about 12% between the $|\eta| < 1$ interval covered by the SCT barrel and the $1 < |\eta| < 2.5$ interval covered primarily by the SCT end-cap. More significant localized drops in efficiency of about 20% are observed over $1 < |\eta| < 1.2$ and $2.3 < |\eta| < 2.5$ corresponding to the transition between the SCT barrel and end-cap and the detector edge respectively. To account for this and other localized variations of the high p_T reconstruction efficiency with pseudorapidity, the parameterizations in Fig. 2 for $p_T > 8$ GeV are multiplied by an η -dependent factor evaluated in intervals of 0.1 units to produce $\varepsilon(p_T, \eta)$.

6. Fragmentation functions and unfolding

Jets used for the fragmentation measurements presented here were required to have $p_{T, \text{jet}}^{\text{jet}} > 85, 92$ and 100 GeV for $R = 0.2, 0.3$, and 0.4 jets, respectively. The jet thresholds for $R = 0.3$ and $R = 0.2$ jets represent the typical energy measured with the smaller jet radii for an $R = 0.4$ jet with $p_T = 100$ GeV. Jets were also required to have either $0 < |\eta| < 1$ or $1.2 < |\eta| < 1.9$. The restriction of the measurement to $|\eta| < 1.9$ avoids the region at the detector edge with reduced efficiency ($|\eta| > 2.3$). The exclusion of the range $1 < |\eta| < 1.2$ removes from the measurement jets whose large- z fragments, which are typically collinear with the jet axis, would be detected in the lower-efficiency η region spanning the gap between SCT barrel and end-cap. While this exclusion does

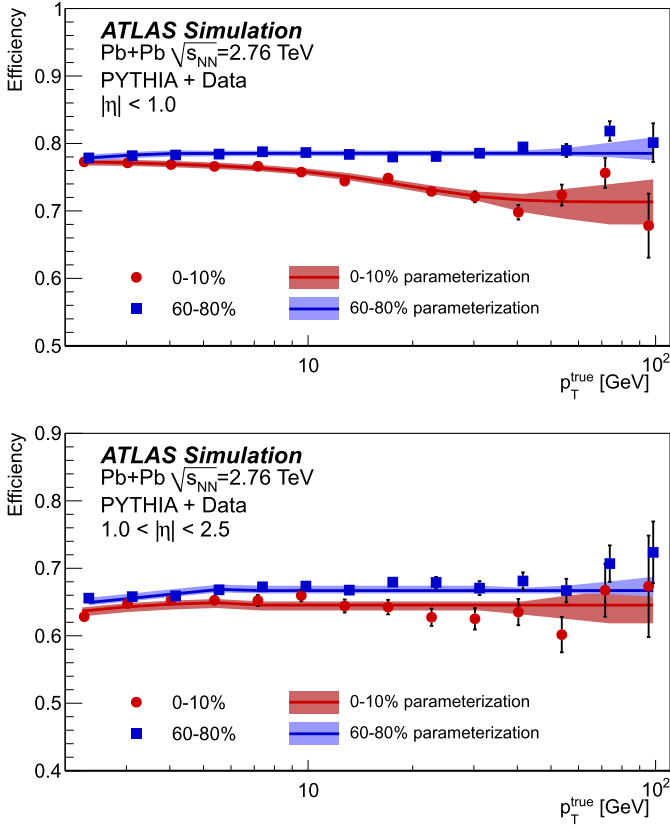


Fig. 2. Charged-particle reconstruction efficiency as a function of truth p_T , for 0–10% (red) and 60–80% (blue) centrality bins in the region $|\eta| < 1$ (top) and $1 < |\eta| < 2.5$ (bottom). The p_T values for the 0–10% points are shifted for clarity. The solid curves show parameterizations of efficiencies. The shaded bands show the systematic uncertainty in the parameterized efficiencies (see text). (For interpretation of the references to color in this figure legend, the reader is referred to the web version of this article.)

not significantly change the result of the measurement, it reduces the systematic uncertainties at large z or p_T^{ch} .

The fragmentation functions were measured for charged particles with $p_T^{\text{ch}} > 2$ GeV within an angular range $\Delta R = 0.4$ of the jet direction for all three R values used in the jet reconstruction. To reduce the effects of the UE broadening of the jet position measurement, for $R = 0.3$ and $R = 0.4$ jets, the jet direction was taken from that of the closest matching $R = 0.2$ jet within $\Delta R = 0.3$ when such a matching jet was found. For each charged particle, the longitudinal jet momentum fraction, z , was calculated according to

$$z = \frac{p_T^{\text{ch}}}{p_T^{\text{jet}}} \cos \Delta R, \quad (4)$$

where ΔR here represents the angle between the charged particle and jet directions.⁴

Charged particles from the UE contribute a p_T^{ch} - and centrality-dependent background to the measurement that must be subtracted to obtain the true fragmentation functions. The contribution of the UE background was separately evaluated for $R = 0.2, 0.3$, and 0.4 jets in events having at least one such jet above the jet p_T thresholds using a grid of $\Delta R = 0.4$ cones that spanned the full coverage of the inner detector. Any such cone having a charged particle with $p_T^{\text{ch}} > 6$ GeV was assumed to be associated

with a real jet in the event and was excluded from the UE background determination. The threshold of 6 GeV was chosen to be high enough to avoid bias of the UE p_T^{ch} distribution.

The resulting per-jet UE charged-particle yields, $dn_{\text{ch}}^{\text{UE}}/dp_T^{\text{ch}}$, were evaluated over $2 < p_T^{\text{ch}} < 6$ GeV as a function of p_T^{ch} , p_T^{jet} , and η^{jet} , averaged over all cones in all events within a given centrality bin according to:

$$\frac{dn_{\text{ch}}^{\text{UE}}}{dp_T^{\text{ch}}} = \frac{1}{N_{\text{cone}}} \frac{\Delta N_{\text{ch}}^{\text{cone}}(p_T^{\text{ch}}, p_T^{\text{jet}}, \eta^{\text{jet}})}{\Delta p_T^{\text{ch}}}. \quad (5)$$

Here N_{cone} represents the number of background cones having a jet of a given radius above the corresponding p_T^{jet} threshold, and $\Delta N_{\text{ch}}^{\text{cone}}$ represents the number of charged particles in a given p_T^{ch} bin in all such cones evaluated for jets with a given p_T^{jet} and η^{jet} . Not shown in Eq. (5) is a correction factor that was applied to each background cone to correct for the difference in the average UE-particle yield at a given p_T^{ch} between the η position of the cone and η^{jet} , and a separate correction factor to account for the difference in the elliptic flow modulation at the ϕ position of the UE cone and ϕ^{jet} . That correction was based on a parameterization of the p_T^{ch} and centrality dependence of previously measured elliptic flow coefficients, v_2 [23].

By evaluating the UE contribution only from events containing jets included in the analysis, the background automatically has the correct distribution of centralities within a given centrality bin. The $dn_{\text{ch}}^{\text{UE}}/dp_T^{\text{ch}}$ is observed to be independent of p_T^{jet} both in the data and MC simulation. That observation excludes the possibility that the upfeeding of jets in p_T^{jet} due to the finite JER could induce a dependence of the UE on jet p_T . However, such upfeeding was observed to induce in the MC events a p_T^{jet} -independent, but centrality-dependent mismatch between the extracted $dn_{\text{ch}}^{\text{UE}}/dp_T^{\text{ch}}$ and the actual UE contribution to reconstructed jets. That mismatch was found to result from intrinsic correlations between the charged-particle density in the UE and the MC p_T^{jet} error, $\Delta p_T^{\text{jet}} = p_{T\text{rec}}^{\text{jet}} - p_{T\text{true}}^{\text{jet}}$. In particular, jets with positive (negative) Δp_T^{jet} are found to have an UE contribution larger (smaller) than jets with $\Delta p_T^{\text{jet}} \sim 0$. Due to the net upfeeding on the falling jet spectrum, the selection of jets above a given p_T^{jet} threshold causes the UE contribution to be larger than that estimated from the above-described procedure. The average fractional mismatch in the estimated UE background was found to be independent of p_T^{ch} and to vary with centrality by factors between 1.04–1.08, 1.07–1.10, and 1.12–1.15 for $R = 0.2, 0.3$, and 0.4 , respectively. The measured $dn_{\text{ch}}^{\text{UE}}/dp_T^{\text{ch}}$ values in the data were corrected by these same factors before being subtracted.

Two different sets of charged-particle fragmentation distributions were measured for each centrality bin and R value:

$$D^{\text{meas}}(p_T) \equiv \frac{1}{\varepsilon} \left(\frac{1}{N_{\text{jet}}} \frac{\Delta N_{\text{ch}}}{\Delta p_T^{\text{ch}}} - \frac{dn_{\text{ch}}^{\text{UE}}}{dp_T} \right), \quad (6)$$

and

$$D^{\text{meas}}(z) \equiv \frac{1}{\varepsilon} \left(\frac{1}{N_{\text{jet}}} \frac{\Delta N_{\text{ch}}}{\Delta z} - \frac{dn_{\text{ch}}^{\text{UE}}}{dp_T} \Big|_{p_T^{\text{ch}}=zp_T^{\text{jet}}} \right), \quad (7)$$

where N_{jet} represents the total number of jets passing the above-described selection cuts in a given centrality bin, and ΔN_{ch} represents the number of measured charged particles within $\Delta R = 0.4$ of the jets in given bins of p_T^{ch} and z , respectively. The efficiency correction, $1/\varepsilon$, was applied on a per-particle basis using the parameterized MC efficiency, $\varepsilon(p_T, \eta)$, assuming $p_{T\text{true}}^{\text{ch}} = p_{T\text{rec}}^{\text{ch}}$. While

⁴ The ΔR is a boost-invariant replacement for the polar angle θ .

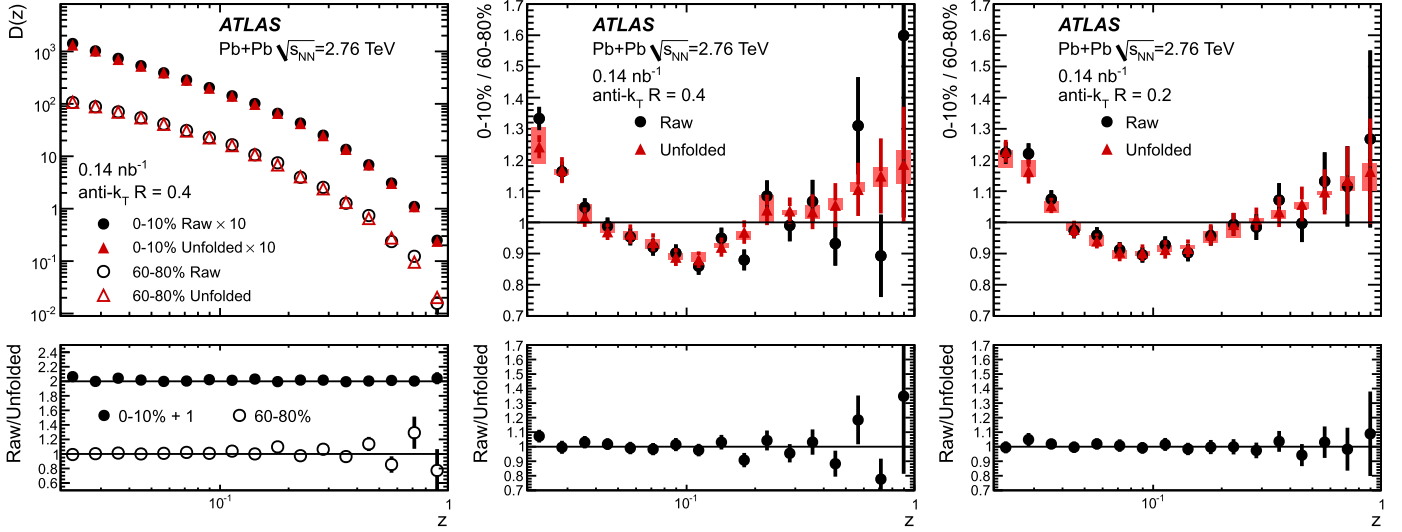


Fig. 3. Measured and unfolded $D(z)$ distributions for $R = 0.4$ and $R = 0.2$ jets in central (0–10%) and peripheral (60–80%) collisions. Top left: $R = 0.4$ $D^{\text{meas}}(z)$ and $D(z)$ distributions, bottom left: ratios of measured to unfolded $R = 0.4$ $D(z)$ distributions with the 0–10% shifted by +1 for clarity. Top middle and right: central-to-peripheral ratios of measured ($R_{D(z)}^{\text{meas}}$) and unfolded ($R_{D(z)}$) distributions for $R = 0.4$ and $R = 0.2$, respectively. Bottom middle and right: ratio of $R_{D(z)}^{\text{meas}}$ to $R_{D(z)}$ for $R = 0.4$ and $R = 0.2$, respectively.

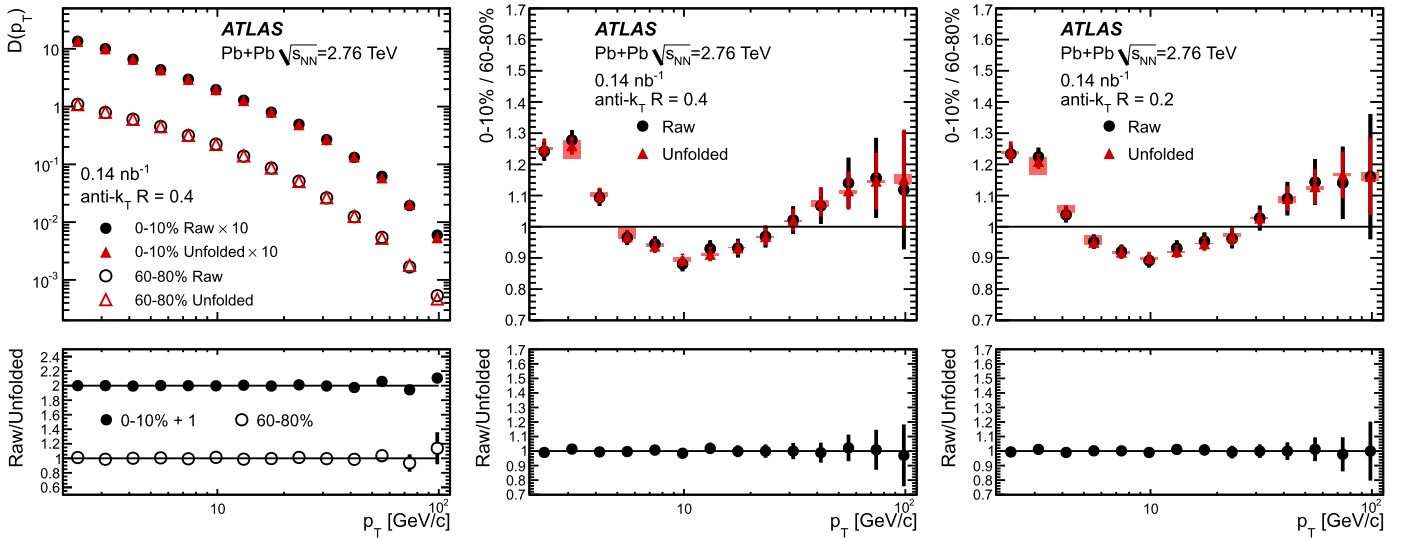


Fig. 4. Measured and unfolded $D(p_T)$ distributions for $R = 0.4$ and $R = 0.2$ jets in central (0–10%) and peripheral (60–80%) collisions. Top left: $R = 0.4$ $D^{\text{meas}}(p_T)$ and $D(p_T)$ distributions, bottom left: ratios of measured to unfolded $R = 0.4$ $D(p_T)$ distributions with the 0–10% shifted by +1 for clarity. Top middle and right: central-to-peripheral ratios of measured ($R_{D(p_T)}^{\text{meas}}$) and unfolded ($R_{D(p_T)}$) distributions for $R = 0.4$ and $R = 0.2$, respectively. Bottom middle and right: ratio of $R_{D(p_T)}^{\text{meas}}$ to $R_{D(p_T)}$ for $R = 0.4$ and $R = 0.2$, respectively.

that assumption is not strictly valid, the efficiency varies sufficiently slowly with $p_{T,\text{true}}^{\text{ch}}$ that the error introduced by this assumption is $\lesssim 1\%$ everywhere.

The measured $D^{\text{meas}}(z)$ distributions for $R = 0.4$ jets in the 0–10% and 60–80% centrality bins are shown in the top left panel in Fig. 3. The top middle panel shows the ratio of $D^{\text{meas}}(z)$ between central (0–10%) and peripheral (60–80%) collisions, $R_{D(z)}^{\text{meas}} \equiv D^{\text{meas}}(z)|_{0-10}/D^{\text{meas}}(z)|_{60-80}$. For comparison, the $D^{\text{meas}}(z)$ ratio is shown on the top right panel for $R = 0.2$ jets. Similar plots are shown in Fig. 4 but for $D^{\text{meas}}(p_T)$. The $D^{\text{meas}}(z)$ ratios for both $R = 0.2$ and $R = 0.4$ indicate an enhanced fragment yield at low z , $z \lesssim 0.04$, in jets in the 0–10% centrality bin compared to jets in the 60–80% centrality bin and a suppressed yield of fragments with $z \sim 0.1$. Similar results are observed in the $D^{\text{meas}}(p_T)$ ratios over the corresponding p_T ranges. The $R = 0.2$ $D^{\text{meas}}(z)$ and the $R = 0.2$ and $R = 0.4$ $D^{\text{meas}}(p_T)$ ratios rise above one for $z \gtrsim 0.2$

or $p_T \gtrsim 25$ GeV. However, the ratios differ from one by only $1-2\sigma(\text{stat})$. No such variations of the $D^{\text{meas}}(z)$ and $D^{\text{meas}}(p_T)$ distributions with centrality as seen in the data are observed in the MC simulation. The central-to-peripheral ratios of MC $D^{\text{meas}}(z)$ and $D^{\text{meas}}(p_T)$ distributions for $R = 0.4$ and $R = 0.2$ jets (not shown) are within 3% of one for all z and p_T .

The $D^{\text{meas}}(p_T)$ and $D^{\text{meas}}(z)$ distributions were unfolded using a one-dimensional Singular Value Decomposition (SVD) method [27] implemented in RooUnfold [28] to remove the effects of charged particle and jet p_T resolution. The SVD method implements a regularized matrix-based unfolding that attempts to “invert” the equation $\mathbf{b} = \mathbf{A}\mathbf{x}$, where \mathbf{x} , is a true spectrum, \mathbf{b} is an observed spectrum, and \mathbf{A} is the “response matrix” that describes the transformation of \mathbf{x} to \mathbf{b} . For $D(p_T)$, the unfolding accounts only for the charged-particle p_T resolution and uses a response matrix derived from the MC data set that describes the distri-

bution of reconstructed p_T^{ch} as a function of MC truth p_T^{ch} . The response matrix $\mathbf{A}(p_T^{\text{ch}}, p_T^{\text{true}})$ is filled using the procedures described in Section 5. The $D(z)$ unfolding simultaneously accounts for both charged particle and jet resolution using a response matrix $\mathbf{A}(z^{\text{rec}}, z^{\text{true}})$ with z^{true} (z^{rec}) calculated using purely truth (fully reconstructed) quantities. A cross-check was performed for the $D(z)$ unfolding that included only the jet energy resolution to ensure that the combination of the two sources of resolution in the one-dimensional unfolding did not distort the result. Because the $D^{\text{meas}}(z)$ and $D^{\text{meas}}(p_T)$ distributions were already corrected for the charged-particle reconstruction efficiency, the response matrices were only populated with truth particles for which a reconstructed particle was obtained and each entry was corrected for reconstruction efficiency so as to not distort the shape of the true distributions.

To ensure that statistical fluctuations in the MC p_T^{jet} or z^{true} distributions do not distort the unfolding, those distributions were smoothed by fitting them to appropriate functional forms. The truth $D(p_T)$ distributions were fit to polynomials in $\ln(p_T)$. The truth $D(z)$ distributions were parameterized using an extension of a standard functional form [29],

$$D(z) = a \cdot z^{d_1} (1 + c - z)^{d_2} \cdot (1 + b \cdot (1 - z)^{d_3}), \quad (8)$$

where a, b, c, d_i were free parameters of the fit. The non-standard additional parameter “ c ” was added to improve the description of the truth distribution at large z . When filling the truth spectra and response matrices, the entries were weighted to match the truth spectra to the fit functions.

The SVD unfolding was performed using a regularization parameter obtained from the ninth singular value ($k = 9$) of the unfolding matrix. Systematic uncertainties in the unfolding due to regularization were evaluated by varying k over the range 5–12 for which the unfolding was observed to be neither significantly biased by regularization nor unstable. The statistical uncertainties in the unfolded spectra were obtained using the pseudo-experiment method [27]. The largest absolute uncertainty obtained over $5 \leq k \leq 12$ was taken to be the statistical uncertainty in the unfolded result.

Unfolded fragmentation functions, $D(z)$, are shown in the top left panel in Fig. 3 and compared to the corresponding $D^{\text{meas}}(z)$ distributions for $R = 0.4$ jets in central (0–10%) and peripheral (60–80%) collisions. Similar results for $D(p_T)$ are shown in Fig. 4. For both figures, the ratios of unfolded to measured distributions are shown in the bottom left panel with the ratio for 0–10% centrality bin offset by +1. Those ratios show that the unfolding has minimal impact on the fragmentation functions in both peripheral and central collisions. Only the largest z point in the 0–10% bin changes by more than 20%.

The middle and top right panels in Fig. 3 (Fig. 4) show for $R = 0.4$ and $R = 0.2$ jets, respectively the ratios of unfolded $D(z)$ ($D(p_T)$) distributions, $R_{D(z)} \equiv D(z)|_{0-10}/D(z)|_{60-80}$ ($R_{D(p_T)} \equiv D(p_T)|_{0-10}/D(p_T)|_{60-80}$), compared to the ratios before unfolding. The unfolding reduces the $D(z)$ ratio slightly at low z but otherwise leaves the shapes unchanged. To evaluate the impact of the unfolding on the difference between central and peripheral fragmentation functions, the middle and bottom right panels in Fig. 3 (Fig. 4) show the ratio of $R_{D(z)}^{\text{meas}}$ ($R_{D(p_T)}^{\text{meas}}$) to $R_{D(z)}$ ($R_{D(p_T)}$). Except for the lowest z point, the ratio is consistent with one over the entire z range. Thus, the features observed in $R_{D(z)}^{\text{meas}}$ ($R_{D(p_T)}^{\text{meas}}$), namely the enhancement at low z (p_T) in central collisions relative to peripheral collisions, the suppression at intermediate z (p_T), and the rise above one at large z (p_T) are robust with respect to the effects of the charged particle and jet p_T resolution.

7. Systematic uncertainties

Systematic uncertainties in the unfolded $D(z)$ and $D(p_T)$ distributions can arise due to uncertainties in the jet energy scale and jet energy resolution, from systematic uncertainties in the unfolding procedure including uncertainties in the shape of the truth distributions, uncertainties in the charged particle reconstruction, and from the UE subtraction procedure.

The systematic uncertainty due to the jet energy scale (JES) has two contributions, an absolute JES uncertainty and an uncertainty in the variation of the JES from peripheral to more central collisions. The absolute JES uncertainty was determined by shifting the transverse momentum of the reconstructed jets according to the evaluation of the jet energy scale uncertainty in Ref. [30]. The typical size of the JES uncertainty for jets used in this study is 2%. The shift in the JES has negligible impact on the ratios between central and peripheral events of $D(p_T)$ and $D(z)$ distributions whereas it has a clear impact on the $D(p_T)$ and $D(z)$ distributions. At high p_T or z the resulting uncertainty reaches 15%. The evaluation of centrality-dependent uncertainty on JES uses the estimates from Ref. [14]. The centrality-dependent JES uncertainty is largest for the most central collisions where it reaches 1.5%. The evaluation of the jet energy resolution (JER) uncertainty follows the procedure applied in proton–proton jet measurements [31]. The typical size of JER uncertainty for jets used in the study is less than 2%. This uncertainty is centrality independent since the dijets in MC are overlaid to real data. The resulting combined systematic uncertainty from JER and centrality-dependent JES on the ratios reaches 6% at high p_T and 10% at high z and it has a similar size in the case of $D(p_T)$ or $D(z)$ distributions as in the case of their ratios.

The systematic uncertainty associated with the unfolding is connected with the sensitivity of the unfolding procedure to the choice of regularization parameter and to the parameterization of the truth distribution. The uncertainty due to the choice of regularization parameter was evaluated by varying k over the range 5–12. The typical systematic uncertainty is found to be smaller than 3% or 2% for the $D(z)$ or $D(p_T)$, respectively. The systematic uncertainty due to the parameterization of the truth distribution was determined from the statistical uncertainties of the fits to these distributions. This systematic uncertainty is below 1% or 2% for the $D(z)$ or $D(p_T)$, respectively.

The estimate of systematic uncertainty due to the tracking efficiency follows methods of the inclusive charged particle measurement [23]. The uncertainty is quantified using the error of the fit of tracking efficiency and by varying the tracking selection criteria. In the intermediate- p_T region the systematic uncertainty is less than 2%. In the low and high p_T region the systematic uncertainty is larger, but less than 8%.

An independent evaluation of potential systematic uncertainties in the central-to-peripheral ratios of $D(z)$ and $D(p_T)$, due to all aspects of the analysis, was obtained by evaluating the deviation from unity of the MC central (0–10%) to peripheral (60–80%) ratios of the fragmentation functions. Since there is no jet quenching employed in MC simulation, the ratios are expected not to show any deviation from unity. No deviation from unity is indeed observed, the largest localized deviation is $\lesssim 4\%$. To quantify the deviations from unity, the MC $R_{D(z)}$ and $R_{D(p_T)}$ ratios were fit by piecewise continuous functions composed of linear functions defined over the z (p_T) ranges $z = 0.02$ – 0.06 ($p_T = 2$ – 6 GeV), $z = 0.06$ – 0.3 ($p_T = 6$ – 30 GeV), and $z > 0.3$ ($p_T > 30$ GeV) with parameters constrained such that the linear functions match at the boundaries. The resulting fits are used as estimates of the systematic uncertainties on all measured $R_{D(z)}$ and $R_{D(p_T)}$ ratios reported in Section 8. This systematic uncertainty is certainly correlated with and may overlap with other systematic uncertainties described above.

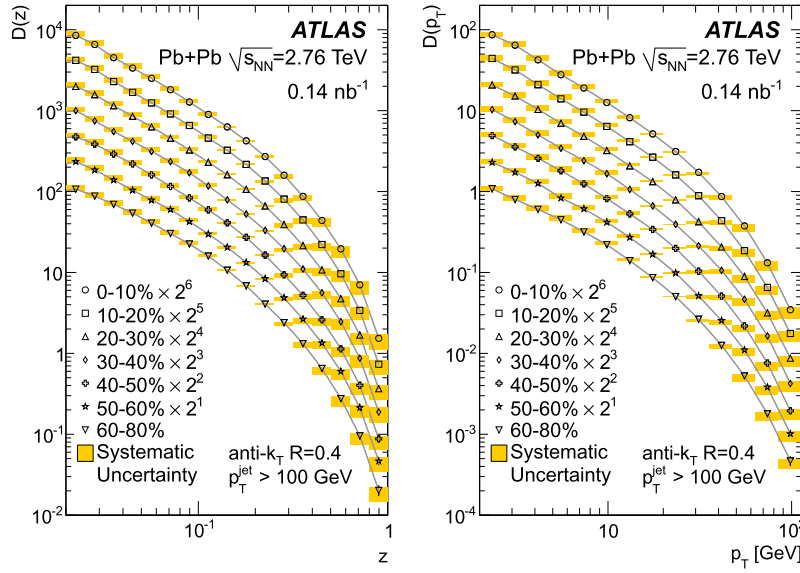


Fig. 5. Unfolded $R = 0.4$ longitudinal charged particle fragmentation function, $D(z)$ and the charged particle transverse momentum distribution, $D(p_T)$, for the seven centrality bins included in this analysis. The statistical uncertainties are everywhere smaller than the points. The yellow shaded error bars indicate systematic uncertainties. Grey lines connecting the central values of distributions are to guide the eye. (For interpretation of the references to color in this figure legend, the reader is referred to the web version of this article.)

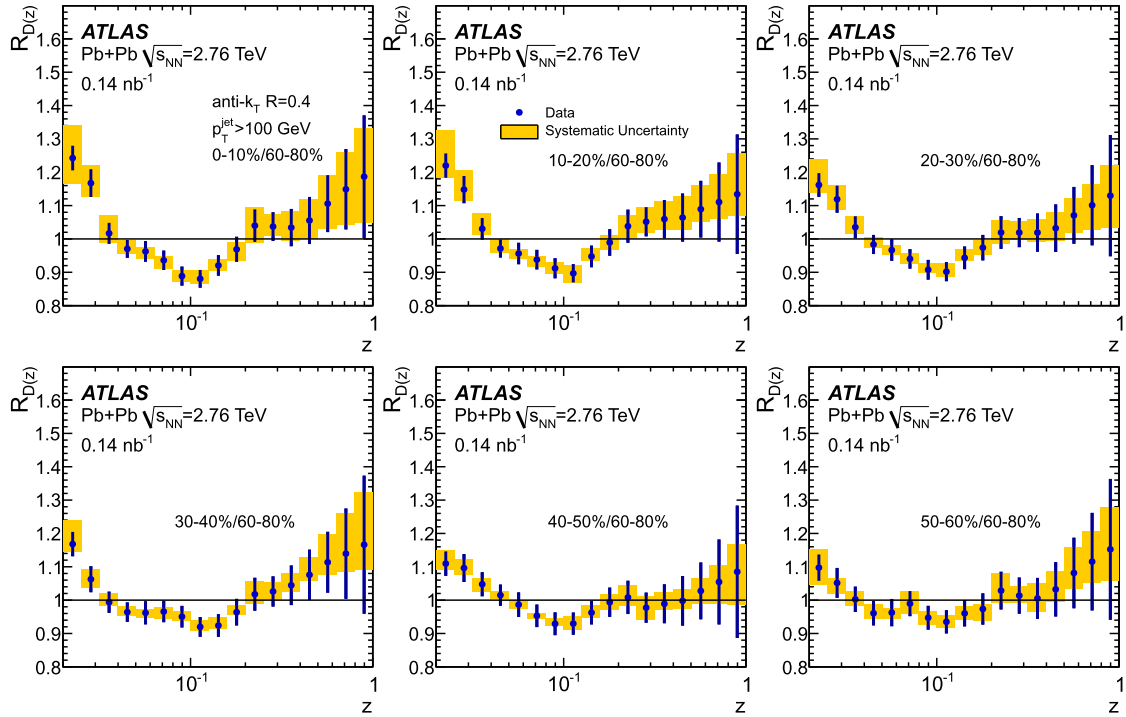


Fig. 6. Ratios of $D(z)$ for six bins in collision centrality to those in peripheral (60–80%) collisions, $D(z)_{\text{cent}}/D(z)_{60-80}$, for $R = 0.4$ jets. The error bars on the data points indicate statistical uncertainties while the yellow shaded bands indicate systematic uncertainties. (For interpretation of the references to color in this figure legend, the reader is referred to the web version of this article.)

8. Results

The unfolded fragmentation functions, $D(z)$ and $D(p_T)$, for $R = 0.4$ jets are shown in Fig. 5 for the seven centrality bins included in the analysis with the distributions for different centralities multiplied by successive values of two for presentation purposes. The shaded error bands indicate systematic uncertainties as discussed in the previous section. The $D(p_T)$ and $D(z)$ distributions have

similar shapes that are characteristic of fragmentation functions with a steep drop at the endpoint.

To evaluate the centrality dependence of the fragmentation functions, ratios were calculated of the $R = 0.4$ $D(z)$ distributions for all centrality bins excluding the peripheral bin to the $D(z)$ measured in the peripheral, 60–80% centrality bin. The results are shown in Fig. 6. The ratios for all centralities show an enhanced yield of low z fragments and a suppressed yield of fragments at

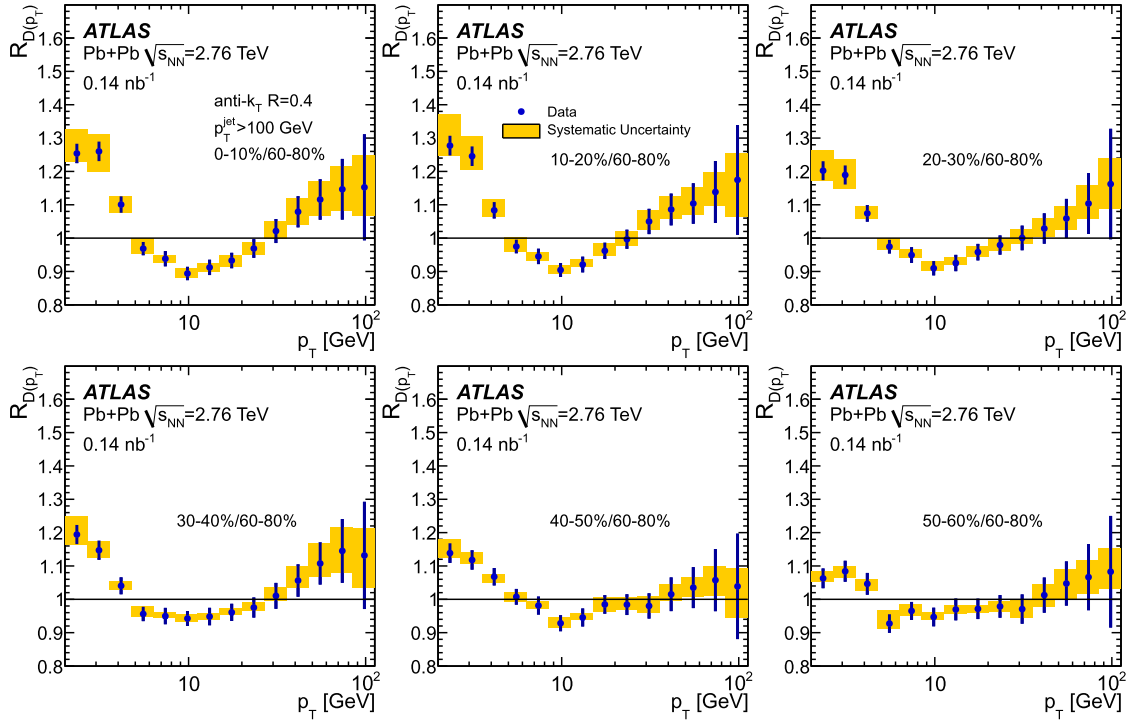


Fig. 7. Ratios of unfolded $D(p_T)$ distributions for six bins in collision centrality to those in peripheral (60–80%) collisions, $D(p_T)|_{\text{cent}}/D(p_T)|_{60-80}$, for $R = 0.4$ jets. The error bars on the data points indicate statistical uncertainties while the yellow shaded bands indicate systematic uncertainties. (For interpretation of the references to color in this figure legend, the reader is referred to the web version of this article.)

intermediate z values in more central collisions relative to the 60–80% centrality bin. For the 0–10% centrality bin, the yield of fragments at $z = 0.02$ is enhanced relative to that in the 60–80% centrality bin by 25% while the yield at $z = 0.1$ is suppressed by about 10%. The size of the observed modifications at low, intermediate, and high z decreases gradually from central to peripheral collisions.

The statistical and systematic uncertainties on $R_{D(z)}$ grow as $z \rightarrow 1$ due to the statistical fluctuations on the $D(z)$ distributions at large z and due to the sensitivity of the steeply falling $D(z)$ distributions to JER and JES systematic uncertainties. The results in Fig. 6 show central values for $R_{D(z)}$ above one at high z for the 0–10% through the 30–40% centrality bins but the $R_{D(z)}$ values differ from one by typically 1σ (stat). Fig. 7 shows ratios of $R = 0.4$ $D(p_T)$ distributions from non-peripheral centrality bins to those in the peripheral, 60–80% centrality bin. The ratios in the figure show the same features as the $D(z)$ ratios, namely an enhancement at low p_T , a suppression at intermediate p_T , and an increase above one at large p_T that is more significant than that seen for $D(z)$. The magnitudes of the deviations from one in the $D(z)$ and $D(p_T)$ ratios are similar in the low, intermediate, and high z and p_T regions. This demonstrates that the modifications observed in Fig. 6 do not result from distortions of the z measurement due to JER and JES.

To further demonstrate that the centrality-dependent modifications observed in $D(z)$ and $D(p_T)$ do not result from unknown UE effects not included in the systematic uncertainties, Fig. 8 shows ratios of $D(z)$ and $D(p_T)$ distributions between central (0–10%) and peripheral (60–80%) collisions for $R = 0.2$ and $R = 0.3$ jets. The fluctuations in the UE are a factor of approximately 100% (30%) smaller for $R = 0.2$ ($R = 0.3$) jets than they are for $R = 0.4$ jets. Nonetheless, the features seen in the $R = 0.4$ $D(z)$ or $D(p_T)$ ratios are also present in the $R = 0.2$ and $R = 0.3$ ratios with the same magnitudes. Due to the reduced systematic uncertainties on $D(z)$ and $D(p_T)$ for $R = 0.2$ and $R = 0.3$ jets compared to $R = 0.4$ jets,

the enhancement in the fragmentation functions at large z or p_T in central collisions is more significant for the smaller jet sizes.

9. Discussion

To quantify the effects of the modifications observed in Fig. 8 on the actual distribution of fragments within the measured jets, the differences in fragmentation functions, $\Delta D(z) = D(z)|_{\text{cent}} - D(z)|_{60-80}$ were calculated and integrals of these distributions, $\int \Delta D(z) dz$ taken over three z ranges chosen to match the observations: 0.02–0.04, 0.04–0.2, and 0.4–1. The last interval was chosen to focus on the region where $R_{D(z)} > 1$. The results are given in Tables 3 and 4 for $R = 0.3$ and $R = 0.2$ jets, respectively. Similar results were obtained for $R = 0.4$ jets but with larger uncertainties. The results presented in the tables indicate an increase in the number of particles with $0.02 < z < 0.04$ of less than one particle per jet in the 0–10% centrality bin relative to the 60–80% centrality bin. A decrease of about 1.5 particles per jet is observed for $0.04 < z < 0.2$. The differences between the integrals of the fragmentation functions over $0.4 < z < 1$ are not significant relative to the uncertainties. The results for $\int \Delta D(z) dz$ shown in the two tables indicate that in the most central collisions a small fraction, $< 2\%$, of the jet transverse momentum is carried by the excess particles in $0.02 < z < 0.04$ for central collisions, but that the depletion in fragment yield in $0.04 < z < 0.2$ accounts on average for about 14% of p_T^{jet} .

To better evaluate the significance of the increase in $R_{D(z)}$ and $R_{D(p_T)}$ above one at large z or p_T , average $R_{D(z)}$ and $R_{D(p_T)}$ ratios were calculated by summing the central and peripheral $D(z)$ or $D(p_T)$ distributions over different regions corresponding to the last n points in the measured distributions, $n = 2-6$. For each resulting average ratio, $\bar{R}_{D(z)}$ or $\bar{R}_{D(p_T)}$, the significance of the deviation from one was evaluated as $(\bar{R}_{D(z)} - 1)/\sigma(\bar{R}_{D(z)})$ or $(\bar{R}_{D(p_T)} - 1)/\sigma(\bar{R}_{D(p_T)})$ where σ represents the combined

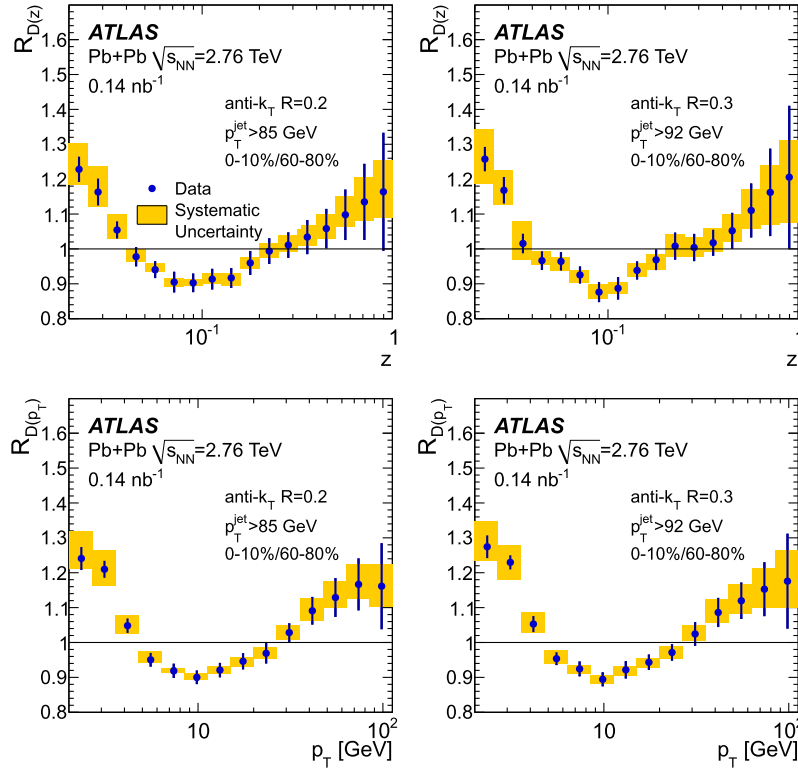


Fig. 8. Ratios of unfolded fragmentation functions, $D(z)$ (top) and $D(p_T)$ (bottom), for central (0–10%) collisions to those in peripheral (60–80%) collisions for $R = 0.2$ (left) and $R = 0.3$ (right) jets. The fragmentation functions were evaluated using charged hadrons within $\Delta R = 0.4$ of the jet axis. The error bars on the data points indicate statistical uncertainties while the yellow shaded bands indicate systematic uncertainties. (For interpretation of the references to color in this figure legend, the reader is referred to the web version of this article.)

Table 3

Differences of $D(z)$ distributions in different centralities with respect to peripheral events for $R = 0.3$ jets. The errors represent combined statistical and systematic uncertainties.

Centrality	$z = 0.02-0.04$		$z = 0.04-0.2$		$z = 0.4-1.0$	
	$\int \Delta D(z)dz$	$\int z \Delta D(z)dz$	$\int \Delta D(z)dz$	$\int z \Delta D(z)dz$	$\int \Delta D(z)dz$	$\int z \Delta D(z)dz$
0–10%	$0.79^{+0.19}_{-0.25}$	$0.020^{+0.005}_{-0.007}$	$-1.7^{+0.6}_{-0.8}$	$-0.14^{+0.04}_{-0.06}$	$0.06^{+0.05}_{-0.04}$	$0.033^{+0.026}_{-0.021}$
10–20%	$0.66^{+0.17}_{-0.18}$	$0.016^{+0.005}_{-0.005}$	$-1.6^{+0.7}_{-0.8}$	$-0.12^{+0.05}_{-0.06}$	$0.05^{+0.05}_{-0.04}$	$0.029^{+0.026}_{-0.021}$
20–30%	$0.52^{+0.13}_{-0.18}$	$0.013^{+0.004}_{-0.005}$	$-1.3^{+0.6}_{-0.6}$	$-0.12^{+0.04}_{-0.04}$	$0.04^{+0.04}_{-0.04}$	$0.025^{+0.024}_{-0.020}$
30–40%	$0.39^{+0.12}_{-0.17}$	$0.009^{+0.004}_{-0.005}$	$-1.3^{+0.6}_{-0.7}$	$-0.10^{+0.04}_{-0.05}$	$0.06^{+0.04}_{-0.04}$	$0.036^{+0.020}_{-0.019}$
40–50%	$0.38^{+0.11}_{-0.15}$	$0.009^{+0.003}_{-0.004}$	$-0.6^{+0.6}_{-0.8}$	$-0.07^{+0.04}_{-0.06}$	$-0.01^{+0.04}_{-0.04}$	$-0.005^{+0.024}_{-0.021}$
50–60%	$0.28^{+0.15}_{-0.21}$	$0.006^{+0.004}_{-0.006}$	$-1.2^{+0.9}_{-0.7}$	$-0.08^{+0.06}_{-0.06}$	$0.04^{+0.04}_{-0.04}$	$0.025^{+0.021}_{-0.021}$

Table 4

Differences of $D(z)$ distributions in different centralities with respect to peripheral events for $R = 0.2$ jets. The errors represent combined statistical and systematic uncertainties.

Centrality	$z = 0.02-0.04$		$z = 0.04-0.2$		$z = 0.4-1.0$	
	$\int \Delta D(z)dz$	$\int z \Delta D(z)dz$	$\int \Delta D(z)dz$	$\int z \Delta D(z)dz$	$\int \Delta D(z)dz$	$\int z \Delta D(z)dz$
0–10%	$0.65^{+0.21}_{-0.20}$	$0.017^{+0.006}_{-0.005}$	$-1.7^{+0.5}_{-0.6}$	$-0.14^{+0.04}_{-0.05}$	$0.07^{+0.05}_{-0.04}$	$0.037^{+0.030}_{-0.022}$
10–20%	$0.60^{+0.16}_{-0.16}$	$0.016^{+0.005}_{-0.004}$	$-1.6^{+0.7}_{-0.7}$	$-0.12^{+0.05}_{-0.05}$	$0.08^{+0.05}_{-0.04}$	$0.046^{+0.029}_{-0.025}$
20–30%	$0.48^{+0.11}_{-0.14}$	$0.013^{+0.003}_{-0.004}$	$-1.6^{+0.6}_{-0.5}$	$-0.13^{+0.04}_{-0.04}$	$0.04^{+0.05}_{-0.04}$	$0.026^{+0.029}_{-0.024}$
30–40%	$0.44^{+0.11}_{-0.15}$	$0.011^{+0.003}_{-0.004}$	$-1.4^{+0.6}_{-0.7}$	$-0.11^{+0.05}_{-0.05}$	$0.07^{+0.04}_{-0.05}$	$0.044^{+0.021}_{-0.028}$
40–50%	$0.33^{+0.09}_{-0.14}$	$0.009^{+0.003}_{-0.004}$	$-1.0^{+0.6}_{-0.8}$	$-0.09^{+0.04}_{-0.06}$	$-0.03^{+0.05}_{-0.04}$	$-0.011^{+0.030}_{-0.020}$
50–60%	$0.27^{+0.12}_{-0.18}$	$0.007^{+0.003}_{-0.005}$	$-1.0^{+0.8}_{-0.7}$	$-0.07^{+0.06}_{-0.06}$	$0.04^{+0.04}_{-0.05}$	$0.027^{+0.024}_{-0.029}$

statistical and systematic uncertainty. Because there is significant cancellation of systematic uncertainties in the ratios, this analysis provides a more sensitive evaluation of the significance of the large- z excess. For $R = 0.4$ jets the combined $R_{D(z)}$ ($R_{D(p_T)}$), differs from one by approximately 1σ (1.5σ) for any of the n values. For $R = 0.2$ jets, $R_{D(z)}$ differs from 1 by approximately 1.5σ for all n values, while $R_{D(p_T)}$ differs from one by 2σ for $n = 3$ –6 corresponding to $p_T > 47.5$ GeV through $p_T > 20$ GeV. The greater significance of the deviations of the $R = 0.2$ $R_{D(p_T)}$ relative to the $R = 0.2$ $R_{D(z)}$ and the $R = 0.4$ $R_{D(z)}$ and $R_{D(p_T)}$ can be attributed to the reduced role of the jet energy resolution in influencing the measurement of the central-to-peripheral ratios for large hadron momenta.

Theoretical predictions for medium modifications of fragmentation functions based on radiative energy loss [32–35] have generally predicted substantial reduction in the yield of high p_T , or large- z fragments and an enhancement at low p_T or low z . The predicted reduction at large z generically results from the radiative energy loss of the leading partons in the shower and the resulting redistribution of the jet energy to lower z hadrons. Instead of a reduction, an enhanced yield of high z fragments is seen in the data. However, the difference between observed behaviour at large z and expectations from theoretical calculations may be at least partially attributed to the fact that the fragmentation functions presented in this paper were evaluated with respect to the energies of quenched jets. In contrast, theoretical analyses of the fragmentation functions of quenched jets are typically evaluated in terms of the initial, unquenched jet energies. However, some recent theoretical analyses [36,37] of jet fragmentation functions using quenched jet energies have shown that jet quenching calculations can reproduce the general features observed in the results presented in this Letter. In addition to direct modifications of the fragmentation function due to quenching, the quenching may indirectly alter the fragmentation function of inclusive jets by altering the relative fraction of quarks and gluons.

The simultaneous effects of quenching on the hadron constituents of jets and the measured jet energies may explain a relative increase of experimental fragmentation functions in central collisions at large z as suggested by the data. Jets that fragment to large- z hadrons may lose less energy than typical jets due to reduced formation or colour-neutralization time [38]. Thus, the fragmentation function measured for inclusive jets may have a higher proportion of jets with large- z hadrons. The results in Ref. [36] indicate such an effect that is qualitatively similar to the data.

10. Conclusions

This Letter has presented measurements by ATLAS of charged-particle fragmentation functions in jets produced in $\sqrt{s_{NN}} = 2.76$ TeV Pb+Pb collisions at the LHC. The measurements were performed using a data set recorded in 2011 with an integrated luminosity of 0.14 nb^{-1} . Jets were reconstructed with the anti- k_t algorithm for distance parameters $R = 0.2, 0.3$, and 0.4 , and the contributions of the underlying event to the jet kinematics and the jet fragment distributions were subtracted. Jet fragments were measured within an angular range $\Delta R = 0.4$ from the jet axes for all three jet sizes. Distributions of per-jet charged-particle transverse momentum, $D(p_T)$, and longitudinal momentum fraction, $D(z)$, were presented for seven bins in collision centrality for jet $p_T > 85, 92$, and 100 GeV, respectively, for $R = 0.2$, $R = 0.3$, and $R = 0.4$ jets. Ratios of fragmentation functions in the different centrality bins to the 60–80% bin were presented and used to evaluate the medium modifications of jet fragmentation. Those ratios show an enhancement in fragment yield in

central collisions for $z \lesssim 0.04$, a reduction in fragment yield for $0.04 \lesssim z \lesssim 0.2$ and an enhancement in the fragment yield for $z > 0.4$. The modifications decrease monotonically with decreasing collision centrality from 0–10% to 50–60%. A similar set of modifications is observed in the $D(p_T)$ distributions over corresponding p_T ranges.

Acknowledgements

We thank CERN for the very successful operation of the LHC, as well as the support staff from our institutions without whom ATLAS could not be operated efficiently.

We acknowledge the support of ANPCyT, Argentina; YerPhI, Armenia; ARC, Australia; BMWFW and FWF, Austria; ANAS, Azerbaijan; SSTC, Belarus; CNPq and FAPESP, Brazil; NSERC, NRC and CFI, Canada; CERN; CONICYT, Chile; CAS, MOST and NSFC, China; COLCIENCIAS, Colombia; MSMT CR, MPO CR and VSC CR, Czech Republic; DNRF, DNSRC and Lundbeck Foundation, Denmark; EPLANET, ERC and NSRF, European Union; IN2P3-CNRS, CEA-DSM/IRFU, France; GNSF, Georgia; BMBF, DFG, HGF, MPG and AvH Foundation, Germany; GSRT and NSRF, Greece; ISF, MINERVA, GIF, I-CORE and Benoziyo Center, Israel; INFN, Italy; MEXT and JSPS, Japan; CNRST, Morocco; FOM and NWO, Netherlands; BRF and RCN, Norway; MNiSW and NCN, Poland; GRICES and FCT, Portugal; MNE/IFA, Romania; MES of Russia and ROSATOM, Russian Federation; JINR; MSTB, Serbia; MSSR, Slovakia; ARRS and MIZŠ, Slovenia; DST/NRF, South Africa; MINECO, Spain; SRC and Wallenberg Foundation, Sweden; SER, SNSF and Cantons of Bern and Geneva, Switzerland; NSC, Taiwan; TAEK, Turkey; STFC, the Royal Society and Leverhulme Trust, United Kingdom; DOE and NSF, United States of America.

The crucial computing support from all WLCG partners is acknowledged gratefully, in particular from CERN and the ATLAS Tier-1 facilities at TRIUMF (Canada), NDGF (Denmark, Norway, Sweden), CC-IN2P3 (France), KIT/GridKA (Germany), INFN-CNAF (Italy), NL-T1 (Netherlands), PIC (Spain), ASGC (Taiwan), RAL (UK) and BNL (USA) and in the Tier-2 facilities worldwide.

References

- [1] A. Majumder, M. Van Leeuwen, *Prog. Part. Nucl. Phys.* **66** (2011) 41–92, arXiv:1002.2206.
- [2] Y. Mehtar-Tani, J.G. Milhano, K. Tywoniuk, *Int. J. Mod. Phys. A* **28** (2013) 1340013, arXiv:1302.2579.
- [3] N. Armesto, B. Cole, C. Gale, W.A. Horowitz, P. Jacobs, et al., *Phys. Rev. C* **86** (2012) 064904, arXiv:1106.1106.
- [4] G.-Y. Qin, B. Muller, *Phys. Rev. Lett.* **106** (2011) 162302, arXiv:1012.5280.
- [5] G. Ovanessian, I. Vitev, *Phys. Lett. B* **706** (2012) 371–378, arXiv:1109.5619.
- [6] J. Casalderrey-Solana, J. Milhano, U. Wiedemann, *J. Phys. G* **38** (2011) 124086, arXiv:1107.1964.
- [7] J. Casalderrey-Solana, Y. Mehtar-Tani, C.A. Salgado, K. Tywoniuk, *Phys. Lett. B* **725** (2013) 357–360, arXiv:1210.7765.
- [8] J.-P. Blaizot, E. Iancu, Y. Mehtar-Tani, *Phys. Rev. Lett.* **111** (2013) 052001, arXiv:1301.6102.
- [9] J. Casalderrey-Solana, D.C. Gulhan, J.G. Milhano, D. Pablos, K. Rajagopal, *J. High Energy Phys.* **1410** (2014) 19, arXiv:1405.3864.
- [10] ATLAS Collaboration, *Phys. Rev. Lett.* **105** (2010) 252303, arXiv:1011.6182.
- [11] CMS Collaboration, *Phys. Rev. C* **84** (2011) 024906, arXiv:1102.1957.
- [12] CMS Collaboration, *Phys. Lett. B* **712** (2012) 176–197, arXiv:1202.5022.
- [13] CMS Collaboration, *Phys. Lett. B* **718** (2013) 773, arXiv:1205.0206.
- [14] ATLAS Collaboration, *Phys. Lett. B* **719** (2013) 220–241, arXiv:1208.1967.
- [15] ALICE Collaboration, *J. High Energy Phys.* **1403** (2014) 013, arXiv:1311.0633.
- [16] T. Renk, *Phys. Rev. C* **85** (2012) 064908, arXiv:1202.4579.
- [17] M. Cacciari, G.P. Salam, G. Soyez, *J. High Energy Phys.* **0804** (2008) 063, arXiv:0802.1189.
- [18] CMS Collaboration, *J. High Energy Phys.* **1210** (2012) 087, arXiv:1205.5872.
- [19] CMS Collaboration, *Phys. Rev. C* **90** (2014) 024908, arXiv:1406.0932.
- [20] ATLAS Collaboration, *J. Instrum.* **3** (2008) S08003.
- [21] ATLAS Collaboration, *J. High Energy Phys.* **1009** (2010) 056, arXiv:1005.5254.
- [22] ATLAS Collaboration, *Phys. Lett. B* **688** (2010) 21–42, arXiv:1003.3124.
- [23] ATLAS Collaboration, *Phys. Lett. B* **707** (2012) 330–348, arXiv:1108.6018.

- [24] ATLAS Collaboration, Eur. Phys. J. C 70 (2010) 823–874, arXiv:1005.4568.
- [25] T. Sjostrand, S. Mrenna, P.Z. Skands, J. High Energy Phys. 0605 (2006) 026, arXiv:hep-ph/0603175.
- [26] S. Agostinelli, et al., Nucl. Instrum. Methods Phys. Res., Sect. A, Accel. Spectrom. Detect. Assoc. Equip. 506 (2003) 250–303.
- [27] A. Hocker, V. Kartvelishvili, Nucl. Instrum. Methods Phys. Res., Sect. A, Accel. Spectrom. Detect. Assoc. Equip. 372 (1996) 469–481, arXiv:hep-ph/9509307.
- [28] <http://hepunix.rlac.uk/~adye/software/unfold/RooUnfold.html>.
- [29] D. Florian, R. Sassot, M. Stratmann, Phys. Rev. D 76 (2007) 074033, arXiv:0707.1506.
- [30] ATLAS Collaboration, Eur. Phys. J. C 73 (2013) 2304, arXiv:1112.6426.
- [31] ATLAS Collaboration, Eur. Phys. J. C 73 (2013) 2306, arXiv:1210.6210.
- [32] N. Borghini, U.A. Wiedemann, arXiv:hep-ph/0506218.
- [33] N. Armesto, L. Cunqueiro, C.A. Salgado, W.-C. Xiang, J. High Energy Phys. 0802 (2008) 048, arXiv:0710.3073.
- [34] N. Armesto, L. Cunqueiro, C.A. Salgado, Eur. Phys. J. C 63 (2009) 679–690, arXiv:0907.1014.
- [35] T. Renk, Phys. Rev. C 79 (2009) 054906, arXiv:0901.2818.
- [36] K.C. Zapp, F. Krauss, U.A. Wiedemann, J. High Energy Phys. 1303 (2013) 080, arXiv:1212.1599.
- [37] D.E. Kharzeev, F. Loshaj, Phys. Rev. D 87 (2013) 077501, arXiv:1212.5857.
- [38] B. Kopeliovich, F. Niedermayer, Sov. J. Nucl. Phys. 42 (1985) 504.

ATLAS Collaboration

G. Aad⁸⁴, B. Abbott¹¹², J. Abdallah¹⁵², S. Abdel Khalek¹¹⁶, O. Abdinov¹¹, R. Aben¹⁰⁶, B. Abi¹¹³, M. Abolins⁸⁹, O.S. AbouZeid¹⁵⁹, H. Abramowicz¹⁵⁴, H. Abreu¹⁵³, R. Abreu³⁰, Y. Abulaiti^{147a,147b}, B.S. Acharya^{165a,165b,a}, L. Adamczyk^{38a}, D.L. Adams²⁵, J. Adelman¹⁷⁷, S. Adomeit⁹⁹, T. Adye¹³⁰, T. Agatonovic-Jovin^{13a}, J.A. Aguilar-Saavedra^{125a,125f}, M. Agustoni¹⁷, S.P. Ahlen²², F. Ahmadov^{64,b}, G. Aielli^{134a,134b}, H. Akerstedt^{147a,147b}, T.P.A. Åkesson⁸⁰, G. Akimoto¹⁵⁶, A.V. Akimov⁹⁵, G.L. Alberghi^{20a,20b}, J. Albert¹⁷⁰, S. Albrand⁵⁵, M.J. Alconada Verzini⁷⁰, M. Aleksa³⁰, I.N. Aleksandrov⁶⁴, C. Alexa^{26a}, G. Alexander¹⁵⁴, G. Alexandre⁴⁹, T. Alexopoulos¹⁰, M. Alhroob^{165a,165c}, G. Alimonti^{90a}, L. Alio⁸⁴, J. Alison³¹, B.M.M. Allbrooke¹⁸, L.J. Allison⁷¹, P.P. Allport⁷³, J. Almond⁸³, A. Aloisio^{103a,103b}, A. Alonso³⁶, F. Alonso⁷⁰, C. Alpigiani⁷⁵, A. Altheimer³⁵, B. Alvarez Gonzalez⁸⁹, M.G. Alviggi^{103a,103b}, K. Amako⁶⁵, Y. Amaral Coutinho^{24a}, C. Amelung²³, D. Amidei⁸⁸, S.P. Amor Dos Santos^{125a,125c}, A. Amorim^{125a,125b}, S. Amoroso⁴⁸, N. Amram¹⁵⁴, G. Amundsen²³, C. Anastopoulos¹⁴⁰, L.S. Ancu⁴⁹, N. Andari³⁰, T. Andeen³⁵, C.F. Anders^{58b}, G. Anders³⁰, K.J. Anderson³¹, A. Andreazza^{90a,90b}, V. Andrei^{58a}, X.S. Anduaga⁷⁰, S. Angelidakis⁹, I. Angelozzi¹⁰⁶, P. Anger⁴⁴, A. Angerami³⁵, F. Anghinolfi³⁰, A.V. Anisenkov¹⁰⁸, N. Anjos^{125a}, A. Annovi⁴⁷, A. Antonaki⁹, M. Antonelli⁴⁷, A. Antonov⁹⁷, J. Antos^{145b}, F. Anulli^{133a}, M. Aoki⁶⁵, L. Aperio Bella¹⁸, R. Apolle^{119,c}, G. Arabidze⁸⁹, I. Aracena¹⁴⁴, Y. Arai⁶⁵, J.P. Araque^{125a}, A.T.H. Arce⁴⁵, J.-F. Arguin⁹⁴, S. Argyropoulos⁴², M. Arik^{19a}, A.J. Armbruster³⁰, O. Arnaez³⁰, V. Arnal⁸¹, H. Arnold⁴⁸, M. Arratia²⁸, O. Arslan²¹, A. Artamonov⁹⁶, G. Artoni²³, S. Asai¹⁵⁶, N. Asbah⁴², A. Ashkenazi¹⁵⁴, B. Åsman^{147a,147b}, L. Asquith⁶, K. Assamagan²⁵, R. Astalos^{145a}, M. Atkinson¹⁶⁶, N.B. Atlay¹⁴², B. Auerbach⁶, K. Augsten¹²⁷, M. Auresseau^{146b}, G. Avolio³⁰, G. Azuelos^{94,d}, Y. Azuma¹⁵⁶, M.A. Baak³⁰, A. Baas^{58a}, C. Bacci^{135a,135b}, H. Bachacou¹³⁷, K. Bachas¹⁵⁵, M. Backes³⁰, M. Backhaus³⁰, J. Backus Mayes¹⁴⁴, E. Badescu^{26a}, P. Bagiacchi^{133a,133b}, P. Bagnaia^{133a,133b}, Y. Bai^{33a}, T. Bain³⁵, J.T. Baines¹³⁰, O.K. Baker¹⁷⁷, P. Balek¹²⁸, F. Balli¹³⁷, E. Banas³⁹, Sw. Banerjee¹⁷⁴, A.A.E. Bannoura¹⁷⁶, V. Bansal¹⁷⁰, H.S. Bansil¹⁸, L. Barak¹⁷³, S.P. Baranov⁹⁵, E.L. Barberio⁸⁷, D. Barberis^{50a,50b}, M. Barbero⁸⁴, T. Barillari¹⁰⁰, M. Barisonzi¹⁷⁶, T. Barklow¹⁴⁴, N. Barlow²⁸, B.M. Barnett¹³⁰, R.M. Barnett¹⁵, Z. Barnovska⁵, A. Baroncelli^{135a}, G. Barone⁴⁹, A.J. Barr¹¹⁹, F. Barreiro⁸¹, J. Barreiro Guimarães da Costa⁵⁷, R. Bartoldus¹⁴⁴, A.E. Barton⁷¹, P. Bartos^{145a}, V. Bartsch¹⁵⁰, A. Bassalat¹¹⁶, A. Basye¹⁶⁶, R.L. Bates⁵³, J.R. Batley²⁸, M. Battaglia¹³⁸, M. Battistin³⁰, F. Bauer¹³⁷, H.S. Bawa^{144,e}, T. Beau⁷⁹, P.H. Beauchemin¹⁶², R. Beccherle^{123a,123b}, P. Bechtel²¹, H.P. Beck¹⁷, K. Becker¹⁷⁶, S. Becker⁹⁹, M. Beckingham¹⁷¹, C. Becot¹¹⁶, A.J. Beddall^{19c}, A. Beddall^{19c}, S. Bedikian¹⁷⁷, V.A. Bednyakov⁶⁴, C.P. Bee¹⁴⁹, L.J. Beemster¹⁰⁶, T.A. Beermann¹⁷⁶, M. Begel²⁵, K. Behr¹¹⁹, C. Belanger-Champagne⁸⁶, P.J. Bell⁴⁹, W.H. Bell⁴⁹, G. Bella¹⁵⁴, L. Bellagamba^{20a}, A. Bellerive²⁹, M. Bellomo⁸⁵, K. Belotskiy⁹⁷, O. Beltramello³⁰, O. Benary¹⁵⁴, D. Bencheikroun^{136a}, K. Bendtz^{147a,147b}, N. Benekos¹⁶⁶, Y. Benhammou¹⁵⁴, E. Benhar Noccioli⁴⁹, J.A. Benitez Garcia^{160b}, D.P. Benjamin⁴⁵, J.R. Bensinger²³, K. Benslama¹³¹, S. Bentvelsen¹⁰⁶, D. Berge¹⁰⁶, E. Bergeaas Kuutmann¹⁶, N. Berger⁵, F. Berghaus¹⁷⁰, J. Beringer¹⁵, C. Bernard²², P. Bernat⁷⁷, C. Bernius⁷⁸, F.U. Bernlochner¹⁷⁰, T. Berry⁷⁶, P. Berta¹²⁸, C. Bertella⁸⁴, G. Bertoli^{147a,147b}, F. Bertolucci^{123a,123b}, D. Bertsche¹¹², M.I. Besana^{90a}, G.J. Besjes¹⁰⁵, O. Bessidskaia^{147a,147b}, M.F. Bessner⁴², N. Besson¹³⁷, C. Betancourt⁴⁸, S. Bethke¹⁰⁰, W. Bhimji⁴⁶, R.M. Bianchi¹²⁴, L. Bianchini²³, M. Bianco³⁰, O. Biebel⁹⁹, S.P. Bieniek⁷⁷, K. Bierwagen⁵⁴, J. Biesiada¹⁵, M. Biglietti^{135a}, J. Bilbao De Mendizabal⁴⁹, H. Bilokon⁴⁷, M. Bindi⁵⁴, S. Binet¹¹⁶, A. Bingul^{19c}, C. Bini^{133a,133b}, C.W. Black¹⁵¹, J.E. Black¹⁴⁴, K.M. Black²², D. Blackburn¹³⁹, R.E. Blair⁶, J.-B. Blanchard¹³⁷, T. Blazek^{145a}, I. Bloch⁴², C. Blocker²³, W. Blum^{82,*}, U. Blumenschein⁵⁴, G.J. Bobbink¹⁰⁶, V.S. Bobrovnikov¹⁰⁸, S.S. Bocchetta⁸⁰, A. Bocci⁴⁵, C. Bock⁹⁹, C.R. Boddy¹¹⁹, M. Boehler⁴⁸, T.T. Boek¹⁷⁶, J.A. Bogaerts³⁰,

A.G. Bogdanchikov¹⁰⁸, A. Bogouch^{91,*}, C. Bohm^{147a}, J. Bohm¹²⁶, V. Boisvert⁷⁶, T. Bold^{38a}, V. Boldea^{26a}, A.S. Boldyrev⁹⁸, M. Bomben⁷⁹, M. Bona⁷⁵, M. Boonekamp¹³⁷, A. Borisov¹²⁹, G. Borissov⁷¹, M. Borri⁸³, S. Borroni⁴², J. Bortfeldt⁹⁹, V. Bortolotto^{135a,135b}, K. Bos¹⁰⁶, D. Boscherini^{20a}, M. Bosman¹², H. Boterenbrood¹⁰⁶, J. Boudreau¹²⁴, J. Bouffard², E.V. Bouhova-Thacker⁷¹, D. Boumediene³⁴, C. Bourdarios¹¹⁶, N. Bousson¹¹³, S. Boutouil^{136d}, A. Boveia³¹, J. Boyd³⁰, I.R. Boyko⁶⁴, J. Bracinik¹⁸, A. Brandt⁸, G. Brandt¹⁵, O. Brandt^{58a}, U. Bratzler¹⁵⁷, B. Brau⁸⁵, J.E. Brau¹¹⁵, H.M. Braun^{176,*}, S.F. Brazzale^{165a,165c}, B. Brelrier¹⁵⁹, K. Brendlinger¹²¹, A.J. Brennan⁸⁷, R. Brenner¹⁶⁷, S. Bressler¹⁷³, K. Bristow^{146c}, T.M. Bristow⁴⁶, D. Britton⁵³, F.M. Brochu²⁸, I. Brock²¹, R. Brock⁸⁹, C. Bromberg⁸⁹, J. Bronner¹⁰⁰, G. Brooijmans³⁵, T. Brooks⁷⁶, W.K. Brooks^{32b}, J. Brosamer¹⁵, E. Brost¹¹⁵, J. Brown⁵⁵, P.A. Bruckman de Renstrom³⁹, D. Bruncko^{145b}, R. Bruneliere⁴⁸, S. Brunet⁶⁰, A. Bruni^{20a}, G. Bruni^{20a}, M. Bruschi^{20a}, L. Bryngemark⁸⁰, T. Buanes¹⁴, Q. Buat¹⁴³, F. Bucci⁴⁹, P. Buchholz¹⁴², R.M. Buckingham¹¹⁹, A.G. Buckley⁵³, S.I. Buda^{26a}, I.A. Budagov⁶⁴, F. Buehrer⁴⁸, L. Bugge¹¹⁸, M.K. Bugge¹¹⁸, O. Bulekov⁹⁷, A.C. Bundock⁷³, H. Burckhart³⁰, S. Burdin⁷³, B. Burghgrave¹⁰⁷, S. Burke¹³⁰, I. Burmeister⁴³, E. Busato³⁴, D. Büscher⁴⁸, V. Büscher⁸², P. Bussey⁵³, C.P. Buszello¹⁶⁷, B. Butler⁵⁷, J.M. Butler²², A.I. Butt³, C.M. Buttar⁵³, J.M. Butterworth⁷⁷, P. Butti¹⁰⁶, W. Buttinger²⁸, A. Buzatu⁵³, M. Byszewski¹⁰, S. Cabrera Urbán¹⁶⁸, D. Caforio^{20a,20b}, O. Cakir^{4a}, P. Calafiura¹⁵, A. Calandri¹³⁷, G. Calderini⁷⁹, P. Calfayan⁹⁹, R. Calkins¹⁰⁷, L.P. Caloba^{24a}, D. Calvet³⁴, S. Calvet³⁴, R. Camacho Toro⁴⁹, S. Camarda⁴², D. Cameron¹¹⁸, L.M. Caminada¹⁵, R. Caminal Armadans¹², S. Campana³⁰, M. Campanelli⁷⁷, A. Campoverde¹⁴⁹, V. Canale^{103a,103b}, A. Canepa^{160a}, M. Cano Bret⁷⁵, J. Cantero⁸¹, R. Cantrill^{125a}, T. Cao⁴⁰, M.D.M. Capeans Garrido³⁰, I. Caprini^{26a}, M. Caprini^{26a}, M. Capua^{37a,37b}, R. Caputo⁸², R. Cardarelli^{134a}, T. Carli³⁰, G. Carlino^{103a}, L. Carminati^{90a,90b}, S. Caron¹⁰⁵, E. Carquin^{32a}, G.D. Carrillo-Montoya^{146c}, J.R. Carter²⁸, J. Carvalho^{125a,125c}, D. Casadei⁷⁷, M.P. Casado¹², M. Casolino¹², E. Castaneda-Miranda^{146b}, A. Castelli¹⁰⁶, V. Castillo Gimenez¹⁶⁸, N.F. Castro^{125a}, P. Catastini⁵⁷, A. Catinaccio³⁰, J.R. Catmore¹¹⁸, A. Cattai³⁰, G. Cattani^{134a,134b}, S. Caughron⁸⁹, V. Cavaliere¹⁶⁶, D. Cavalli^{90a}, M. Cavalli-Sforza¹², V. Cavasinni^{123a,123b}, F. Ceradini^{135a,135b}, B. Cerio⁴⁵, K. Cerny¹²⁸, A.S. Cerqueira^{24b}, A. Cerri¹⁵⁰, L. Cerrito⁷⁵, F. Cerutti¹⁵, M. Cerv³⁰, A. Cervelli¹⁷, S.A. Cetin^{19b}, A. Chafaq^{136a}, D. Chakraborty¹⁰⁷, I. Chalupkova¹²⁸, P. Chang¹⁶⁶, B. Chapleau⁸⁶, J.D. Chapman²⁸, D. Charfeddine¹¹⁶, D.G. Charlton¹⁸, C.C. Chau¹⁵⁹, C.A. Chavez Barajas¹⁵⁰, S. Cheatham⁸⁶, A. Chegwidden⁸⁹, S. Chekanov⁶, S.V. Chekulaev^{160a}, G.A. Chelkov^{64,f}, M.A. Chelstowska⁸⁸, C. Chen⁶³, H. Chen²⁵, K. Chen¹⁴⁹, L. Chen^{33d,g}, S. Chen^{33c}, X. Chen^{146c}, Y. Chen³⁵, H.C. Cheng⁸⁸, Y. Cheng³¹, A. Cheplakov⁶⁴, R. Cherkaoui El Moursli^{136e}, V. Chernyatin^{25,*}, E. Cheu⁷, L. Chevalier¹³⁷, V. Chiarella⁴⁷, G. Chiefari^{103a,103b}, J.T. Childers⁶, A. Chilingarov⁷¹, G. Chiodini^{72a}, A.S. Chisholm¹⁸, R.T. Chislett⁷⁷, A. Chitan^{26a}, M.V. Chizhov⁶⁴, S. Chouridou⁹, B.K.B. Chow⁹⁹, D. Chromek-Burckhart³⁰, M.L. Chu¹⁵², J. Chudoba¹²⁶, J.J. Chwastowski³⁹, L. Chytka¹¹⁴, G. Ciapetti^{133a,133b}, A.K. Ciftci^{4a}, R. Ciftci^{4a}, D. Cinca⁵³, V. Cindro⁷⁴, A. Ciocio¹⁵, P. Cirkovic^{13b}, Z.H. Citron¹⁷³, M. Citterio^{90a}, M. Ciubancan^{26a}, A. Clark⁴⁹, P.J. Clark⁴⁶, R.N. Clarke¹⁵, W. Cleland¹²⁴, J.C. Clemens⁸⁴, C. Clement^{147a,147b}, Y. Coadou⁸⁴, M. Cobal^{165a,165c}, A. Coccaro¹³⁹, J. Cochran⁶³, L. Coffey²³, J.G. Cogan¹⁴⁴, J. Coggeshall¹⁶⁶, B. Cole³⁵, S. Cole¹⁰⁷, A.P. Colijn¹⁰⁶, J. Collot⁵⁵, T. Colombo^{58c}, G. Colon⁸⁵, G. Compostella¹⁰⁰, P. Conde Muiño^{125a,125b}, E. Coniavitis⁴⁸, M.C. Conidi¹², S.H. Connell^{146b}, I.A. Connelly⁷⁶, S.M. Consonni^{90a,90b}, V. Consorti⁴⁸, S. Constantinescu^{26a}, C. Conta^{120a,120b}, G. Conti⁵⁷, F. Conventi^{103a,h}, M. Cooke¹⁵, B.D. Cooper⁷⁷, A.M. Cooper-Sarkar¹¹⁹, N.J. Cooper-Smith⁷⁶, K. Copic¹⁵, T. Cornelissen¹⁷⁶, M. Corradi^{20a}, F. Corriveau^{86,i}, A. Corso-Radu¹⁶⁴, A. Cortes-Gonzalez¹², G. Cortiana¹⁰⁰, G. Costa^{90a}, M.J. Costa¹⁶⁸, D. Costanzo¹⁴⁰, D. Côté⁸, G. Cottin²⁸, G. Cowan⁷⁶, B.E. Cox⁸³, K. Cranmer¹⁰⁹, G. Cree²⁹, S. Crépé-Renaudin⁵⁵, F. Crescioli⁷⁹, W.A. Cribbs^{147a,147b}, M. Crispin Ortuzar¹¹⁹, M. Cristinziani²¹, V. Croft¹⁰⁵, G. Crosetti^{37a,37b}, C.-M. Cuciuc^{26a}, T. Cuhadar Donszelmann¹⁴⁰, J. Cummings¹⁷⁷, M. Curatolo⁴⁷, C. Cuthbert¹⁵¹, H. Czirr¹⁴², P. Czodrowski³, Z. Czyzula¹⁷⁷, S. D'Auria⁵³, M. D'Onofrio⁷³, M.J. Da Cunha Sargedass De Sousa^{125a,125b}, C. Da Via⁸³, W. Dabrowski^{38a}, A. Dainca¹¹⁹, T. Dai⁸⁸, O. Dale¹⁴, F. Dallaire⁹⁴, C. Dallapiccola⁸⁵, M. Dam³⁶, A.C. Daniells¹⁸, H.O. Danielsson³⁰, M. Dano Hoffmann¹³⁷, V. Dao¹⁰⁵, G. Darbo^{50a}, S. Darmora⁸, J.A. Dassoulas⁴², A. Dattagupta⁶⁰, W. Davey²¹, C. David¹⁷⁰, T. Davidek¹²⁸, E. Davies^{119,c}, M. Davies¹⁵⁴, O. Davignon⁷⁹, A.R. Davison⁷⁷, P. Davison⁷⁷, Y. Davygora^{58a}, E. Dawe¹⁴³, I. Dawson¹⁴⁰, R.K. Daya-Ishmukhametova⁸⁵, K. De⁸,

R. de Asmundis ^{103a}, S. De Castro ^{20a,20b}, S. De Cecco ⁷⁹, N. De Groot ¹⁰⁵, P. de Jong ¹⁰⁶, H. De la Torre ⁸¹, F. De Lorenzi ⁶³, L. De Nooij ¹⁰⁶, D. De Pedis ^{133a}, A. De Salvo ^{133a}, U. De Sanctis ^{165a,165b}, A. De Santo ¹⁵⁰, J.B. De Vivie De Regie ¹¹⁶, W.J. Dearnaley ⁷¹, R. Debbé ²⁵, C. Debenedetti ¹³⁸, B. Dechenaux ⁵⁵, D.V. Dedovich ⁶⁴, I. Deigaard ¹⁰⁶, J. Del Peso ⁸¹, T. Del Prete ^{123a,123b}, F. Deliot ¹³⁷, C.M. Delitzsch ⁴⁹, M. Deliyergiyev ⁷⁴, A. Dell'Acqua ³⁰, L. Dell'Asta ²², M. Dell'Orso ^{123a,123b}, M. Della Pietra ^{103a,h}, D. della Volpe ⁴⁹, M. Delmastro ⁵, P.A. Delsart ⁵⁵, C. Deluca ¹⁰⁶, S. Demers ¹⁷⁷, M. Demichev ⁶⁴, A. Demilly ⁷⁹, S.P. Denisov ¹²⁹, D. Derendarz ³⁹, J.E. Derkaoui ^{136d}, F. Derue ⁷⁹, P. Dervan ⁷³, K. Desch ²¹, C. Deterre ⁴², P.O. Deviveiros ¹⁰⁶, A. Dewhurst ¹³⁰, S. Dhaliwal ¹⁰⁶, A. Di Ciaccio ^{134a,134b}, L. Di Ciaccio ⁵, A. Di Domenico ^{133a,133b}, C. Di Donato ^{103a,103b}, A. Di Girolamo ³⁰, B. Di Girolamo ³⁰, A. Di Mattia ¹⁵³, B. Di Micco ^{135a,135b}, R. Di Nardo ⁴⁷, A. Di Simone ⁴⁸, R. Di Sipio ^{20a,20b}, D. Di Valentino ²⁹, F.A. Dias ⁴⁶, M.A. Diaz ^{32a}, E.B. Diehl ⁸⁸, J. Dietrich ⁴², T.A. Dietzsch ^{58a}, S. Diglio ⁸⁴, A. Dimitrievska ^{13a}, J. Dingfelder ²¹, C. Dionisi ^{133a,133b}, P. Dita ^{26a}, S. Dita ^{26a}, F. Dittus ³⁰, F. Djama ⁸⁴, T. Djobava ^{51b}, M.A.B. do Vale ^{24c}, A. Do Valle Wemans ^{125a,125g}, T.K.O. Doan ⁵, D. Dobos ³⁰, C. Doglioni ⁴⁹, T. Doherty ⁵³, T. Dohmae ¹⁵⁶, J. Dolejsi ¹²⁸, Z. Dolezal ¹²⁸, B.A. Dolgoshein ^{97,*}, M. Donadelli ^{24d}, S. Donati ^{123a,123b}, P. Dondero ^{120a,120b}, J. Donini ³⁴, J. Dopke ¹³⁰, A. Doria ^{103a}, M.T. Dova ⁷⁰, A.T. Doyle ⁵³, M. Dris ¹⁰, J. Dubbert ⁸⁸, S. Dube ¹⁵, E. Dubreuil ³⁴, E. Duchovni ¹⁷³, G. Duckeck ⁹⁹, O.A. Ducu ^{26a}, D. Duda ¹⁷⁶, A. Dudarev ³⁰, F. Dudziak ⁶³, L. Dufлот ¹¹⁶, L. Duguid ⁷⁶, M. Dührssen ³⁰, M. Dunford ^{58a}, H. Duran Yildiz ^{4a}, M. Düren ⁵², A. Durglishvili ^{51b}, M. Dwuznik ^{38a}, M. Dyndal ^{38a}, J. Ebke ⁹⁹, W. Edson ², N.C. Edwards ⁴⁶, W. Ehrenfeld ²¹, T. Eifert ¹⁴⁴, G. Eigen ¹⁴, K. Einsweiler ¹⁵, T. Ekelof ¹⁶⁷, M. El Kacimi ^{136c}, M. Ellert ¹⁶⁷, S. Elles ⁵, F. Ellinghaus ⁸², N. Ellis ³⁰, J. Elmsheuser ⁹⁹, M. Elsing ³⁰, D. Emeliyanov ¹³⁰, Y. Enari ¹⁵⁶, O.C. Endner ⁸², M. Endo ¹¹⁷, R. Engelmann ¹⁴⁹, J. Erdmann ¹⁷⁷, A. Ereditato ¹⁷, D. Eriksson ^{147a}, G. Ernis ¹⁷⁶, J. Ernst ², M. Ernst ²⁵, J. Ernwein ¹³⁷, D. Errede ¹⁶⁶, S. Errede ¹⁶⁶, E. Ertel ⁸², M. Escalier ¹¹⁶, H. Esch ⁴³, C. Escobar ¹²⁴, B. Esposito ⁴⁷, A.I. Etiennevre ¹³⁷, E. Etzion ¹⁵⁴, H. Evans ⁶⁰, A. Ezhilov ¹²², L. Fabbri ^{20a,20b}, G. Facini ³¹, R.M. Fakhruddinov ¹²⁹, S. Falciano ^{133a}, R.J. Falla ⁷⁷, J. Faltova ¹²⁸, Y. Fang ^{33a}, M. Fanti ^{90a,90b}, A. Farbin ⁸, A. Farilla ^{135a}, T. Farooque ¹², S. Farrell ¹⁶⁴, S.M. Farrington ¹⁷¹, P. Farthouat ³⁰, F. Fassi ¹⁶⁸, P. Fassnacht ³⁰, D. Fassoulidis ⁹, A. Favareto ^{50a,50b}, L. Fayard ¹¹⁶, P. Federic ^{145a}, O.L. Fedin ^{122,j}, W. Fedorko ¹⁶⁹, M. Fehling-Kaschek ⁴⁸, S. Feigl ³⁰, L. Feligioni ⁸⁴, C. Feng ^{33d}, E.J. Feng ⁶, H. Feng ⁸⁸, A.B. Fenyuk ¹²⁹, S. Fernandez Perez ³⁰, S. Ferrag ⁵³, J. Ferrando ⁵³, A. Ferrari ¹⁶⁷, P. Ferrari ¹⁰⁶, R. Ferrari ^{120a}, D.E. Ferreira de Lima ⁵³, A. Ferrer ¹⁶⁸, D. Ferrere ⁴⁹, C. Ferretti ⁸⁸, A. Ferretto Parodi ^{50a,50b}, M. Fiascaris ³¹, F. Fiedler ⁸², A. Filipčič ⁷⁴, M. Filipuzzi ⁴², F. Filthaut ¹⁰⁵, M. Fincke-Keeler ¹⁷⁰, K.D. Finelli ¹⁵¹, M.C.N. Fiolhais ^{125a,125c}, L. Fiorini ¹⁶⁸, A. Firan ⁴⁰, A. Fischer ², J. Fischer ¹⁷⁶, W.C. Fisher ⁸⁹, E.A. Fitzgerald ²³, M. Flechl ⁴⁸, I. Fleck ¹⁴², P. Fleischmann ⁸⁸, S. Fleischmann ¹⁷⁶, G.T. Fletcher ¹⁴⁰, G. Fletcher ⁷⁵, T. Flick ¹⁷⁶, A. Floderus ⁸⁰, L.R. Flores Castillo ^{174,k}, A.C. Florez Bustos ^{160b}, M.J. Flowerdew ¹⁰⁰, A. Formica ¹³⁷, A. Forti ⁸³, D. Fortin ^{160a}, D. Fournier ¹¹⁶, H. Fox ⁷¹, S. Fracchia ¹², P. Francavilla ⁷⁹, M. Franchini ^{20a,20b}, S. Franchino ³⁰, D. Francis ³⁰, M. Franklin ⁵⁷, S. Franz ⁶¹, M. Fraternali ^{120a,120b}, S.T. French ²⁸, C. Friedrich ⁴², F. Friedrich ⁴⁴, D. Froidevaux ³⁰, J.A. Frost ²⁸, C. Fukunaga ¹⁵⁷, E. Fullana Torregrosa ⁸², B.G. Fulsom ¹⁴⁴, J. Fuster ¹⁶⁸, C. Gabaldon ⁵⁵, O. Gabizon ¹⁷³, A. Gabrielli ^{20a,20b}, A. Gabrielli ^{133a,133b}, S. Gadatsch ¹⁰⁶, S. Gadomski ⁴⁹, G. Gagliardi ^{50a,50b}, P. Gagnon ⁶⁰, C. Galea ¹⁰⁵, B. Galhardo ^{125a,125c}, E.J. Gallas ¹¹⁹, V. Gallo ¹⁷, B.J. Gallop ¹³⁰, P. Gallus ¹²⁷, G. Galster ³⁶, K.K. Gan ¹¹⁰, R.P. Gandrajula ⁶², J. Gao ^{33b,g}, Y.S. Gao ^{144,e}, F.M. Garay Walls ⁴⁶, F. Garbersson ¹⁷⁷, C. García ¹⁶⁸, J.E. García Navarro ¹⁶⁸, M. Garcia-Sciveres ¹⁵, R.W. Gardner ³¹, N. Garelli ¹⁴⁴, V. Garonne ³⁰, C. Gatti ⁴⁷, G. Gaudio ^{120a}, B. Gaur ¹⁴², L. Gauthier ⁹⁴, P. Gauzzi ^{133a,133b}, I.L. Gavrilenko ⁹⁵, C. Gay ¹⁶⁹, G. Gaycken ²¹, E.N. Gazis ¹⁰, P. Ge ^{33d}, Z. Gece ¹⁶⁹, C.N.P. Gee ¹³⁰, D.A.A. Geerts ¹⁰⁶, Ch. Geich-Gimbel ²¹, K. Gellerstedt ^{147a,147b}, C. Gemme ^{50a}, A. Gemmell ⁵³, M.H. Genest ⁵⁵, S. Gentile ^{133a,133b}, M. George ⁵⁴, S. George ⁷⁶, D. Gerbaudo ¹⁶⁴, A. Gershon ¹⁵⁴, H. Ghazlane ^{136b}, N. Ghodbane ³⁴, B. Giacobbe ^{20a}, S. Giagu ^{133a,133b}, V. Giangiobbe ¹², P. Giannetti ^{123a,123b}, F. Gianotti ³⁰, B. Gibbard ²⁵, S.M. Gibson ⁷⁶, M. Gilchriese ¹⁵, T.P.S. Gillam ²⁸, D. Gillberg ³⁰, G. Gilles ³⁴, D.M. Gingrich ^{3,d}, N. Giokaris ⁹, M.P. Giordani ^{165a,165c}, R. Giordano ^{103a,103b}, F.M. Giorgi ^{20a}, F.M. Giorgi ¹⁶, P.F. Giraud ¹³⁷, D. Giugni ^{90a}, C. Giuliani ⁴⁸, M. Giulini ^{58b}, B.K. Gjelsten ¹¹⁸, S. Gkaitatzis ¹⁵⁵, I. Gkialas ^{155,l}, L.K. Gladilin ⁹⁸, C. Glasman ⁸¹, J. Glatzer ³⁰, P.C.F. Glaysher ⁴⁶, A. Glazov ⁴², G.L. Glonti ⁶⁴, M. Goblirsch-Kolb ¹⁰⁰, J.R. Goddard ⁷⁵, J. Godfrey ¹⁴³, J. Godlewski ³⁰, C. Goeringer ⁸², S. Goldfarb ⁸⁸, T. Golling ¹⁷⁷, D. Golubkov ¹²⁹, A. Gomes ^{125a,125b,125d}, L.S. Gomez Fajardo ⁴², R. Gonçalves ^{125a},

J. Goncalves Pinto Firmino Da Costa¹³⁷, L. Gonella²¹, S. González de la Hoz¹⁶⁸, G. Gonzalez Parra¹², S. Gonzalez-Sevilla⁴⁹, L. Goossens³⁰, P.A. Gorbounov⁹⁶, H.A. Gordon²⁵, I. Gorelov¹⁰⁴, B. Gorini³⁰, E. Gorini^{72a,72b}, A. Gorišek⁷⁴, E. Gornicki³⁹, A.T. Goshaw⁶, C. Gössling⁴³, M.I. Gostkin⁶⁴, M. Gouighri^{136a}, D. Goujdami^{136c}, M.P. Goulette⁴⁹, A.G. Goussiou¹³⁹, C. Goy⁵, S. Gozpinar²³, H.M.X. Grabas¹³⁷, L. Graber⁵⁴, I. Grabowska-Bold^{38a}, P. Grafström^{20a,20b}, K.-J. Grahn⁴², J. Gramling⁴⁹, E. Gramstad¹¹⁸, S. Grancagnolo¹⁶, V. Grassi¹⁴⁹, V. Gratchev¹²², H.M. Gray³⁰, E. Graziani^{135a}, O.G. Grebenyuk¹²², Z.D. Greenwood^{78,m}, K. Gregersen⁷⁷, I.M. Gregor⁴², P. Grenier¹⁴⁴, J. Griffiths⁸, A.A. Grillo¹³⁸, K. Grimm⁷¹, S. Grinstein^{12,n}, Ph. Gris³⁴, Y.V. Grishkevich⁹⁸, J.-F. Grivaz¹¹⁶, J.P. Grohs⁴⁴, A. Grohsjean⁴², E. Gross¹⁷³, J. Grosse-Knetter⁵⁴, G.C. Grossi^{134a,134b}, J. Groth-Jensen¹⁷³, Z.J. Grout¹⁵⁰, L. Guan^{33b}, F. Guescini⁴⁹, D. Guest¹⁷⁷, O. Gueta¹⁵⁴, C. Guicheney³⁴, E. Guido^{50a,50b}, T. Guillemin¹¹⁶, S. Guindon², U. Gul⁵³, C. Gumpert⁴⁴, J. Gunther¹²⁷, J. Guo³⁵, S. Gupta¹¹⁹, P. Gutierrez¹¹², N.G. Gutierrez Ortiz⁵³, C. Gutsche⁷⁷, N. Guttman¹⁵⁴, C. Guyot¹³⁷, C. Gwenlan¹¹⁹, C.B. Gwilliam⁷³, A. Haas¹⁰⁹, C. Haber¹⁵, H.K. Hadavand⁸, N. Haddad^{136e}, P. Haefner²¹, S. Hageböck²¹, Z. Hajduk³⁹, H. Hakobyan¹⁷⁸, M. Haleem⁴², D. Hall¹¹⁹, G. Halladjian⁸⁹, K. Hamacher¹⁷⁶, P. Hamal¹¹⁴, K. Hamano¹⁷⁰, M. Hamer⁵⁴, A. Hamilton^{146a}, S. Hamilton¹⁶², G.N. Hamity^{146c}, P.G. Hamnett⁴², L. Han^{33b}, K. Hanagaki¹¹⁷, K. Hanawa¹⁵⁶, M. Hance¹⁵, P. Hanke^{58a}, R. Hanna¹³⁷, J.B. Hansen³⁶, J.D. Hansen³⁶, P.H. Hansen³⁶, K. Hara¹⁶¹, A.S. Hard¹⁷⁴, T. Harenberg¹⁷⁶, F. Hariri¹¹⁶, S. Harkusha⁹¹, D. Harper⁸⁸, R.D. Harrington⁴⁶, O.M. Harris¹³⁹, P.F. Harrison¹⁷¹, F. Hartjes¹⁰⁶, S. Hasegawa¹⁰², Y. Hasegawa¹⁴¹, A. Hasib¹¹², S. Hassani¹³⁷, S. Haug¹⁷, M. Hauschild³⁰, R. Hauser⁸⁹, M. Havranek¹²⁶, C.M. Hawkes¹⁸, R.J. Hawkins³⁰, A.D. Hawkins⁸⁰, T. Hayashi¹⁶¹, D. Hayden⁸⁹, C.P. Hays¹¹⁹, H.S. Hayward⁷³, S.J. Haywood¹³⁰, S.J. Head¹⁸, T. Heck⁸², V. Hedberg⁸⁰, L. Heelan⁸, S. Heim¹²¹, T. Heim¹⁷⁶, B. Heinemann¹⁵, L. Heinrich¹⁰⁹, J. Hejbal¹²⁶, L. Helary²², C. Heller⁹⁹, M. Heller³⁰, S. Hellman^{147a,147b}, D. Hellmich²¹, C. Helsens³⁰, J. Henderson¹¹⁹, R.C.W. Henderson⁷¹, Y. Heng¹⁷⁴, C. Hengler⁴², A. Henrichs¹⁷⁷, A.M. Henriques Correia³⁰, S. Henrot-Versille¹¹⁶, C. Hensel⁵⁴, G.H. Herbert¹⁶, Y. Hernández Jiménez¹⁶⁸, R. Herrberg-Schubert¹⁶, G. Herten⁴⁸, R. Hertenberger⁹⁹, L. Hervas³⁰, G.G. Hesketh⁷⁷, N.P. Hessey¹⁰⁶, R. Hickling⁷⁵, E. Higón-Rodríguez¹⁶⁸, E. Hill¹⁷⁰, J.C. Hill²⁸, K.H. Hiller⁴², S. Hillert²¹, S.J. Hillier¹⁸, I. Hinchliffe¹⁵, E. Hines¹²¹, M. Hirose¹⁵⁸, D. Hirschbuehl¹⁷⁶, J. Hobbs¹⁴⁹, N. Hod¹⁰⁶, M.C. Hodgkinson¹⁴⁰, P. Hodgson¹⁴⁰, A. Hoecker³⁰, M.R. Hoefkamp¹⁰⁴, J. Hoffman⁴⁰, D. Hoffmann⁸⁴, J.I. Hofmann^{58a}, M. Hohlfeld⁸², T.R. Holmes¹⁵, T.M. Hong¹²¹, L. Hooft van Huysduynen¹⁰⁹, J.-Y. Hostachy⁵⁵, S. Hou¹⁵², A. Hoummada^{136a}, J. Howard¹¹⁹, J. Howarth⁴², M. Hrabovsky¹¹⁴, I. Hristova¹⁶, J. Hrivnac¹¹⁶, T. Hryn'ova⁵, C. Hsu^{146c}, P.J. Hsu⁸², S.-C. Hsu¹³⁹, D. Hu³⁵, X. Hu²⁵, Y. Huang⁴², Z. Hubacek³⁰, F. Hubaut⁸⁴, F. Huegging²¹, T.B. Huffman¹¹⁹, E.W. Hughes³⁵, G. Hughes⁷¹, M. Huhtinen³⁰, T.A. Hülsing⁸², M. Hurwitz¹⁵, N. Huseynov^{64,b}, J. Huston⁸⁹, J. Huth⁵⁷, G. Iacobucci⁴⁹, G. Iakovidis¹⁰, I. Ibragimov¹⁴², L. Iconomidou-Fayard¹¹⁶, E. Ideal¹⁷⁷, P. Iengo^{103a}, O. Igonkina¹⁰⁶, T. Iizawa¹⁷², Y. Ikegami⁶⁵, K. Ikematsu¹⁴², M. Ikeno⁶⁵, Y. Ilchenko³¹, D. Iliadis¹⁵⁵, N. Ilic¹⁵⁹, Y. Inamaru⁶⁶, T. Ince¹⁰⁰, P. Ioannou⁹, M. Iodice^{135a}, K. Iordanidou⁹, V. Ippolito⁵⁷, A. Irles Quiles¹⁶⁸, C. Isaksson¹⁶⁷, M. Ishino⁶⁷, M. Ishitsuka¹⁵⁸, R. Ishmukhametov¹¹⁰, C. Issever¹¹⁹, S. Istin^{19a}, J.M. Iturbe Ponce⁸³, R. Iuppa^{134a,134b}, J. Ivarsson⁸⁰, W. Iwanski³⁹, H. Iwasaki⁶⁵, J.M. Izen⁴¹, V. Izzo^{103a}, B. Jackson¹²¹, M. Jackson⁷³, P. Jackson¹, M.R. Jaekel³⁰, V. Jain², K. Jakobs⁴⁸, S. Jakobsen³⁰, T. Jakoubek¹²⁶, J. Jakubek¹²⁷, D.O. Jamin¹⁵², D.K. Jana⁷⁸, E. Jansen⁷⁷, H. Jansen³⁰, J. Janssen²¹, M. Janus¹⁷¹, G. Jarlskog⁸⁰, N. Javadov^{64,b}, T. Javůrek⁴⁸, L. Jeanty¹⁵, J. Jejelava^{51a,o}, G.-Y. Jeng¹⁵¹, D. Jennens⁸⁷, P. Jenni^{48,p}, J. Jentsch⁴³, C. Jeske¹⁷¹, S. Jézéquel⁵, H. Ji¹⁷⁴, W. Ji⁸², J. Jia¹⁴⁹, Y. Jiang^{33b}, M. Jimenez Belenguer⁴², S. Jin^{33a}, A. Jinaru^{26a}, O. Jinnouchi¹⁵⁸, M.D. Joergensen³⁶, K.E. Johansson^{147a,147b}, P. Johansson¹⁴⁰, K.A. Johns⁷, K. Jon-And^{147a,147b}, G. Jones¹⁷¹, R.W.L. Jones⁷¹, T.J. Jones⁷³, J. Jongmanns^{58a}, P.M. Jorge^{125a,125b}, K.D. Joshi⁸³, J. Jovicevic¹⁴⁸, X. Ju¹⁷⁴, C.A. Jung⁴³, R.M. Jungst³⁰, P. Jussel⁶¹, A. Juste Rozas^{12,n}, M. Kaci¹⁶⁸, A. Kaczmarska³⁹, M. Kado¹¹⁶, H. Kagan¹¹⁰, M. Kagan¹⁴⁴, E. Kajomovitz⁴⁵, C.W. Kalderon¹¹⁹, S. Kama⁴⁰, A. Kamenshchikov¹²⁹, N. Kanaya¹⁵⁶, M. Kaneda³⁰, S. Kaneti²⁸, V.A. Kantserov⁹⁷, J. Kanzaki⁶⁵, B. Kaplan¹⁰⁹, A. Kapliy³¹, D. Kar⁵³, K. Karakostas¹⁰, N. Karastathis¹⁰, M. Karnevskiy⁸², S.N. Karpov⁶⁴, K. Karthik¹⁰⁹, V. Kartvelishvili⁷¹, A.N. Karyukhin¹²⁹, L. Kashif¹⁷⁴, G. Kasieczka^{58b}, R.D. Kass¹¹⁰, A. Kastanas¹⁴, Y. Kataoka¹⁵⁶, A. Katre⁴⁹, J. Katzy⁴², V. Kaushik⁷, K. Kawagoe⁶⁹, T. Kawamoto¹⁵⁶, G. Kawamura⁵⁴, S. Kazama¹⁵⁶, V.F. Kazanin¹⁰⁸, M.Y. Kazarinov⁶⁴, R. Keeler¹⁷⁰, R. Kehoe⁴⁰, M. Keil⁵⁴, J.S. Keller⁴², J.J. Kempster⁷⁶, H. Keoshkerian⁵,

O. Kepka¹²⁶, B.P. Kerševan⁷⁴, S. Kersten¹⁷⁶, K. Kessoku¹⁵⁶, J. Keung¹⁵⁹, F. Khalil-zada¹¹, H. Khandanyan^{147a,147b}, A. Khanov¹¹³, A. Khodinov⁹⁷, A. Khomich^{58a}, T.J. Khoo²⁸, G. Khoriauli²¹, A. Khoroshilov¹⁷⁶, V. Khovanskiy⁹⁶, E. Khramov⁶⁴, J. Khubua^{51b}, H.Y. Kim⁸, H. Kim^{147a,147b}, S.H. Kim¹⁶¹, N. Kimura¹⁷², O. Kind¹⁶, B.T. King⁷³, M. King¹⁶⁸, R.S.B. King¹¹⁹, S.B. King¹⁶⁹, J. Kirk¹³⁰, A.E. Kiryunin¹⁰⁰, T. Kishimoto⁶⁶, D. Kisielewska^{38a}, F. Kiss⁴⁸, T. Kittelmann¹²⁴, K. Kiuchi¹⁶¹, E. Kladiva^{145b}, M. Klein⁷³, U. Klein⁷³, K. Kleinknecht⁸², P. Klimek^{147a,147b}, A. Klimentov²⁵, R. Klingenberg⁴³, J.A. Klinger⁸³, T. Klioutchnikova³⁰, P.F. Klok¹⁰⁵, E.-E. Kluge^{58a}, P. Kluit¹⁰⁶, S. Kluth¹⁰⁰, E. Kneringer⁶¹, E.B.F.G. Knoop⁸⁴, A. Knue⁵³, D. Kobayashi¹⁵⁸, T. Kobayashi¹⁵⁶, M. Kobel⁴⁴, M. Kocian¹⁴⁴, P. Kodys¹²⁸, P. Koevesarki²¹, T. Koffas²⁹, E. Koffeman¹⁰⁶, L.A. Kogan¹¹⁹, S. Kohlmann¹⁷⁶, Z. Kohout¹²⁷, T. Kohriki⁶⁵, T. Koi¹⁴⁴, H. Kolanoski¹⁶, I. Koletsou⁵, J. Koll⁸⁹, A.A. Komar^{95,*}, Y. Komori¹⁵⁶, T. Kondo⁶⁵, N. Kondrashova⁴², K. Köneke⁴⁸, A.C. König¹⁰⁵, S. König⁸², T. Kono^{65,q}, R. Konoplich^{109,r}, N. Konstantinidis⁷⁷, R. Kopeliansky¹⁵³, S. Koperny^{38a}, L. Köpke⁸², A.K. Kopp⁴⁸, K. Korcyl³⁹, K. Kordas¹⁵⁵, A. Korn⁷⁷, A.A. Korol^{108,s}, I. Korolkov¹², E.V. Korolkova¹⁴⁰, V.A. Korotkov¹²⁹, O. Kortner¹⁰⁰, S. Kortner¹⁰⁰, V.V. Kostyukhin²¹, V.M. Kotov⁶⁴, A. Kotwal⁴⁵, C. Kourkoumelis⁹, V. Kouskoura¹⁵⁵, A. Koutsman^{160a}, R. Kowalewski¹⁷⁰, T.Z. Kowalski^{38a}, W. Kozanecki¹³⁷, A.S. Kozhin¹²⁹, V. Kral¹²⁷, V.A. Kramarenko⁹⁸, G. Kramberger⁷⁴, D. Krasnopevtsev⁹⁷, M.W. Krasny⁷⁹, A. Krasznahorkay³⁰, J.K. Kraus²¹, A. Kravchenko²⁵, S. Kreiss¹⁰⁹, M. Kretz^{58c}, J. Kretzschmar⁷³, K. Kreutzfeldt⁵², P. Krieger¹⁵⁹, K. Kroeninger⁵⁴, H. Kroha¹⁰⁰, J. Kroll¹²¹, J. Kroseberg²¹, J. Krstic^{13a}, U. Kruchonak⁶⁴, H. Krüger²¹, T. Kruker¹⁷, N. Krumnack⁶³, Z.V. Krumshteyn⁶⁴, A. Kruse¹⁷⁴, M.C. Kruse⁴⁵, M. Kruskal²², T. Kubota⁸⁷, S. Kuday^{4a}, S. Kuehn⁴⁸, A. Kugel^{58c}, A. Kuhl¹³⁸, T. Kuhl⁴², V. Kukhtin⁶⁴, Y. Kulchitsky⁹¹, S. Kuleshov^{32b}, M. Kuna^{133a,133b}, J. Kunkle¹²¹, A. Kupco¹²⁶, H. Kurashige⁶⁶, Y.A. Kurochkin⁹¹, R. Kurumida⁶⁶, V. Kus¹²⁶, E.S. Kuwertz¹⁴⁸, M. Kuze¹⁵⁸, J. Kvita¹¹⁴, A. La Rosa⁴⁹, L. La Rotonda^{37a,37b}, C. Lacasta¹⁶⁸, F. Lacava^{133a,133b}, J. Lacey²⁹, H. Lacker¹⁶, D. Lacour⁷⁹, V.R. Lacuesta¹⁶⁸, E. Ladygin⁶⁴, R. Lafaye⁵, B. Laforge⁷⁹, T. Lagouri¹⁷⁷, S. Lai⁴⁸, H. Laier^{58a}, L. Lambourne⁷⁷, S. Lammers⁶⁰, C.L. Lampen⁷, W. Lampl⁷, E. Lançon¹³⁷, U. Landgraf⁴⁸, M.P.J. Landon⁷⁵, V.S. Lang^{58a}, A.J. Lankford¹⁶⁴, F. Lanni²⁵, K. Lantzsch³⁰, S. Laplace⁷⁹, C. Lapoire²¹, J.F. Laporte¹³⁷, T. Lari^{90a}, M. Lassnig³⁰, P. Laurelli⁴⁷, W. Lavrijsen¹⁵, A.T. Law¹³⁸, P. Laycock⁷³, B.T. Le⁵⁵, O. Le Dortz⁷⁹, E. Le Guirriec⁸⁴, E. Le Menedeu¹², T. LeCompte⁶, F. Ledroit-Guillon⁵⁵, C.A. Lee¹⁵², H. Lee¹⁰⁶, J.S.H. Lee¹¹⁷, S.C. Lee¹⁵², L. Lee¹⁷⁷, G. Lefebvre⁷⁹, M. Lefebvre¹⁷⁰, F. Legger⁹⁹, C. Leggett¹⁵, A. Lehan⁷³, M. Lehmacher²¹, G. Lehmann Miotto³⁰, X. Lei⁷, W.A. Leight²⁹, A. Leisos¹⁵⁵, A.G. Leister¹⁷⁷, M.A.L. Leite^{24d}, R. Leitner¹²⁸, D. Lellouch¹⁷³, B. Lemmer⁵⁴, K.J.C. Leney⁷⁷, T. Lenz¹⁰⁶, G. Lenzen¹⁷⁶, B. Lenzi³⁰, R. Leone⁷, S. Leone^{123a,123b}, K. Leonhardt⁴⁴, C. Leonidopoulos⁴⁶, S. Leontsinis¹⁰, C. Leroy⁹⁴, C.G. Lester²⁸, C.M. Lester¹²¹, M. Levchenko¹²², J. Levêque⁵, D. Levin⁸⁸, L.J. Levinson¹⁷³, M. Levy¹⁸, A. Lewis¹¹⁹, G.H. Lewis¹⁰⁹, A.M. Leyko²¹, M. Leyton⁴¹, B. Li^{33b,t}, B. Li⁸⁴, H. Li¹⁴⁹, H.L. Li³¹, L. Li⁴⁵, L. Li^{33e}, S. Li⁴⁵, Y. Li^{33c,u}, Z. Liang¹³⁸, H. Liao³⁴, B. Liberti^{134a}, P. Lichard³⁰, K. Lie¹⁶⁶, J. Liebal²¹, W. Liebig¹⁴, C. Limbach²¹, A. Limosani⁸⁷, S.C. Lin^{152,v}, T.H. Lin⁸², F. Linde¹⁰⁶, B.E. Lindquist¹⁴⁹, J.T. Linnemann⁸⁹, E. Lipeles¹²¹, A. Lipniacka¹⁴, M. Lisovsky⁴², T.M. Liss¹⁶⁶, D. Lissauer²⁵, A. Lister¹⁶⁹, A.M. Litke¹³⁸, B. Liu¹⁵², D. Liu¹⁵², J.B. Liu^{33b}, K. Liu^{33b,w}, L. Liu⁸⁸, M. Liu⁴⁵, M. Liu^{33b}, Y. Liu^{33b}, M. Livan^{120a,120b}, S.S.A. Livermore¹¹⁹, A. Lleres⁵⁵, J. Llorente Merino⁸¹, S.L. Lloyd⁷⁵, F. Lo Sterzo¹⁵², E. Lobodzinska⁴², P. Loch⁷, W.S. Lockman¹³⁸, T. Loddienkoetter²¹, F.K. Loebinger⁸³, A.E. Loevschall-Jensen³⁶, A. Loginov¹⁷⁷, C.W. Loh¹⁶⁹, T. Lohse¹⁶, K. Lohwasser⁴², M. Lokajicek¹²⁶, V.P. Lombardo⁵, B.A. Long²², J.D. Long⁸⁸, R.E. Long⁷¹, L. Lopes^{125a}, D. Lopez Mateos⁵⁷, B. Lopez Paredes¹⁴⁰, I. Lopez Paz¹², J. Lorenz⁹⁹, N. Lorenzo Martinez⁶⁰, M. Losada¹⁶³, P. Loscutoff¹⁵, X. Lou⁴¹, A. Lounis¹¹⁶, J. Love⁶, P.A. Love⁷¹, A.J. Lowe^{144,e}, F. Lu^{33a}, H.J. Lubatti¹³⁹, C. Luci^{133a,133b}, A. Lucotte⁵⁵, F. Luehring⁶⁰, W. Lukas⁶¹, L. Luminari^{133a}, O. Lundberg^{147a,147b}, B. Lund-Jensen¹⁴⁸, M. Lungwitz⁸², D. Lynn²⁵, R. Lysak¹²⁶, E. Lytken⁸⁰, H. Ma²⁵, L.L. Ma^{33d}, G. Maccarrone⁴⁷, A. Macchiolo¹⁰⁰, J. Machado Miguens^{125a,125b}, D. Macina³⁰, D. Madaffari⁸⁴, R. Madar⁴⁸, H.J. Maddocks⁷¹, W.F. Mader⁴⁴, A. Madsen¹⁶⁷, M. Maeno⁸, T. Maeno²⁵, E. Magradze⁵⁴, K. Mahboubi⁴⁸, J. Mahlstedt¹⁰⁶, S. Mahmoud⁷³, C. Maiani¹³⁷, C. Maidantchik^{24a}, A.A. Maier¹⁰⁰, A. Maio^{125a,125b,125d}, S. Majewski¹¹⁵, Y. Makida⁶⁵, N. Makovec¹¹⁶, P. Mal^{137,x}, B. Malaescu⁷⁹, Pa. Malecki³⁹, V.P. Maleev¹²², F. Malek⁵⁵, U. Mallik⁶², D. Malon⁶, C. Malone¹⁴⁴, S. Maltezos¹⁰, V.M. Malyshev¹⁰⁸, S. Malyukov³⁰, J. Mamuzic^{13b}, B. Mandelli³⁰, L. Mandelli^{90a}, I. Mandić⁷⁴, R. Mandrysch⁶², J. Maneira^{125a,125b},

A. Manfredini¹⁰⁰, L. Manhaes de Andrade Filho^{24b}, J.A. Manjarres Ramos^{160b}, A. Mann⁹⁹, P.M. Manning¹³⁸, A. Manousakis-Katsikakis⁹, B. Mansoulie¹³⁷, R. Mantifel⁸⁶, L. Mapelli³⁰, L. March¹⁶⁸, J.F. Marchand²⁹, G. Marchiori⁷⁹, M. Marcisovsky¹²⁶, C.P. Marino¹⁷⁰, M. Marjanovic^{13a}, C.N. Marques^{125a}, F. Marroquim^{24a}, S.P. Marsden⁸³, Z. Marshall¹⁵, L.F. Marti¹⁷, S. Marti-Garcia¹⁶⁸, B. Martin³⁰, B. Martin⁸⁹, T.A. Martin¹⁷¹, V.J. Martin⁴⁶, B. Martin dit Latour¹⁴, H. Martinez¹³⁷, M. Martinez^{12,n}, S. Martin-Haugh¹³⁰, A.C. Martyniuk⁷⁷, M. Marx¹³⁹, F. Marzano^{133a}, A. Marzin³⁰, L. Masetti⁸², T. Mashimo¹⁵⁶, R. Mashinistov⁹⁵, J. Masik⁸³, A.L. Maslennikov¹⁰⁸, I. Massa^{20a,20b}, N. Massol⁵, P. Mastrandrea¹⁴⁹, A. Mastroberardino^{37a,37b}, T. Masubuchi¹⁵⁶, P. Mättig¹⁷⁶, J. Mattmann⁸², J. Maurer^{26a}, S.J. Maxfield⁷³, D.A. Maximov^{108,s}, R. Mazini¹⁵², L. Mazzaferro^{134a,134b}, G. Mc Goldrick¹⁵⁹, S.P. Mc Kee⁸⁸, A. McCarn⁸⁸, R.L. McCarthy¹⁴⁹, T.G. McCarthy²⁹, N.A. McCubbin¹³⁰, K.W. McFarlane^{56,*}, J.A. Mcfayden⁷⁷, G. Mchedlidze⁵⁴, S.J. McMahon¹³⁰, R.A. McPherson^{170,i}, A. Meade⁸⁵, J. Mechnich¹⁰⁶, M. Medinnis⁴², S. Meehan³¹, S. Mehlhase⁹⁹, A. Mehta⁷³, K. Meier^{58a}, C. Meineck⁹⁹, B. Meirose⁸⁰, C. Melachrinou³¹, B.R. Mellado Garcia^{146c}, F. Meloni¹⁷, A. Mengarelli^{20a,20b}, S. Menke¹⁰⁰, E. Meoni¹⁶², K.M. Mercurio⁵⁷, S. Mergelmeyer²¹, N. Meric¹³⁷, P. Mermoud⁴⁹, L. Merola^{103a,103b}, C. Meroni^{90a}, F.S. Merritt³¹, H. Merritt¹¹⁰, A. Messina^{30,y}, J. Metcalfe²⁵, A.S. Mete¹⁶⁴, C. Meyer⁸², C. Meyer³¹, J-P. Meyer¹³⁷, J. Meyer³⁰, R.P. Middleton¹³⁰, S. Migas⁷³, L. Mijović²¹, G. Mikenberg¹⁷³, M. Mikestikova¹²⁶, M. Mikuž⁷⁴, D.W. Miller³¹, C. Mills⁴⁶, A. Milov¹⁷³, D.A. Milstead^{147a,147b}, D. Milstein¹⁷³, A.A. Minaenko¹²⁹, I.A. Minashvili⁶⁴, A.I. Mincer¹⁰⁹, B. Mindur^{38a}, M. Mineev⁶⁴, Y. Ming¹⁷⁴, L.M. Mir¹², G. Mirabelli^{133a}, T. Mitani¹⁷², J. Mitrevski⁹⁹, V.A. Mitsou¹⁶⁸, S. Mitsui⁶⁵, A. Miucci⁴⁹, P.S. Miyagawa¹⁴⁰, J.U. Mjörnmark⁸⁰, T. Moa^{147a,147b}, K. Mochizuki⁸⁴, S. Mohapatra³⁵, W. Mohr⁴⁸, S. Molander^{147a,147b}, R. Moles-Valls¹⁶⁸, K. Mönig⁴², C. Monini⁵⁵, J. Monk³⁶, E. Monnier⁸⁴, J. Montejo Berlingen¹², F. Monticelli⁷⁰, S. Monzani^{133a,133b}, R.W. Moore³, A. Moraes⁵³, N. Morange⁶², D. Moreno⁸², M. Moreno Llácer⁵⁴, P. Morettini^{50a}, M. Morgenstern⁴⁴, M. Morii⁵⁷, S. Moritz⁸², A.K. Morley¹⁴⁸, G. Mornacchi³⁰, J.D. Morris⁷⁵, L. Morvaj¹⁰², H.G. Moser¹⁰⁰, M. Mosidze^{51b}, J. Moss¹¹⁰, K. Motohashi¹⁵⁸, R. Mount¹⁴⁴, E. Mountricha²⁵, S.V. Mouraviev^{95,*}, E.J.W. Moyse⁸⁵, S. Muanza⁸⁴, R.D. Mudd¹⁸, F. Mueller^{58a}, J. Mueller¹²⁴, K. Mueller²¹, T. Mueller²⁸, T. Mueller⁸², D. Muenstermann⁴⁹, Y. Munwes¹⁵⁴, J.A. Murillo Quijada¹⁸, W.J. Murray^{171,130}, H. Musheghyan⁵⁴, E. Musto¹⁵³, A.G. Myagkov^{129,z}, M. Myska¹²⁷, O. Nackenhorst⁵⁴, J. Nadal⁵⁴, K. Nagai⁶¹, R. Nagai¹⁵⁸, Y. Nagai⁸⁴, K. Nagano⁶⁵, A. Nagarkar¹¹⁰, Y. Nagasaka⁵⁹, M. Nagel¹⁰⁰, A.M. Nairz³⁰, Y. Nakahama³⁰, K. Nakamura⁶⁵, T. Nakamura¹⁵⁶, I. Nakano¹¹¹, H. Namasivayam⁴¹, G. Nanava²¹, R. Narayan^{58b}, T. Nattermann²¹, T. Naumann⁴², G. Navarro¹⁶³, R. Nayyar⁷, H.A. Neal⁸⁸, P.Yu. Nechaeva⁹⁵, T.J. Neep⁸³, P.D. Nef¹⁴⁴, A. Negri^{120a,120b}, G. Negri³⁰, M. Negrini^{20a}, S. Nektarijevic⁴⁹, A. Nelson¹⁶⁴, T.K. Nelson¹⁴⁴, S. Nemecek¹²⁶, P. Nemethy¹⁰⁹, A.A. Nepomuceno^{24a}, M. Nessi^{30,aa}, M.S. Neubauer¹⁶⁶, M. Neumann¹⁷⁶, R.M. Neves¹⁰⁹, P. Nevski²⁵, P.R. Newman¹⁸, D.H. Nguyen⁶, R.B. Nickerson¹¹⁹, R. Nicolaidou¹³⁷, B. Niquevert³⁰, J. Nielsen¹³⁸, N. Nikiforou³⁵, A. Nikiforov¹⁶, V. Nikolaenko^{129,z}, I. Nikolic-Audit⁷⁹, K. Nikolics⁴⁹, K. Nikolopoulos¹⁸, P. Nilsson⁸, Y. Ninomiya¹⁵⁶, A. Nisati^{133a}, R. Nisius¹⁰⁰, T. Nobe¹⁵⁸, L. Nodulman⁶, M. Nomachi¹¹⁷, I. Nomidis¹⁵⁵, S. Norberg¹¹², M. Nordberg³⁰, S. Nowak¹⁰⁰, M. Nozaki⁶⁵, L. Nozka¹¹⁴, K. Ntekas¹⁰, G. Nunes Hanninger⁸⁷, T. Nunnemann⁹⁹, E. Nurse⁷⁷, F. Nuti⁸⁷, B.J. O'Brien⁴⁶, F. O'grady⁷, D.C. O'Neil¹⁴³, V. O'Shea⁵³, F.G. Oakham^{29,d}, H. Oberlack¹⁰⁰, T. Obermann²¹, J. Ocariz⁷⁹, A. Ochi⁶⁶, M.I. Ochoa⁷⁷, S. Oda⁶⁹, S. Odaka⁶⁵, H. Ogren⁶⁰, A. Oh⁸³, S.H. Oh⁴⁵, C.C. Ohm³⁰, H. Ohman¹⁶⁷, T. Ohshima¹⁰², W. Okamura¹¹⁷, H. Okawa²⁵, Y. Okumura³¹, T. Okuyama¹⁵⁶, A. Olariu^{26a}, A.G. Olchevski⁶⁴, S.A. Olivares Pino⁴⁶, D. Oliveira Damazio²⁵, E. Oliver Garcia¹⁶⁸, A. Olszewski³⁹, J. Olszowska³⁹, A. Onofre^{125a,125e}, P.U.E. Onyisi^{31,ab}, C.J. Oram^{160a}, M.J. Oreglia³¹, Y. Oren¹⁵⁴, D. Orestano^{135a,135b}, N. Orlando^{72a,72b}, C. Oropeza Barrera⁵³, R.S. Orr¹⁵⁹, B. Osculati^{50a,50b}, R. Ospanov¹²¹, G. Otero y Garzon²⁷, H. Otono⁶⁹, M. Ouchrif^{136d}, E.A. Ouellette¹⁷⁰, F. Ould-Saada¹¹⁸, A. Ouraou¹³⁷, K.P. Oussoren¹⁰⁶, Q. Ouyang^{33a}, A. Ovcharova¹⁵, M. Owen⁸³, V.E. Ozcan^{19a}, N. Ozturk⁸, K. Pachal¹¹⁹, A. Pacheco Pages¹², C. Padilla Aranda¹², M. Pagáčová⁴⁸, S. Pagan Griso¹⁵, E. Paganis¹⁴⁰, C. Pahl¹⁰⁰, F. Paige²⁵, P. Pais⁸⁵, K. Pajchel¹¹⁸, G. Palacino^{160b}, S. Palestini³⁰, M. Palka^{38b}, D. Pallin³⁴, A. Palma^{125a,125b}, J.D. Palmer¹⁸, Y.B. Pan¹⁷⁴, E. Panagiotopoulou¹⁰, J.G. Panduro Vazquez⁷⁶, P. Pani¹⁰⁶, N. Panikashvili⁸⁸, S. Panitkin²⁵, D. Pantea^{26a}, L. Paolozzi^{134a,134b}, Th.D. Papadopoulos¹⁰, K. Papageorgiou^{155,l}, A. Paramonov⁶, D. Paredes Hernandez³⁴, M.A. Parker²⁸, F. Parodi^{50a,50b}, J.A. Parsons³⁵, U. Parzefall⁴⁸, E. Pasqualucci^{133a}, S. Passaggio^{50a}, A. Passeri^{135a}, F. Pastore^{135a,135b,*},

Fr. Pastore⁷⁶, G. Pásztor²⁹, S. Patarraia¹⁷⁶, N.D. Patel¹⁵¹, J.R. Pater⁸³, S. Patricelli^{103a,103b}, T. Pauly³⁰, J. Pearce¹⁷⁰, M. Pedersen¹¹⁸, S. Pedraza Lopez¹⁶⁸, R. Pedro^{125a,125b}, S.V. Peleganchuk¹⁰⁸, D. Pelikan¹⁶⁷, H. Peng^{33b}, B. Penning³¹, J. Penwell⁶⁰, D.V. Perepelitsa²⁵, E. Perez Codina^{160a}, M.T. Pérez García-Estañ¹⁶⁸, V. Perez Reale³⁵, L. Perini^{90a,90b}, H. Pernegger³⁰, R. Perrino^{72a}, R. Peschke⁴², V.D. Peshekhonov⁶⁴, K. Peters³⁰, R.F.Y. Peters⁸³, B.A. Petersen³⁰, T.C. Petersen³⁶, E. Petit⁴², A. Petridis^{147a,147b}, C. Petridou¹⁵⁵, E. Petrolo^{133a}, F. Petrucci^{135a,135b}, N.E. Pettersson¹⁵⁸, R. Pezoa^{32b}, P.W. Phillips¹³⁰, G. Piacquadio¹⁴⁴, E. Pianori¹⁷¹, A. Picazio⁴⁹, E. Piccaro⁷⁵, M. Piccinini^{20a,20b}, R. Piegaia²⁷, D.T. Pignotti¹¹⁰, J.E. Pilcher³¹, A.D. Pilkington⁷⁷, J. Pina^{125a,125b,125d}, M. Pinamonti^{165a,165c,ac}, A. Pinder¹¹⁹, J.L. Pinfold³, A. Pingel³⁶, B. Pinto^{125a}, S. Pires⁷⁹, M. Pitt¹⁷³, C. Pizio^{90a,90b}, L. Plazak^{145a}, M.-A. Pleier²⁵, V. Pleskot¹²⁸, E. Plotnikova⁶⁴, P. Plucinski^{147a,147b}, S. Poddar^{58a}, F. Podlyski³⁴, R. Poettgen⁸², L. Poggioli¹¹⁶, D. Pohl²¹, M. Pohl⁴⁹, G. Polesello^{120a}, A. Policicchio^{37a,37b}, R. Polifka¹⁵⁹, A. Polini^{20a}, C.S. Pollard⁴⁵, V. Polychronakos²⁵, K. Pommès³⁰, L. Pontecorvo^{133a}, B.G. Pope⁸⁹, G.A. Popeneciu^{26b}, D.S. Popovic^{13a}, A. Poppleton³⁰, X. Portell Bueso¹², S. Pospisil¹²⁷, K. Potamianos¹⁵, I.N. Potrap⁶⁴, C.J. Potter¹⁵⁰, C.T. Potter¹¹⁵, G. Poulard³⁰, J. Poveda⁶⁰, V. Pozdnyakov⁶⁴, P. Pralavorio⁸⁴, A. Pranko¹⁵, S. Prasad³⁰, R. Pravahan⁸, S. Prell⁶³, D. Price⁸³, J. Price⁷³, L.E. Price⁶, D. Prieur¹²⁴, M. Primavera^{72a}, M. Proissl⁴⁶, K. Prokofiev⁴⁷, F. Prokoshin^{32b}, E. Protopapadaki¹³⁷, S. Protopopescu²⁵, J. Proudfoot⁶, M. Przybycien^{38a}, H. Przysieznik⁵, E. Ptacek¹¹⁵, D. Puddu^{135a,135b}, E. Pueschel⁸⁵, D. Puldon¹⁴⁹, M. Purohit^{25,ad}, P. Puzo¹¹⁶, J. Qian⁸⁸, G. Qin⁵³, Y. Qin⁸³, A. Quadt⁵⁴, D.R. Quarrie¹⁵, W.B. Quayle^{165a,165b}, M. Queitsch-Maitland⁸³, D. Quilty⁵³, A. Qureshi^{160b}, V. Radeka²⁵, V. Radescu⁴², S.K. Radhakrishnan¹⁴⁹, P. Radloff¹¹⁵, P. Rados⁸⁷, F. Ragusa^{90a,90b}, G. Rahal¹⁷⁹, S. Rajagopalan²⁵, M. Rammensee³⁰, A.S. Randle-Conde⁴⁰, C. Rangel-Smith¹⁶⁷, K. Rao¹⁶⁴, F. Rauscher⁹⁹, T.C. Rave⁴⁸, T. Ravenscroft⁵³, M. Raymond³⁰, A.L. Read¹¹⁸, N.P. Readioff⁷³, D.M. Rebuzzi^{120a,120b}, A. Redelbach¹⁷⁵, G. Redlinger²⁵, R. Reece¹³⁸, K. Reeves⁴¹, L. Rehnisch¹⁶, H. Reisin²⁷, M. Relich¹⁶⁴, C. Rembser³⁰, H. Ren^{33a}, Z.L. Ren¹⁵², A. Renaud¹¹⁶, M. Rescigno^{133a}, S. Resconi^{90a}, O.L. Rezanova^{108,s}, P. Reznicek¹²⁸, R. Rezvani⁹⁴, R. Richter¹⁰⁰, M. Ridel⁷⁹, P. Rieck¹⁶, J. Rieger⁵⁴, M. Rijssenbeek¹⁴⁹, A. Rimoldi^{120a,120b}, L. Rinaldi^{20a}, E. Ritsch⁶¹, I. Riu¹², F. Rizatdinova¹¹³, E. Rizvi⁷⁵, S.H. Robertson^{86,i}, A. Robichaud-Veronneau⁸⁶, D. Robinson²⁸, J.E.M. Robinson⁸³, A. Robson⁵³, C. Roda^{123a,123b}, L. Rodrigues³⁰, S. Roe³⁰, O. Røhne¹¹⁸, S. Rolli¹⁶², A. Romaniouk⁹⁷, M. Romano^{20a,20b}, E. Romero Adam¹⁶⁸, N. Rompotis¹³⁹, L. Roos⁷⁹, E. Ros¹⁶⁸, S. Rosati^{133a}, K. Rosbach⁴⁹, M. Rose⁷⁶, P.L. Rosendahl¹⁴, O. Rosenthal¹⁴², V. Rossetti^{147a,147b}, E. Rossi^{103a,103b}, L.P. Rossi^{50a}, R. Rosten¹³⁹, M. Rotaru^{26a}, I. Roth¹⁷³, J. Rothberg¹³⁹, D. Rousseau¹¹⁶, C.R. Royon¹³⁷, A. Rozanov⁸⁴, Y. Rozen¹⁵³, X. Ruan^{146c}, F. Rubbo¹², I. Rubinskiy⁴², V.I. Rud⁹⁸, C. Rudolph⁴⁴, M.S. Rudolph¹⁵⁹, F. Rühr⁴⁸, A. Ruiz-Martinez³⁰, Z. Rurikova⁴⁸, N.A. Rusakovich⁶⁴, A. Ruschke⁹⁹, J.P. Rutherford⁷, N. Ruthmann⁴⁸, Y.F. Ryabov¹²², M. Rybar¹²⁸, G. Rybkin¹¹⁶, N.C. Ryder¹¹⁹, A.F. Saavedra¹⁵¹, S. Sacerdoti²⁷, A. Saddique³, I. Sadeh¹⁵⁴, H.F.-W. Sadrozinski¹³⁸, R. Sadykov⁶⁴, F. Safai Tehrani^{133a}, H. Sakamoto¹⁵⁶, Y. Sakurai¹⁷², G. Salamanna^{135a,135b}, A. Salamon^{134a}, M. Saleem¹¹², D. Salek¹⁰⁶, P.H. Sales De Bruin¹³⁹, D. Saliagic¹⁰⁰, A. Salnikov¹⁴⁴, J. Salt¹⁶⁸, D. Salvatore^{37a,37b}, F. Salvatore¹⁵⁰, A. Salvucci¹⁰⁵, A. Salzburger³⁰, D. Sampsonidis¹⁵⁵, A. Sanchez^{103a,103b}, J. Sánchez¹⁶⁸, V. Sanchez Martinez¹⁶⁸, H. Sandaker¹⁴, R.L. Sandbach⁷⁵, H.G. Sander⁸², M.P. Sanders⁹⁹, M. Sandhoff¹⁷⁶, T. Sandoval²⁸, C. Sandoval¹⁶³, R. Sandstroem¹⁰⁰, D.P.C. Sankey¹³⁰, A. Sansoni⁴⁷, C. Santoni³⁴, R. Santonico^{134a,134b}, H. Santos^{125a}, I. Santoyo Castillo¹⁵⁰, K. Sapp¹²⁴, A. Saponov⁶⁴, J.G. Saraiva^{125a,125d}, B. Sarrazin²¹, G. Sartisoehn¹⁷⁶, O. Sasaki⁶⁵, Y. Sasaki¹⁵⁶, G. Sauvage^{5,*}, E. Sauvan⁵, P. Savard^{159,d}, D.O. Savu³⁰, C. Sawyer¹¹⁹, L. Sawyer^{78,m}, D.H. Saxon⁵³, J. Saxon¹²¹, C. Sbarra^{20a}, A. Sbrizzi³, T. Scanlon⁷⁷, D.A. Scannicchio¹⁶⁴, M. Scarcella¹⁵¹, V. Scarfone^{37a,37b}, J. Schaarschmidt¹⁷³, P. Schacht¹⁰⁰, D. Schaefer¹²¹, R. Schaefer⁴², S. Schaepe²¹, S. Schaetzel^{58b}, U. Schäfer⁸², A.C. Schaffer¹¹⁶, D. Schaile⁹⁹, R.D. Schamberger¹⁴⁹, V. Scharf^{58a}, V.A. Schegelsky¹²², D. Scheirich¹²⁸, M. Schernau¹⁶⁴, M.I. Scherzer³⁵, C. Schiavi^{50a,50b}, J. Schieck⁹⁹, C. Schillo⁴⁸, M. Schioppa^{37a,37b}, S. Schlenker³⁰, E. Schmidt⁴⁸, K. Schmieden³⁰, C. Schmitt⁸², C. Schmitt⁹⁹, S. Schmitt^{58b}, B. Schneider¹⁷, Y.J. Schnellbach⁷³, U. Schnoor⁴⁴, L. Schoeffel¹³⁷, A. Schoening^{58b}, B.D. Schoenrock⁸⁹, A.L.S. Schorlemmer⁵⁴, M. Schott⁸², D. Schouten^{160a}, J. Schovancova²⁵, S. Schramm¹⁵⁹, M. Schreyer¹⁷⁵, C. Schroeder⁸², N. Schuh⁸², M.J. Schultens²¹, H.-C. Schultz-Coulon^{58a}, H. Schulz¹⁶, M. Schumacher⁴⁸, B.A. Schumm¹³⁸, Ph. Schune¹³⁷,

C. Schwanenberger⁸³, A. Schwartzman¹⁴⁴, Ph. Schwegler¹⁰⁰, Ph. Schwemling¹³⁷, R. Schwienhorst⁸⁹, J. Schwindling¹³⁷, T. Schwindt²¹, M. Schwoerer⁵, F.G. Sciaccia¹⁷, E. Scifo¹¹⁶, G. Sciolla²³, W.G. Scott¹³⁰, F. Scuri^{123a,123b}, F. Scutti²¹, J. Searcy⁸⁸, G. Sedov⁴², E. Sedykh¹²², S.C. Seidel¹⁰⁴, A. Seiden¹³⁸, F. Seifert¹²⁷, J.M. Seixas^{24a}, G. Sekhniaidze^{103a}, S.J. Sekula⁴⁰, K.E. Selbach⁴⁶, D.M. Seliverstov^{122,*}, G. Sellers⁷³, N. Semprini-Cesari^{20a,20b}, C. Serfon³⁰, L. Serin¹¹⁶, L. Serkin⁵⁴, T. Serre⁸⁴, R. Seuster^{160a}, H. Severini¹¹², T. Sfiligoi⁷⁴, F. Sforza¹⁰⁰, A. Sfyrila³⁰, E. Shabalina⁵⁴, M. Shamim¹¹⁵, L.Y. Shan^{33a}, R. Shang¹⁶⁶, J.T. Shank²², M. Shapiro¹⁵, P.B. Shatalov⁹⁶, K. Shaw^{165a,165b}, C.Y. Shehu¹⁵⁰, P. Sherwood⁷⁷, L. Shi^{152,ae}, S. Shimizu⁶⁶, C.O. Shimmin¹⁶⁴, M. Shimojima¹⁰¹, M. Shiyakova⁶⁴, A. Shmeleva⁹⁵, M.J. Shochet³¹, D. Short¹¹⁹, S. Shrestha⁶³, E. Shulga⁹⁷, M.A. Shupe⁷, S. Shushkevich⁴², P. Sicho¹²⁶, O. Sidiropoulou¹⁵⁵, D. Sidorov¹¹³, A. Sidoti^{133a}, F. Siegert⁴⁴, Dj. Sijacki^{13a}, J. Silva^{125a,125d}, Y. Silver¹⁵⁴, D. Silverstein¹⁴⁴, S.B. Silverstein^{147a}, V. Simak¹²⁷, O. Simard⁵, Lj. Simic^{13a}, S. Simion¹¹⁶, E. Simioni⁸², B. Simmons⁷⁷, R. Simoniello^{90a,90b}, M. Simonyan³⁶, P. Sinervo¹⁵⁹, N.B. Sinev¹¹⁵, V. Sipica¹⁴², G. Siragusa¹⁷⁵, A. Sircar⁷⁸, A.N. Sisakyan^{64,*}, S.Yu. Sivoklokov⁹⁸, J. Sjölin^{147a,147b}, T.B. Sjursen¹⁴, H.P. Skottowe⁵⁷, K.Yu. Skovpen¹⁰⁸, P. Skubic¹¹², M. Slater¹⁸, T. Slavicek¹²⁷, K. Sliwa¹⁶², V. Smakhtin¹⁷³, B.H. Smart⁴⁶, L. Smestad¹⁴, S.Yu. Smirnov⁹⁷, Y. Smirnov⁹⁷, L.N. Smirnova^{98,af}, O. Smirnova⁸⁰, K.M. Smith⁵³, M. Smizanska⁷¹, K. Smolek¹²⁷, A.A. Snesarev⁹⁵, G. Snidero⁷⁵, S. Snyder²⁵, R. Sobie^{170,i}, F. Socher⁴⁴, A. Soffer¹⁵⁴, D.A. Soh^{152,ae}, C.A. Solans³⁰, M. Solar¹²⁷, J. Solc¹²⁷, E.Yu. Soldatov⁹⁷, U. Soldevila¹⁶⁸, E. Solfaroli Camillocci^{133a,133b}, A.A. Solodkov¹²⁹, A. Soloshenko⁶⁴, O.V. Solovyanov¹²⁹, V. Solovyev¹²², P. Sommer⁴⁸, H.Y. Song^{33b}, N. Soni¹, A. Sood¹⁵, A. Sopczak¹²⁷, B. Sopko¹²⁷, V. Sopko¹²⁷, V. Sorin¹², M. Sosebee⁸, R. Soualah^{165a,165c}, P. Soueid⁹⁴, A.M. Soukharev¹⁰⁸, D. South⁴², S. Spagnolo^{72a,72b}, F. Spanò⁷⁶, W.R. Spearman⁵⁷, R. Spighi^{20a}, G. Spigo³⁰, M. Spousta¹²⁸, T. Spreitzer¹⁵⁹, B. Spurlock⁸, R.D. St. Denis^{53,*}, S. Staerz⁴⁴, J. Stahlman¹²¹, R. Stamen^{58a}, E. Stanecka³⁹, R.W. Stanek⁶, C. Stanescu^{135a}, M. Stanescu-Bellu⁴², M.M. Stanitzki⁴², S. Stapnes¹¹⁸, E.A. Starchenko¹²⁹, J. Stark⁵⁵, P. Staroba¹²⁶, P. Starovoitov⁴², R. Staszewski³⁹, P. Stavina^{145a,*}, P. Steinberg²⁵, B. Stelzer¹⁴³, H.J. Stelzer³⁰, O. Stelzer-Chilton^{160a}, H. Stenzel⁵², S. Stern¹⁰⁰, G.A. Stewart⁵³, J.A. Stillings²¹, M.C. Stockton⁸⁶, M. Stoebe⁸⁶, G. Stoicea^{26a}, P. Stolte⁵⁴, S. Stonjek¹⁰⁰, A.R. Stradling⁸, A. Straessner⁴⁴, M.E. Stramaglia¹⁷, J. Strandberg¹⁴⁸, S. Strandberg^{147a,147b}, A. Strandlie¹¹⁸, E. Strauss¹⁴⁴, M. Strauss¹¹², P. Strizenec^{145b}, R. Ströhmer¹⁷⁵, D.M. Strom¹¹⁵, R. Stroynowski⁴⁰, S.A. Stucci¹⁷, B. Stugu¹⁴, N.A. Styles⁴², D. Su¹⁴⁴, J. Su¹²⁴, R. Subramaniam⁷⁸, A. Succurro¹², Y. Sugaya¹¹⁷, C. Suhr¹⁰⁷, M. Suk¹²⁷, V.V. Sulin⁹⁵, S. Sultansoy^{4c}, T. Sumida⁶⁷, X. Sun^{33a}, J.E. Sundermann⁴⁸, K. Suruliz¹⁴⁰, G. Susinno^{37a,37b}, M.R. Sutton¹⁵⁰, Y. Suzuki⁶⁵, M. Svatos¹²⁶, S. Swedish¹⁶⁹, M. Swiatlowski¹⁴⁴, I. Sykora^{145a}, T. Sykora¹²⁸, D. Ta⁸⁹, C. Taccini^{135a,135b}, K. Tackmann⁴², J. Taenzer¹⁵⁹, A. Taffard¹⁶⁴, R. Tafirout^{160a}, N. Taiblum¹⁵⁴, H. Takai²⁵, R. Takashima⁶⁸, H. Takeda⁶⁶, T. Takeshita¹⁴¹, Y. Takubo⁶⁵, M. Talby⁸⁴, A.A. Talyshev^{108,s}, J.Y.C. Tam¹⁷⁵, K.G. Tan⁸⁷, J. Tanaka¹⁵⁶, R. Tanaka¹¹⁶, S. Tanaka¹³², S. Tanaka⁶⁵, A.J. Tanasijczuk¹⁴³, B.B. Tannenwald¹¹⁰, N. Tannoury²¹, S. Tapprogge⁸², S. Tarem¹⁵³, F. Tarrade²⁹, G.F. Tartarelli^{90a}, P. Tas¹²⁸, M. Tasevsky¹²⁶, T. Tashiro⁶⁷, E. Tassi^{37a,37b}, A. Tavares Delgado^{125a,125b}, Y. Tayalati^{136d}, F.E. Taylor⁹³, G.N. Taylor⁸⁷, W. Taylor^{160b}, F.A. Teischinger³⁰, M. Teixeira Dias Castanheira⁷⁵, P. Teixeira-Dias⁷⁶, K.K. Temming⁴⁸, H. Ten Kate³⁰, P.K. Teng¹⁵², J.J. Teoh¹¹⁷, S. Terada⁶⁵, K. Terashi¹⁵⁶, J. Terron⁸¹, S. Terzo¹⁰⁰, M. Testa⁴⁷, R.J. Teuscher^{159,i}, J. Therhaag²¹, T. Theveneaux-Pelzer³⁴, J.P. Thomas¹⁸, J. Thomas-Wilsker⁷⁶, E.N. Thompson³⁵, P.D. Thompson¹⁸, P.D. Thompson¹⁵⁹, A.S. Thompson⁵³, L.A. Thomsen³⁶, E. Thomson¹²¹, M. Thomson²⁸, W.M. Thong⁸⁷, R.P. Thun^{88,*}, F. Tian³⁵, M.J. Tibbetts¹⁵, V.O. Tikhomirov^{95,ag}, Yu.A. Tikhonov^{108,s}, S. Timoshenko⁹⁷, E. Tiouchichine⁸⁴, P. Tipton¹⁷⁷, S. Tisserant⁸⁴, T. Todorov⁵, S. Todorova-Nova¹²⁸, B. Toggerson⁷, J. Tojo⁶⁹, S. Tokár^{145a}, K. Tokushuku⁶⁵, K. Tollefson⁸⁹, L. Tomlinson⁸³, M. Tomoto¹⁰², L. Tompkins³¹, K. Toms¹⁰⁴, N.D. Topilin⁶⁴, E. Torrence¹¹⁵, H. Torres¹⁴³, E. Torró Pastor¹⁶⁸, J. Toth^{84,ah}, F. Touchard⁸⁴, D.R. Tovey¹⁴⁰, H.L. Tran¹¹⁶, T. Trefzger¹⁷⁵, L. Tremblet³⁰, A. Tricoli³⁰, I.M. Trigger^{160a}, S. Trincaz-Duvold⁷⁹, M.F. Tripiana¹², W. Trischuk¹⁵⁹, B. Trocmé⁵⁵, C. Troncon^{90a}, M. Trotter-McDonald¹⁴³, M. Trovatelli^{135a,135b}, P. True⁸⁹, M. Trzebinski³⁹, A. Trzupek³⁹, C. Tsarouchas³⁰, J.C.-L. Tseng¹¹⁹, P.V. Tsiarehshka⁹¹, D. Tsiou¹³⁷, G. Tsipolitis¹⁰, N. Tsirintanis⁹, S. Tsiskaridze¹², V. Tsiskaridze⁴⁸, E.G. Tskhadadze^{51a}, I.I. Tsukerman⁹⁶, V. Tsulaia¹⁵, S. Tsuno⁶⁵, D. Tsybychev¹⁴⁹, A. Tudorache^{26a}, V. Tudorache^{26a}, A.N. Tuna¹²¹, S.A. Tupputi^{20a,20b}, S. Turchikhin^{98,af}, D. Turecek¹²⁷, I. Turk Cakir^{4d}, R. Turra^{90a,90b}, P.M. Tuts³⁵, A. Tykhonov⁴⁹, M. Tylmad^{147a,147b}, M. Tyndel¹³⁰, K. Uchida²¹, I. Ueda¹⁵⁶

R. Ueno²⁹, M. Ughetto⁸⁴, M. Ugland¹⁴, M. Uhlenbrock²¹, F. Ukegawa¹⁶¹, G. Unal³⁰, A. Undrus²⁵, G. Unel¹⁶⁴, F.C. Ungaro⁴⁸, Y. Unno⁶⁵, D. Urbaniec³⁵, P. Urquijo⁸⁷, G. Usai⁸, A. Usanova⁶¹, L. Vacavant⁸⁴, V. Vacek¹²⁷, B. Vachon⁸⁶, N. Valencic¹⁰⁶, S. Valentinetti^{20a,20b}, A. Valero¹⁶⁸, L. Valery³⁴, S. Valkar¹²⁸, E. Valladolid Gallego¹⁶⁸, S. Vallecorsa⁴⁹, J.A. Valls Ferrer¹⁶⁸, W. Van Den Wollenberg¹⁰⁶, P.C. Van Der Deijl¹⁰⁶, R. van der Geer¹⁰⁶, H. van der Graaf¹⁰⁶, R. Van Der Leeuw¹⁰⁶, D. van der Ster³⁰, N. van Eldik³⁰, P. van Gemmeren⁶, J. Van Nieuwkoop¹⁴³, I. van Vulpen¹⁰⁶, M.C. van Woerden³⁰, M. Vanadia^{133a,133b}, W. Vandelli³⁰, R. Vanguri¹²¹, A. Vaniachine⁶, P. Vankov⁴², F. Vannucci⁷⁹, G. Vardanyan¹⁷⁸, R. Vari^{133a}, E.W. Varnes⁷, T. Varol⁸⁵, D. Varouchas⁷⁹, A. Vartapetian⁸, K.E. Varvell¹⁵¹, F. Vazeille³⁴, T. Vazquez Schroeder⁵⁴, J. Veatch⁷, F. Veloso^{125a,125c}, S. Veneziano^{133a}, A. Ventura^{72a,72b}, D. Ventura⁸⁵, M. Venturi¹⁷⁰, N. Venturi¹⁵⁹, A. Venturini²³, V. Vercesi^{120a}, M. Verducci^{133a,133b}, W. Verkerke¹⁰⁶, J.C. Vermeulen¹⁰⁶, A. Vest⁴⁴, M.C. Vetterli^{143,d}, O. Viazlo⁸⁰, I. Vichou¹⁶⁶, T. Vickey^{146c,ai}, O.E. Vickey Boeriu^{146c}, G.H.A. Viehhauser¹¹⁹, S. Viel¹⁶⁹, R. Vigne³⁰, M. Villa^{20a,20b}, M. Villaplana Perez^{90a,90b}, E. Vilucchi⁴⁷, M.G. Vinciter²⁹, V.B. Vinogradov⁶⁴, J. Virzi¹⁵, I. Vivarelli¹⁵⁰, F. Vives Vaque³, S. Vlachos¹⁰, D. Vladoiu⁹⁹, M. Vlasak¹²⁷, A. Vogel²¹, M. Vogel^{32a}, P. Vokac¹²⁷, G. Volpi^{123a,123b}, M. Volpi⁸⁷, H. von der Schmitt¹⁰⁰, H. von Radziewski⁴⁸, E. von Toerne²¹, V. Vorobel¹²⁸, K. Vorobev⁹⁷, M. Vos¹⁶⁸, R. Voss³⁰, J.H. Vossebeld⁷³, N. Vranjes¹³⁷, M. Vranjes Milosavljevic¹⁰⁶, V. Vrba¹²⁶, M. Vreeswijk¹⁰⁶, T. Vu Anh⁴⁸, R. Vuillermet³⁰, I. Vukotic³¹, Z. Vykydal¹²⁷, P. Wagner²¹, W. Wagner¹⁷⁶, H. Wahlberg⁷⁰, S. Wahrmund⁴⁴, J. Wakabayashi¹⁰², J. Walder⁷¹, R. Walker⁹⁹, W. Walkowiak¹⁴², R. Wall¹⁷⁷, P. Waller⁷³, B. Walsh¹⁷⁷, C. Wang^{152,qj}, C. Wang⁴⁵, F. Wang¹⁷⁴, H. Wang¹⁵, H. Wang⁴⁰, J. Wang⁴², J. Wang^{33a}, K. Wang⁸⁶, R. Wang¹⁰⁴, S.M. Wang¹⁵², T. Wang²¹, X. Wang¹⁷⁷, C. Wanotayaroj¹¹⁵, A. Warburton⁸⁶, C.P. Ward²⁸, D.R. Wardrope⁷⁷, M. Warsinsky⁴⁸, A. Washbrook⁴⁶, C. Wasicki⁴², P.M. Watkins¹⁸, A.T. Watson¹⁸, I.J. Watson¹⁵¹, M.F. Watson¹⁸, G. Watts¹³⁹, S. Watts⁸³, B.M. Waugh⁷⁷, S. Webb⁸³, M.S. Weber¹⁷, S.W. Weber¹⁷⁵, J.S. Webster³¹, A.R. Weidberg¹¹⁹, P. Weigell¹⁰⁰, B. Weinert⁶⁰, J. Weingarten⁵⁴, C. Weiser⁴⁸, H. Weits¹⁰⁶, P.S. Wells³⁰, T. Wenaus²⁵, D. Wendland¹⁶, Z. Weng^{152,ae}, T. Wengler³⁰, S. Wenig³⁰, N. Wermes²¹, M. Werner⁴⁸, P. Werner³⁰, M. Wessels^{58a}, J. Wetter¹⁶², K. Whalen²⁹, A. White⁸, M.J. White¹, R. White^{32b}, S. White^{123a,123b}, D. Whiteson¹⁶⁴, D. Wicke¹⁷⁶, F.J. Wickens¹³⁰, W. Wiedenmann¹⁷⁴, M. Wielers¹³⁰, P. Wienemann²¹, C. Wiglesworth³⁶, L.A.M. Wiik-Fuchs²¹, P.A. Wijeratne⁷⁷, A. Wildauer¹⁰⁰, M.A. Wildt^{42,ak}, H.G. Wilkens³⁰, J.Z. Will⁹⁹, H.H. Williams¹²¹, S. Williams²⁸, C. Willis⁸⁹, S. Willocq⁸⁵, A. Wilson⁸⁸, J.A. Wilson¹⁸, I. Wingerter-Seez⁵, F. Winklmeier¹¹⁵, B.T. Winter²¹, M. Wittgen¹⁴⁴, T. Wittig⁴³, J. Wittkowski⁹⁹, S.J. Wollstadt⁸², M.W. Wolter³⁹, H. Wolters^{125a,125c}, B.K. Wosiek³⁹, J. Wotschack³⁰, M.J. Woudstra⁸³, K.W. Wozniak³⁹, M. Wright⁵³, M. Wu⁵⁵, S.L. Wu¹⁷⁴, X. Wu⁴⁹, Y. Wu⁸⁸, E. Wulf³⁵, T.R. Wyatt⁸³, B.M. Wynne⁴⁶, S. Xella³⁶, M. Xiao¹³⁷, D. Xu^{33a}, L. Xu^{33b,al}, B. Yabsley¹⁵¹, S. Yacoob^{146b,am}, M. Yamada⁶⁵, H. Yamaguchi¹⁵⁶, Y. Yamaguchi¹¹⁷, A. Yamamoto⁶⁵, K. Yamamoto⁶³, S. Yamamoto¹⁵⁶, T. Yamamura¹⁵⁶, T. Yamanaka¹⁵⁶, K. Yamauchi¹⁰², Y. Yamazaki⁶⁶, Z. Yan²², H. Yang^{33e}, H. Yang¹⁷⁴, U.K. Yang⁸³, Y. Yang¹¹⁰, S. Yanush⁹², L. Yao^{33a}, W.-M. Yao¹⁵, Y. Yasu⁶⁵, E. Yatsenko⁴², K.H. Yau Wong²¹, J. Ye⁴⁰, S. Ye²⁵, A.L. Yen⁵⁷, E. Yildirim⁴², M. Yilmaz^{4b}, R. Yoosoofmiya¹²⁴, K. Yorita¹⁷², R. Yoshida⁶, K. Yoshihara¹⁵⁶, C. Young¹⁴⁴, C.J.S. Young³⁰, S. Youssef²², D.R. Yu¹⁵, J. Yu⁸, J.M. Yu⁸⁸, J. Yu¹¹³, L. Yuan⁶⁶, A. Yurkewicz¹⁰⁷, I. Yusuf^{28,an}, B. Zabinski³⁹, R. Zaidan⁶², A.M. Zaitsev^{129,z}, A. Zaman¹⁴⁹, S. Zambito²³, L. Zanello^{133a,133b}, D. Zanzi¹⁰⁰, C. Zeitnitz¹⁷⁶, M. Zeman¹²⁷, A. Zemla^{38a}, K. Zengel²³, O. Zenin¹²⁹, T. Ženiš^{145a}, D. Zerwas¹¹⁶, G. Zevi della Porta⁵⁷, D. Zhang⁸⁸, F. Zhang¹⁷⁴, H. Zhang⁸⁹, J. Zhang⁶, L. Zhang¹⁵², X. Zhang^{33d}, Z. Zhang¹¹⁶, Z. Zhao^{33b}, A. Zhemchugov⁶⁴, J. Zhong¹¹⁹, B. Zhou⁸⁸, L. Zhou³⁵, N. Zhou¹⁶⁴, C.G. Zhu^{33d}, H. Zhu^{33a}, J. Zhu⁸⁸, Y. Zhu^{33b}, X. Zhuang^{33a}, K. Zhukov⁹⁵, A. Zibell¹⁷⁵, D. Zieminska⁶⁰, N.I. Zimine⁶⁴, C. Zimmermann⁸², R. Zimmermann²¹, S. Zimmermann²¹, S. Zimmermann⁴⁸, Z. Zinonos⁵⁴, M. Ziolkowski¹⁴², G. Zobernig¹⁷⁴, A. Zoccoli^{20a,20b}, M. zur Nedden¹⁶, G. Zurzolo^{103a,103b}, V. Zutshi¹⁰⁷, L. Zwalinski³⁰

¹ Department of Physics, University of Adelaide, Adelaide, Australia² Physics Department, SUNY Albany, Albany, NY, United States³ Department of Physics, University of Alberta, Edmonton, AB, Canada⁴ (a) Department of Physics, Ankara University, Ankara; (b) Department of Physics, Gazi University, Ankara; (c) Division of Physics, TOBB University of Economics and Technology, Ankara;

(d) Turkish Atomic Energy Authority, Ankara, Turkey

⁵ LAPP, CNRS/IN2P3 and Université de Savoie, Annecy-le-Vieux, France⁶ High Energy Physics Division, Argonne National Laboratory, Argonne, IL, United States

- ⁷ Department of Physics, University of Arizona, Tucson, AZ, United States
- ⁸ Department of Physics, The University of Texas at Arlington, Arlington, TX, United States
- ⁹ Physics Department, University of Athens, Athens, Greece
- ¹⁰ Physics Department, National Technical University of Athens, Zografou, Greece
- ¹¹ Institute of Physics, Azerbaijan Academy of Sciences, Baku, Azerbaijan
- ¹² Institut de Física d'Altes Energies and Departament de Física de la Universitat Autònoma de Barcelona, Barcelona, Spain
- ¹³ ^(a) Institute of Physics, University of Belgrade, Belgrade; ^(b) Vinca Institute of Nuclear Sciences, University of Belgrade, Belgrade, Serbia
- ¹⁴ Department for Physics and Technology, University of Bergen, Bergen, Norway
- ¹⁵ Physics Division, Lawrence Berkeley National Laboratory and University of California, Berkeley, CA, United States
- ¹⁶ Department of Physics, Humboldt University, Berlin, Germany
- ¹⁷ Albert Einstein Center for Fundamental Physics and Laboratory for High Energy Physics, University of Bern, Bern, Switzerland
- ¹⁸ School of Physics and Astronomy, University of Birmingham, Birmingham, United Kingdom
- ¹⁹ ^(a) Department of Physics, Bogazici University, Istanbul; ^(b) Department of Physics, Dogus University, Istanbul; ^(c) Department of Physics Engineering, Gaziantep University, Gaziantep, Turkey
- ²⁰ ^(a) INFN Sezione di Bologna; ^(b) Dipartimento di Fisica e Astronomia, Università di Bologna, Bologna, Italy
- ²¹ Physikalisches Institut, University of Bonn, Bonn, Germany
- ²² Department of Physics, Boston University, Boston, MA, United States
- ²³ Department of Physics, Brandeis University, Waltham, MA, United States
- ²⁴ ^(a) Universidade Federal do Rio De Janeiro COPPE/EE/IF, Rio de Janeiro; ^(b) Federal University of Juiz de Fora (UFJF), Juiz de Fora; ^(c) Federal University of Sao Joao del Rei (UFSJ), Sao Joao del Rei; ^(d) Instituto de Física, Universidade de Sao Paulo, Sao Paulo, Brazil
- ²⁵ Physics Department, Brookhaven National Laboratory, Upton, NY, United States
- ²⁶ ^(a) National Institute of Physics and Nuclear Engineering, Bucharest; ^(b) National Institute for Research and Development of Isotopic and Molecular Technologies, Physics Department, Cluj Napoca; ^(c) University Politehnica Bucharest, Bucharest; ^(d) West University in Timisoara, Timisoara, Romania
- ²⁷ Departamento de Física, Universidad de Buenos Aires, Buenos Aires, Argentina
- ²⁸ Cavendish Laboratory, University of Cambridge, Cambridge, United Kingdom
- ²⁹ Department of Physics, Carleton University, Ottawa, ON, Canada
- ³⁰ CERN, Geneva, Switzerland
- ³¹ Enrico Fermi Institute, University of Chicago, Chicago, IL, United States
- ³² ^(a) Departamento de Física, Pontificia Universidad Católica de Chile, Santiago; ^(b) Departamento de Física, Universidad Técnica Federico Santa María, Valparaíso, Chile
- ³³ ^(a) Institute of High Energy Physics, Chinese Academy of Sciences, Beijing; ^(b) Department of Modern Physics, University of Science and Technology of China, Anhui; ^(c) Department of Physics, Nanjing University, Jiangsu; ^(d) School of Physics, Shandong University, Shandong; ^(e) Physics Department, Shanghai Jiao Tong University, Shanghai, China
- ³⁴ Laboratoire de Physique Corpusculaire, Clermont Université et Université Blaise Pascal and CNRS/IN2P3, Clermont-Ferrand, France
- ³⁵ Nevis Laboratory, Columbia University, Irvington, NY, United States
- ³⁶ Niels Bohr Institute, University of Copenhagen, Copenhagen, Denmark
- ³⁷ ^(a) INFN Gruppo Collegato di Cosenza, Laboratori Nazionali di Frascati; ^(b) Dipartimento di Fisica, Università della Calabria, Rende, Italy
- ³⁸ ^(a) AGH University of Science and Technology, Faculty of Physics and Applied Computer Science, Krakow; ^(b) Marian Smoluchowski Institute of Physics, Jagiellonian University, Krakow, Poland
- ³⁹ The Henryk Niewodniczanski Institute of Nuclear Physics, Polish Academy of Sciences, Krakow, Poland
- ⁴⁰ Physics Department, Southern Methodist University, Dallas, TX, United States
- ⁴¹ Physics Department, University of Texas at Dallas, Richardson, TX, United States
- ⁴² DESY, Hamburg and Zeuthen, Germany
- ⁴³ Institut für Experimentelle Physik IV, Technische Universität Dortmund, Dortmund, Germany
- ⁴⁴ Institut für Kern- und Teilchenphysik, Technische Universität Dresden, Dresden, Germany
- ⁴⁵ Department of Physics, Duke University, Durham, NC, United States
- ⁴⁶ SUPA – School of Physics and Astronomy, University of Edinburgh, Edinburgh, United Kingdom
- ⁴⁷ INFN Laboratori Nazionali di Frascati, Frascati, Italy
- ⁴⁸ Fakultät für Mathematik und Physik, Albert-Ludwigs-Universität, Freiburg, Germany
- ⁴⁹ Section de Physique, Université de Genève, Geneva, Switzerland
- ⁵⁰ ^(a) INFN Sezione di Genova; ^(b) Dipartimento di Fisica, Università di Genova, Genova, Italy
- ⁵¹ ^(a) E. Andronikashvili Institute of Physics, Iv. Javakishvili Tbilisi State University, Tbilisi; ^(b) High Energy Physics Institute, Tbilisi State University, Tbilisi, Georgia
- ⁵² II Physikalisches Institut, Justus-Liebig-Universität Giessen, Giessen, Germany
- ⁵³ SUPA – School of Physics and Astronomy, University of Glasgow, Glasgow, United Kingdom
- ⁵⁴ II Physikalisches Institut, Georg-August-Universität, Göttingen, Germany
- ⁵⁵ Laboratoire de Physique Subatomique et de Cosmologie, Université Grenoble-Alpes, CNRS/IN2P3, Grenoble, France
- ⁵⁶ Department of Physics, Hampton University, Hampton, VA, United States
- ⁵⁷ Laboratory for Particle Physics and Cosmology, Harvard University, Cambridge, MA, United States
- ⁵⁸ ^(a) Kirchhoff-Institut für Physik, Ruprecht-Karls-Universität Heidelberg, Heidelberg; ^(b) Physikalisches Institut, Ruprecht-Karls-Universität Heidelberg, Heidelberg; ^(c) ZITI Institut für technische Informatik, Ruprecht-Karls-Universität Heidelberg, Mannheim, Germany
- ⁵⁹ Faculty of Applied Information Science, Hiroshima Institute of Technology, Hiroshima, Japan
- ⁶⁰ Department of Physics, Indiana University, Bloomington, IN, United States
- ⁶¹ Institut für Astro- und Teilchenphysik, Leopold-Franzens-Universität, Innsbruck, Austria
- ⁶² University of Iowa, Iowa City, IA, United States
- ⁶³ Department of Physics and Astronomy, Iowa State University, Ames, IA, United States
- ⁶⁴ Joint Institute for Nuclear Research, JINR Dubna, Dubna, Russia
- ⁶⁵ KEK, High Energy Accelerator Research Organization, Tsukuba, Japan
- ⁶⁶ Graduate School of Science, Kobe University, Kobe, Japan
- ⁶⁷ Faculty of Science, Kyoto University, Kyoto, Japan
- ⁶⁸ Kyoto University of Education, Kyoto, Japan
- ⁶⁹ Department of Physics, Kyushu University, Fukuoka, Japan
- ⁷⁰ Instituto de Física La Plata, Universidad Nacional de La Plata and CONICET, La Plata, Argentina
- ⁷¹ Physics Department, Lancaster University, Lancaster, United Kingdom
- ⁷² ^(a) INFN Sezione di Lecce; ^(b) Dipartimento di Matematica e Fisica, Università del Salento, Lecce, Italy
- ⁷³ Oliver Lodge Laboratory, University of Liverpool, Liverpool, United Kingdom
- ⁷⁴ Department of Physics, Jozef Stefan Institute and University of Ljubljana, Ljubljana, Slovenia
- ⁷⁵ School of Physics and Astronomy, Queen Mary University of London, London, United Kingdom
- ⁷⁶ Department of Physics, Royal Holloway University of London, Surrey, United Kingdom
- ⁷⁷ Department of Physics and Astronomy, University College London, London, United Kingdom
- ⁷⁸ Louisiana Tech University, Ruston, LA, United States
- ⁷⁹ Laboratoire de Physique Nucléaire et de Hautes Energies, UPMC and Université Paris-Diderot and CNRS/IN2P3, Paris, France

- ⁸⁰ Fysiska institutionen, Lunds universitet, Lund, Sweden
- ⁸¹ Departamento de Física Teórica C-15, Universidad Autónoma de Madrid, Madrid, Spain
- ⁸² Institut für Physik, Universität Mainz, Mainz, Germany
- ⁸³ School of Physics and Astronomy, University of Manchester, Manchester, United Kingdom
- ⁸⁴ CPPM, Aix-Marseille Université and CNRS/IN2P3, Marseille, France
- ⁸⁵ Department of Physics, University of Massachusetts, Amherst, MA, United States
- ⁸⁶ Department of Physics, McGill University, Montreal, QC, Canada
- ⁸⁷ School of Physics, University of Melbourne, Victoria, Australia
- ⁸⁸ Department of Physics, The University of Michigan, Ann Arbor, MI, United States
- ⁸⁹ Department of Physics and Astronomy, Michigan State University, East Lansing, MI, United States
- ⁹⁰ ^(a) INFN Sezione di Milano; ^(b) Dipartimento di Fisica, Università di Milano, Milano, Italy
- ⁹¹ B.I. Stepanov Institute of Physics, National Academy of Sciences of Belarus, Minsk, Belarus
- ⁹² National Scientific and Educational Centre for Particle and High Energy Physics, Minsk, Belarus
- ⁹³ Department of Physics, Massachusetts Institute of Technology, Cambridge, MA, United States
- ⁹⁴ Group of Particle Physics, University of Montreal, Montreal, QC, Canada
- ⁹⁵ P.N. Lebedev Institute of Physics, Academy of Sciences, Moscow, Russia
- ⁹⁶ Institute for Theoretical and Experimental Physics (ITEP), Moscow, Russia
- ⁹⁷ Moscow Engineering and Physics Institute (MEPhI), Moscow, Russia
- ⁹⁸ D.V. Skobel'syn Institute of Nuclear Physics, M.V. Lomonosov Moscow State University, Moscow, Russia
- ⁹⁹ Fakultät für Physik, Ludwig-Maximilians-Universität München, München, Germany
- ¹⁰⁰ Max-Planck-Institut für Physik (Werner-Heisenberg-Institut), München, Germany
- ¹⁰¹ Nagasaki Institute of Applied Science, Nagasaki, Japan
- ¹⁰² Graduate School of Science and Kobayashi–Maskawa Institute, Nagoya University, Nagoya, Japan
- ¹⁰³ ^(a) INFN Sezione di Napoli; ^(b) Dipartimento di Fisica, Università di Napoli, Napoli, Italy
- ¹⁰⁴ Department of Physics and Astronomy, University of New Mexico, Albuquerque, NM, United States
- ¹⁰⁵ Institute for Mathematics, Astrophysics and Particle Physics, Radboud University Nijmegen/Nikhef, Nijmegen, Netherlands
- ¹⁰⁶ Nikhef National Institute for Subatomic Physics and University of Amsterdam, Amsterdam, Netherlands
- ¹⁰⁷ Department of Physics, Northern Illinois University, DeKalb, IL, United States
- ¹⁰⁸ Budker Institute of Nuclear Physics, SB RAS, Novosibirsk, Russia
- ¹⁰⁹ Department of Physics, New York University, New York, NY, United States
- ¹¹⁰ Ohio State University, Columbus, OH, United States
- ¹¹¹ Faculty of Science, Okayama University, Okayama, Japan
- ¹¹² Homer L. Dodge Department of Physics and Astronomy, University of Oklahoma, Norman, OK, United States
- ¹¹³ Department of Physics, Oklahoma State University, Stillwater, OK, United States
- ¹¹⁴ Palacký University, RCPTM, Olomouc, Czech Republic
- ¹¹⁵ Center for High Energy Physics, University of Oregon, Eugene, OR, United States
- ¹¹⁶ LAL, Université Paris-Sud and CNRS/IN2P3, Orsay, France
- ¹¹⁷ Graduate School of Science, Osaka University, Osaka, Japan
- ¹¹⁸ Department of Physics, University of Oslo, Oslo, Norway
- ¹¹⁹ Department of Physics, Oxford University, Oxford, United Kingdom
- ¹²⁰ ^(a) INFN Sezione di Pavia; ^(b) Dipartimento di Fisica, Università di Pavia, Pavia, Italy
- ¹²¹ Department of Physics, University of Pennsylvania, Philadelphia, PA, United States
- ¹²² Petersburg Nuclear Physics Institute, Gatchina, Russia
- ¹²³ ^(a) INFN Sezione di Pisa; ^(b) Dipartimento di Fisica E. Fermi, Università di Pisa, Pisa, Italy
- ¹²⁴ Department of Physics and Astronomy, University of Pittsburgh, Pittsburgh, PA, United States
- ¹²⁵ ^(a) Laboratório de Instrumentação e Física Experimental de Partículas – LIP, Lisboa; ^(b) Faculdade de Ciências, Universidade de Lisboa, Lisboa; ^(c) Department of Physics, University of Coimbra, Coimbra; ^(d) Centro de Física Nuclear da Universidade de Lisboa, Lisboa; ^(e) Departamento de Física, Universidade do Minho, Braga; ^(f) Departamento de Física Teórica y del Cosmos and CAFPE, Universidad de Granada, Granada (Spain); ^(g) Dep Física and CEFITEC of Faculdade de Ciências e Tecnologia, Universidade Nova de Lisboa, Caparica, Portugal
- ¹²⁶ Institute of Physics, Academy of Sciences of the Czech Republic, Praha, Czech Republic
- ¹²⁷ Czech Technical University in Prague, Praha, Czech Republic
- ¹²⁸ Faculty of Mathematics and Physics, Charles University in Prague, Praha, Czech Republic
- ¹²⁹ State Research Center Institute for High Energy Physics, Protvino, Russia
- ¹³⁰ Particle Physics Department, Rutherford Appleton Laboratory, Didcot, United Kingdom
- ¹³¹ Physics Department, University of Regina, Regina, SK, Canada
- ¹³² Ritsumeikan University, Kusatsu, Shiga, Japan
- ¹³³ ^(a) INFN Sezione di Roma; ^(b) Dipartimento di Fisica, Sapienza Università di Roma, Roma, Italy
- ¹³⁴ ^(a) INFN Sezione di Roma Tor Vergata; ^(b) Dipartimento di Fisica, Università di Roma Tor Vergata, Roma, Italy
- ¹³⁵ ^(a) INFN Sezione di Roma Tre; ^(b) Dipartimento di Matematica e Fisica, Università Roma Tre, Roma, Italy
- ¹³⁶ ^(a) Faculté des Sciences Ain Chock, Réseau Universitaire de Physique des Hautes Energies – Université Hassan II, Casablanca; ^(b) Centre National de l'Energie des Sciences Techniques Nucleaires, Rabat; ^(c) Faculté des Sciences Semlalia, Université Cadi Ayyad, LPHEA, Marrakech; ^(d) Faculté des Sciences, Université Mohamed Premier and LPTPM, Oujda;
- ¹³⁷ ^(e) Faculté des sciences, Université Mohammed V-Agdal, Rabat, Morocco
- ¹³⁸ DSM/IRFU (Institut de Recherches sur les Lois Fondamentales de l'Univers), CEA Saclay (Commissariat à l'Energie Atomique et aux Energies Alternatives), Gif-sur-Yvette, France
- ¹³⁹ Santa Cruz Institute for Particle Physics, University of California Santa Cruz, Santa Cruz, CA, United States
- ¹⁴⁰ Department of Physics, University of Washington, Seattle, WA, United States
- ¹⁴¹ Department of Physics and Astronomy, University of Sheffield, Sheffield, United Kingdom
- ¹⁴² Department of Physics, Shinshu University, Nagano, Japan
- ¹⁴³ Fachbereich Physik, Universität Siegen, Siegen, Germany
- ¹⁴⁴ Department of Physics, Simon Fraser University, Burnaby, BC, Canada
- ¹⁴⁵ SLAC National Accelerator Laboratory, Stanford, CA, United States
- ¹⁴⁶ ^(a) Faculty of Mathematics, Physics & Informatics, Comenius University, Bratislava; ^(b) Department of Subnuclear Physics, Institute of Experimental Physics of the Slovak Academy of Sciences, Kosice, Slovak Republic
- ¹⁴⁷ ^(a) Department of Physics, University of Cape Town, Cape Town; ^(b) Department of Physics, University of Johannesburg, Johannesburg; ^(c) School of Physics, University of the Witwatersrand, Johannesburg, South Africa
- ¹⁴⁸ ^(a) Department of Physics, Stockholm University; ^(b) The Oskar Klein Centre, Stockholm, Sweden
- ¹⁴⁹ Physics Department, Royal Institute of Technology, Stockholm, Sweden
- ¹⁵⁰ Departments of Physics & Astronomy and Chemistry, Stony Brook University, Stony Brook, NY, United States
- ¹⁵¹ Department of Physics and Astronomy, University of Sussex, Brighton, United Kingdom
- ¹⁵² School of Physics, University of Sydney, Sydney, Australia
- ¹⁵³ Institute of Physics, Academia Sinica, Taipei, Taiwan

- ¹⁵³ Department of Physics, Technion: Israel Institute of Technology, Haifa, Israel
¹⁵⁴ Raymond and Beverly Sackler School of Physics and Astronomy, Tel Aviv University, Tel Aviv, Israel
¹⁵⁵ Department of Physics, Aristotle University of Thessaloniki, Thessaloniki, Greece
¹⁵⁶ International Center for Elementary Particle Physics and Department of Physics, The University of Tokyo, Tokyo, Japan
¹⁵⁷ Graduate School of Science and Technology, Tokyo Metropolitan University, Tokyo, Japan
¹⁵⁸ Department of Physics, Tokyo Institute of Technology, Tokyo, Japan
¹⁵⁹ Department of Physics, University of Toronto, Toronto, ON, Canada
¹⁶⁰ ^(a) TRIUMF, Vancouver, BC; ^(b) Department of Physics and Astronomy, York University, Toronto, ON, Canada
¹⁶¹ Faculty of Pure and Applied Sciences, University of Tsukuba, Tsukuba, Japan
¹⁶² Department of Physics and Astronomy, Tufts University, Medford, MA, United States
¹⁶³ Centro de Investigaciones, Universidad Antonio Narino, Bogota, Colombia
¹⁶⁴ Department of Physics and Astronomy, University of California Irvine, Irvine, CA, United States
¹⁶⁵ ^(a) INFN Gruppo Collegato di Udine, Sezione di Trieste, Udine; ^(b) ICTP, Trieste; ^(c) Dipartimento di Chimica, Fisica e Ambiente, Università di Udine, Udine, Italy
¹⁶⁶ Department of Physics, University of Illinois, Urbana, IL, United States
¹⁶⁷ Department of Physics and Astronomy, University of Uppsala, Uppsala, Sweden
¹⁶⁸ Instituto de Física Corpuscular (IFIC) and Departamento de Física Atómica, Molecular y Nuclear and Departamento de Ingeniería Electrónica and Instituto de Microelectrónica de Barcelona (IMB-CNM), University of Valencia and CSIC, Valencia, Spain
¹⁶⁹ Department of Physics, University of British Columbia, Vancouver, BC, Canada
¹⁷⁰ Department of Physics and Astronomy, University of Victoria, Victoria, BC, Canada
¹⁷¹ Department of Physics, University of Warwick, Coventry, United Kingdom
¹⁷² Waseda University, Tokyo, Japan
¹⁷³ Department of Particle Physics, The Weizmann Institute of Science, Rehovot, Israel
¹⁷⁴ Department of Physics, University of Wisconsin, Madison, WI, United States
¹⁷⁵ Fakultät für Physik und Astronomie, Julius-Maximilians-Universität, Würzburg, Germany
¹⁷⁶ Fachbereich C Physik, Bergische Universität Wuppertal, Wuppertal, Germany
¹⁷⁷ Department of Physics, Yale University, New Haven, CT, United States
¹⁷⁸ Yerevan Physics Institute, Yerevan, Armenia
¹⁷⁹ Centre de Calcul de l'Institut National de Physique Nucléaire et de Physique des Particules (IN2P3), Villeurbanne, France

- ^a Also at Department of Physics, King's College London, London, United Kingdom.
^b Also at Institute of Physics, Azerbaijan Academy of Sciences, Baku, Azerbaijan.
^c Also at Particle Physics Department, Rutherford Appleton Laboratory, Didcot, United Kingdom.
^d Also at TRIUMF, Vancouver, BC, Canada.
^e Also at Department of Physics, California State University, Fresno, CA, United States.
^f Also at Tomsk State University, Tomsk, Russia.
^g Also at CPPM, Aix-Marseille Université and CNRS/IN2P3, Marseille, France.
^h Also at Università di Napoli Parthenope, Napoli, Italy.
ⁱ Also at Institute of Particle Physics (IPP), Canada.
^j Also at Department of Physics, St. Petersburg State Polytechnical University, St. Petersburg, Russia.
^k Also at Chinese University of Hong Kong, China.
^l Also at Department of Financial and Management Engineering, University of the Aegean, Chios, Greece.
^m Also at Louisiana Tech University, Ruston, LA, United States.
ⁿ Also at Institutio Catalana de Recerca i Estudis Avancats, ICREA, Barcelona, Spain.
^o Also at Institute of Theoretical Physics, Ilia State University, Tbilisi, Georgia.
^p Also at CERN, Geneva, Switzerland.
^q Also at Ochadai Academic Production, Ochanomizu University, Tokyo, Japan.
^r Also at Manhattan College, New York, NY, United States.
^s Also at Novosibirsk State University, Novosibirsk, Russia.
^t Also at Institute of Physics, Academia Sinica, Taipei, Taiwan.
^u Also at LAL, Université Paris-Sud and CNRS/IN2P3, Orsay, France.
^v Also at Academia Sinica Grid Computing, Institute of Physics, Academia Sinica, Taipei, Taiwan.
^w Also at Laboratoire de Physique Nucléaire et de Hautes Energies, UPMC and Université Paris-Diderot and CNRS/IN2P3, Paris, France.
^x Also at School of Physical Sciences, National Institute of Science Education and Research, Bhubaneswar, India.
^y Also at Dipartimento di Fisica, Sapienza Università di Roma, Roma, Italy.
^z Also at Moscow Institute of Physics and Technology State University, Dolgoprudny, Russia.
^{aa} Also at Section de Physique, Université de Genève, Geneva, Switzerland.
^{ab} Also at Department of Physics, The University of Texas at Austin, Austin, TX, United States.
^{ac} Also at International School for Advanced Studies (SISSA), Trieste, Italy.
^{ad} Also at Department of Physics and Astronomy, University of South Carolina, Columbia, SC, United States.
^{ae} Also at School of Physics and Engineering, Sun Yat-sen University, Guangzhou, China.
^{af} Also at Faculty of Physics, M.V. Lomonosov Moscow State University, Moscow, Russia.
^{ag} Also at Moscow Engineering and Physics Institute (MEPhI), Moscow, Russia.
^{ah} Also at Institute for Particle and Nuclear Physics, Wigner Research Centre for Physics, Budapest, Hungary.
^{ai} Also at Department of Physics, Oxford University, Oxford, United Kingdom.
^{aj} Also at Department of Physics, Nanjing University, Jiangsu, China.
^{ak} Also at Institut für Experimentalphysik, Universität Hamburg, Hamburg, Germany.
^{al} Also at Department of Physics, The University of Michigan, Ann Arbor, MI, United States.
^{am} Also at Discipline of Physics, University of KwaZulu-Natal, Durban, South Africa.
^{an} Also at University of Malaya, Department of Physics, Kuala Lumpur, Malaysia.
^{*} Deceased.